Strategies for surface immobilization of whole bacteriophages: A review

Larry O'connell, Pierre R. Marcoux, Yoann Roupioz

Strategies for Surface Immobilization of Whole Bacteriophages: A Review

Larry O'Connell[1,2], *Pierre R. Marcoux*[1], *Yoann Roupioz*[2,*]

[1] Univ. Grenoble Alpes, CEA, LETI, F38054 Grenoble, France

[2] Univ. Grenoble Alpes, CNRS, CEA, IRIG, SyMMES, 38000 Grenoble, France

[*]Correspondence: yoann.roupioz@cea.fr; Tel.:+33-4-38-78-98-79

Keywords: Biomaterials, Biosensing, Functional surfaces, Surface functionalization, Bacteriophage

Abstract

Bacteriophage immobilization is a key unit operation in emerging biotechnologies, enabling many new possibilities for biodetection of pathogenic microbes at low concentration, production of materials with novel antimicrobial properties, and fundamental research on bacteriophages themselves.

Wild type bacteriophages exhibit extreme binding specificity for a single species – and often for a particular subspecies – of bacteria. Since their specificity originates in epitope recognition by capsid proteins, which can be altered by chemical or genetic modification, their binding specificity may also be redirected towards arbitrary substrates or a variety of analytes in

addition to bacteria. The immobilization of bacteriophages on planar and particulate substrates is thus an area of active and increasing scientific interest.

This review assembles the knowledge gained so far in the immobilization of whole phage particles, summarizing the main chemistries and presenting the current state-of-the-art both for an audience well-versed in bioconjugation methods as well as for those who are new to the field.

Introduction

Bacteriophages, obligate intracellular parasitic viruses that replicate only in their host bacterium, are the most numerous replicating biological entity on Earth, with an estimated 10^{31} phage particles contained within the biosphere, compared to an estimated 10^{30} bacterial cells [1,2]. Indeed, the estimated *daily* turnover of 15% of all bacterial cells due to phage lysis is a testament to their crucial role in microbiological ecology [3].

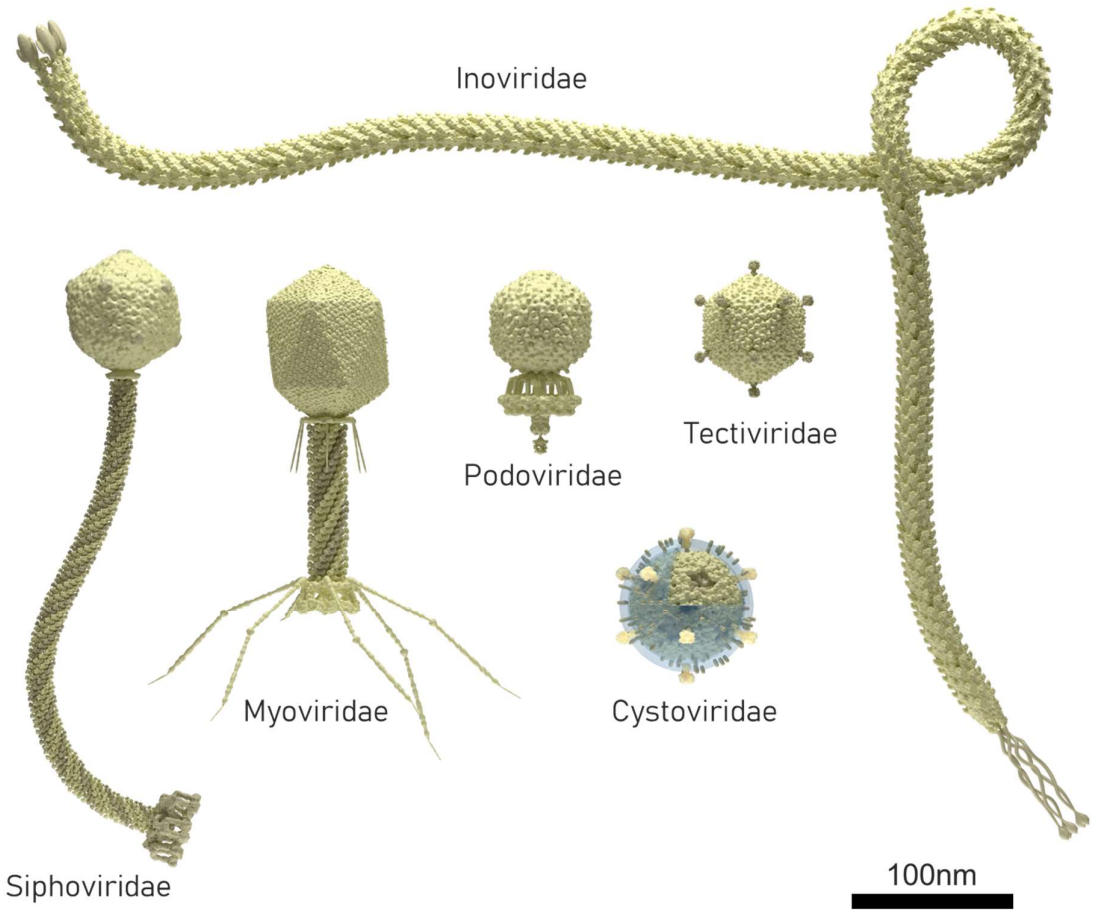

Figure 1. Illustrations of the bacteriophage morphologies that appear most often in the phage-functionalization literature. The *Inoviridae* family comprises filamentous phages and includes fd and M13. The *Myoviridae* family features long contractile-tailed phages and includes the well-known T4 coliphage. The *Siphoviridae* family features long non-contractile-tailed phages and includes D29. Meanwhile, the *Podoviridae* family are short-tailed and include P22. Relative scales are approximate.

Phage structure exhibits large variation which falls within a few stereotyped forms (**Erreur ! Source du renvoi introuvable.**). A small number of phage morphologies are over-represented

in the phage immobilization literature and include: long contractile-tailed phages (*Myoviridae* e.g. T4), long non-contractile-tailed phages (*Siphoviridae*), short-tailed phages (*Podoviridae* e.g. T7 or P68), filamentous phages (*Inoviridae* e.g. M13 and fd) [4]. Less frequently seen in the phage immobilization literature are tailless phages families *Tectiviridae* (comprising non-tailed icosahedonal phages, such as PRD1) and *Cystoviridae* (featuring an outer lipid membrane and no tail, such as phage phi6). Phages are also described in terms of their replication cycle. *Lytic phages* terminate their replicative cycle with the biochemical lysis of their host, rupturing the cell membrane and releasing up to several hundred progeny virions in one burst. In contrast, upon infection of a suitable host, temperate phages incorporate their genetic material into that of the bacterial cell and may lay dormant before shifting to a lytic cycle, or may instead continually produce a smaller number of phages which are shed from the host on a continuous basis [5].

History

Bacteriophages were independently discovered by microbiologists Frederick Twort in London in 1915 and by Felix d'Herelle in Paris in 1917 [6].It should be noted that extensive research on phage phenomena was also carried out in Poland during the interwar period[7], as well as in Brazil. Indeed, the oft-cited pioneering 1919 work by d'Hérelle in the use of phage to treat dysentary in French soldiers was followed relatively soon afterwards by similar trials in 1923 in both Poland[7] and Brazil[8].

Such research eventually led to the widespread use of phages in the Soviet Union for the treatment of routine bacterial infections, with phage therapy being extensively mobilized to meet the needs of the Soviet military beginning in 1939 with the Winter War with Finland, and later in World War II [9].

Meanwhile in the West, the discovery by Alexander Fleming in 1928 of penicillin, a broad spectrum antibiotic, led to a paradigm shift in medicine that relied heavily on the widespread administration of what was seen at the time as a "magic bullet".

The geopolitical paranoia of the Cold War and a lack of scientific rigor in reporting of early soviet phage therapy studies resulted in a progressive dismissal of phage therapy in Western medicine [10]. In the 1970s, up to 70 patients per year underwent phage therapy to treat bone and joint infections (BJI) in Croix Rousse Hospital, Lyon [11]. However, non soviet-aligned states instead pursued a policy of unfettered use of antibiotics [12], the profligate administration of which has now led to widespread antimicrobial resistance (AMR), threatening to return medicine to the "dark ages" before widespread availability of microbial control [13]. With the World Health Organization (WHO) announcement in 2014 that AMR was no longer a looming threat but a contemporary crisis [14], the problem of antibiotic resistance is proving increasingly salient [15].

In a global context where common pathogenic bacterial strains are rapidly gaining new resistance mechanisms, the pharmaceutical sector is largely withdrawing from the antibiotic discovery field, which has led to a failure to discover any new classes of antimicrobial agents in over three decades [16,17].

A growing appreciation for the importance of antibiotic stewardship and the urgency of identifying novel therapies has led to renewed interest in phage therapy as a plausible replacement for antibiotics [18]. In the field of biodetection, too, researchers have leveraged the high specificity of bacteriophages for their hosts to create biosensors with single strain specificity for a variety of common human pathogens and with extremely low detection limits. New use cases are also being explored, including the use of phages for antimicrobial, bioactive packaging [19,20] or as nanostructural scaffolds for various supramolecular structures [21].

Within this context, biomedical, agricultural, and environmental monitoring applications of bacteriophages would be aided by well-characterized, repeatable, versatile, and (ideally) morphology-agnostic immobilization methods.

State of the art

The literature concerning phage-functionalization of substrates falls into three main categories, with some overlap:

- Coupling to a transducer for the specific detection of bacteria or other analytes.

  Starting in earnest in 2005 [22], the last 15 years have seen bacteriophages immobilized on biosensors using a variety of transduction mechanisms, towards the detection of a large variety of target analytes including bacteria and their spores [23–28], antibodies [29–32], prostate specific antigen [32–34], enzymes [35,36], cancer biomarkers [37], and glucose [38].

- As a biosorbent layer for species-targeted biocontrol and anti-fouling

  The incorporation of bacteriophages into materials (e.g. food packaging and wound dressing) can confer them targeted anti-bacterial properties which can help reduce the proliferation of bacteria in foodstuffs or surrounding wounds. Such bioactive materials have been demonstrated in food packaging that targets *Listeria* [20,39], *Escherichia coli* [20,39,40], and *Salmonella* [19]. Bioactive fabrics have been demonstrated with specific antimicrobial action against *Pseudomonas aeruginosa* [41] and *E. coli* [42].

- As a structural scaffold for supramolecular nanostructure fabrication

  The tessellated and highly redundant structure of bacteriophage capsids, together with their chemical uniformity and physical monodispersity, also opens up the possibility of bottom-up fabrication of highly ordered supramolecular structures [21,43]. Liquid crystalline bacteriophage films [21,43] have been proposed for use as tissue regenerating scaffolds [44], piezoelectric energy harvesting [45], and colorimetric sensors [46].

Across all applications, the vast majority of papers reviewed demonstrate immobilization of classic phages such as the lytic T4 coliphage, or the temperate M13 and fd phages. However, examples are also to be found of successful immobilization of various other phages of the *Autographiviridae* [29,47–49], *Tectiviridae* [50–52], *Herelleviridae* [53], *Leviviridae* [50,53], *Myoviridae* [39,50–64], *Siphoviridae* [39,41,53,60,65,66] and *Podoviridae* [50,53,57,58,67–72] families.

Viral properties involved in immobilization

When considering the immobilization of bacteriophages on surfaces or particles, we should first consider what properties of the phage, which moieties and/or surface charges, can be modified or leveraged for chemical and/or physical interaction with the surface or intermediate linker molecules. The vast majority of bacteriophages exhibit an outermost protein layer which encapsulates genetic material on the interior (with the exception of *Cystoviridae*, which encapsulated the capsid in a lipid envelope). Bacteriophage capsids are composed of proteins which are in turn composed of long chains of amino acid subunits, which display primary amine ($-NH_2$) groups on their N-terminus, and carboxyl groups (-COOH) on their C-terminus (**Erreur ! Source du renvoi introuvable.**). Both the amine and carboxyl groups of polypeptide amino-termini are frequent targets for immobilization chemistry, but in the specific case of bacteriophages, the termini available for conjugation will be greatly outnumbered by amino acid side chains.

Amino acids vary in the composition of their side chains, with some side chains endowing a polarity, charge, or hydrophobic/hydrophilic character, each of which may be leveraged in isolation or in combination for the purposes of conjugation. For example, two amino acids in particular, cysteine and methionine, contain sulfhydryl side chains which interact strongly with gold, a common substrate for bio-functionalization. The amino acids lysine, arginine, asparagine, and glutamine feature a second primary amine group on the side chain in addition to their N-terminus.

Each amino acid also has a characteristic isoelectric point which determines the pH below which the side chain is protonated in aqueous solutions. The local hydrophobic character and charge of a phage is the result of an aggregate sum of the local constituent amino acids. The isoelectric point of a bacteriophage dictates the charge it presents to the solution and thus its stability and resilience against aggregation[73–75]. There is significant evidence that tailed bacteriophages – which make up over 95% of described phages [76] – have a net dipole moment,

with a negatively charged head and positively charged tail and tail fibers at physiological pH[39,77,78].

Genes coding amino acids on the outer bacteriophage surface can also be targeted for site-specific genetic engineering and mutagenesis, altering them in order to introduce new functional groups in order to optimize their chemical and/or physical characteristics for the purposes of immobilization [38,48,79–89].

To summarize, when developing immobilization strategies, the researcher has at their disposal:

- Primary amine groups ($-NH_2$), present at the N amino-termini of proteins and in the side chains of lysine, arginine, asparagine, and glutamine
- Carboxylic groups (−COOH), present at the C amino-termini of proteins and in the side chains of aspartic and glutamic acid
- Sulfhydryl side chains (−SH) of the amino acids cysteine and methionine
- The local and overall charge of the phage
- The dipole moment of the phage
- Site-directed genetic engineering of the phage coat

It is starting from this basis that the full suite of immobilization strategies can be derived.

Immobilizing biological entities on surface or nanoparticle substrates can lead to conformational and other changes that impede their original function. When choosing an immobilization strategy, it is important to consider what purpose the phage immobilization is serving. Is the goal to maximize analyte capture itself? Or is it rather to maximize the limit of detection (LOD) of a biosensor? Is the surface to be used for the purpose of biocontrol (e.g. wound dressing or food packaging)? What kind of environment will the phage-functionalized surface be used in? Is it important that the phage maintains the same infectivity as its non-immobilized form? Is it important that the phage be oriented in a given direction relative to the substrate?

The answers to each of these questions places different requirements on the surface chemistry and optimal phage density. For example, Naidoo *et al.* have found that bacterial capture efficiency only correlates with increasing phage surface density up to a certain threshold, beyond which the capture efficiency actually decreases [58]. However, in a biocontrol context

where shedding of phage particles from a substrate may be desirable, this effect may not be problematic and we may indeed aim to achieve a maximal surface density limited only by geometric constraints.

Consideration of the end result is needed in order to optimize the immobilization strategy. Phage density may represent only a proximal measure for a different performance metric of the phage-functionalized substrate. The researcher may indeed aim for lower phage surface densities depending on the application, and one should not necessarily aim to maximize surface density for its own sake.

Scope and organization of the review

This review groups the literature based on immobilization technique, rather than grouping by substrate, phage, or detection scheme (in the case of biosensors). This arrangement makes the particularities and commonalities between immobilization strategies more apparent.

This review does not treat the immobilization of phage-derived proteins (e.g. endolysins or recombinant coat proteins), since this has been treated elsewhere and overlaps with general strategies for protein immobilization, a topic too large for a single review. For an excellent treatment of protein immobilization, see Hermanson [90]. Likewise, this review does not treat phage immobilization on chromatographic columns or microtiter plates, since this falls in the category of phage display literature, thoroughly reviewed in Hust and Lim [91].

The most common substrates are briefly described, as well as the scientific interest in phage-functionalization in each case. Thereafter, the most common and successful immobilization strategies are outlined with reference to their application in the literature, grouped into covalent chemistries, non-covalent and physical methods (e.g. physisorption, electrostatic adsorption, avidin-biotin linkage etc.), and finally genetic modification techniques, which are treated separately since they exist as a modification of the bacteriophage itself but facilitate the preceding chemisorptive and physisorptive immobilization strategies.

Oriented immobilization

A phage's host range and ability to replicate is largely based on its ability to specifically recognize cells of its host bacterial strain *via* the phage's receptor-binding domains (RBDs) – epitope-recognizing regions on the phage capsid. This initiating event is a *sina qua non* and relies on serendipitous encounters between the RBDs and a bacterial cell surface.

Over 95% of described phages are tailed [76]. and thus have an inherent asymmetric, bilateral geometry; having a preferred orientation with regards to attachment to their host cell. For a conjugated phage to retain its binding and replicative capacity, it must be oriented on the surface such that its RBDs are exposed to the environment, and hence any host cells that may be present [92]. Such a tail-upward orientation will hereafter be referred to simply as "oriented" immobilization. Most authors simply accept the lower bacterial capture associated with random phage orientation, relying on immobilization of a sufficiently large number of phages that includes a small subpopulation of serendipitously tail-upward oriented phages. Nevertheless, Nogueira *et al.* recognize that maximizing tail exposure is a key criterion for maintaining immobilized phage infectivity [41]. and Hosseinidoust *et al.* conclude in an influential review paper that the main hurdle to designing efficient phage-based biosensors appears to be controlling the orientation of the immobilized phages [92].

The bacteriophage head presents a net negative charge, while the tail fibers present a net positive charge [77]. Thus, the dipole moment of a phage particle causes the head to be oriented towards a positively charged surface [78]. In addition to local charge distribution, many phages such as T7, present an overall net negative charge [93,94].

In most circumstances there is a strong entropic preference towards horizontal alignment of tailed and filamentous phages. However, as we shall see, a significant minority of the studies reviewed have taken advantage of the local charge or other properties of bacteriophage capsids to claim oriented immobilization as a result of their protocols (**Figure 2**). Frequently, however,

insufficient evidence and/or no clear mechanisms are presented to prove oriented immobilization has been achieved. This is partly due to the difficulty in determining the orientation of nanoscale objects, but post-functionalization characterization techniques do exist that can help justify such claims.

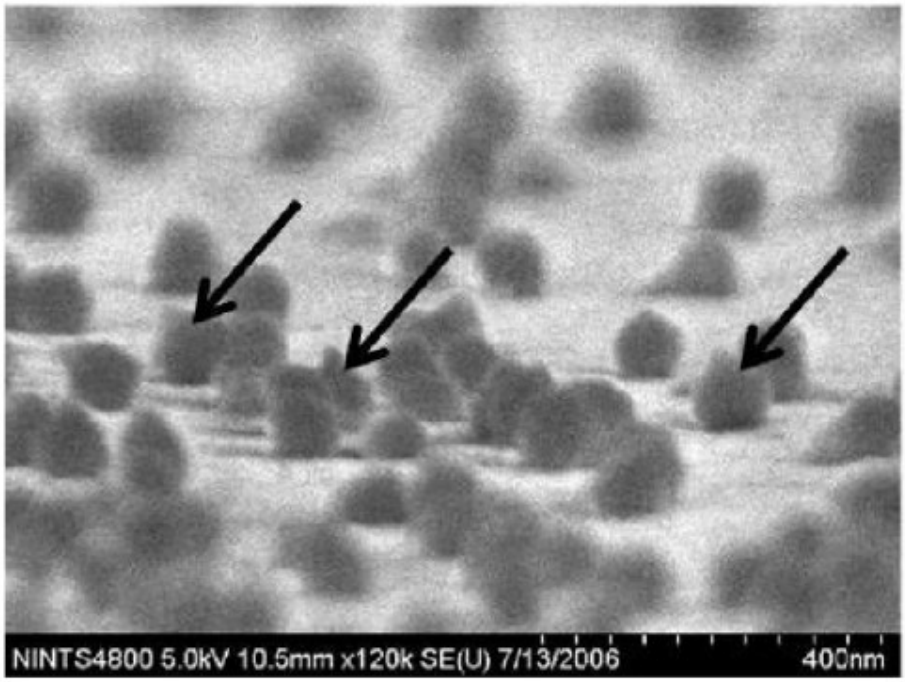

Figure 2. Scanning electron micrograph of *in vivo* biotinylated T4 phage, immobilized on a streptavidin-coated gold surface. Arrows indicate phage particles with tail-up orientation. Reproduced from *Tolba et al.* [83].

A note on surface density

A high phage surface density is not the sole criterion for high phage infectivity and/or bacterial capture. For example, Tawil *et al.* found that phages were immobilized on gold with double the density when cross-linked *via* L-cysteine compared to glutaraldehyde, but that no significant difference was found in the bound phages' lytic behavior [72]. Similarly, Leppänen *et al.* rigorously compared infectivity and phage surface density after surface treatments with different combinations of 11-MUA and (3-aminopropyl)triethoxysilane (APTES), concluding

that a higher phage density did not always result in a higher infectivity [95]. Indeed, Naidoo *et al.* achieved an impressive surface density of 199±2 phages/μm^2 but found that – above a value of a 18.9±0.8 phages/μm^2 – higher phage density led to a *reduction* in total bacterial capture [58].

These results suggest that careful consideration and design of the surface functionalization can lead to dramatically improved activity and/or bacterial capture of phage-functionalized surfaces.

Common substrates

Gold

Gold surfaces are by far the most popular surface for phage functionalization, serving as the substrate in just over half of all papers reviewed on this topic. Gold exhibits ideal properties for functionalization with many biological entities [90], and for bacteriophages the case is no different. Gold is biocompatible, non-oxidizable, readily available, easily cleaned, and its deposition on a variety of substrates is a mature technology [96–98]. Gold also exhibits a very high binding affinity for sulfhydryl (R-SH, aka thiol) groups of around 200 kJ/mol, which also permits easy formation of self-assembled monolayers [98]. Thiol groups are frequently found – or easily introduced – in most target ligands for the purpose of immobilization [98].

Facilitating bioconjugation is the principal motivation behind the deposition of a gold layer on transducers that do not involve the intrinsic properties of gold itself (e.g. magnetoelastic or quartz crystal microbalance (QCM) biosensors, which instead rely on the resonance of an underlying amorphous ferromagnetic material [99] or quartz crystal [100], respectively). However, gold also exhibits ideal properties where its biocompatibility and ease of conjugation is a happy coincidence. Gold features a high density of easily polarizable free electrons – a prerequisite for strong interaction with electromagnetic fields [101] – making it an ideal material for use in

surface plasmon resonance (SPR). For SPR, there are effectively only two metals with appropriate properties: gold and silver [102]. While silver actually yields a superior SPR effect, it is less biocompatible and less chemically stable – particularly towards oxidation – compared to gold, and so the latter has become the *de facto* default for SPR biosensors [101,102].

Magnetic beads

Magnetic bead surfaces are a frequent substrate for phage conjugation since, once functionalized, they can be used for immunomagnetic separation (also sometimes referred to as phagomagnetic separation) and concentration of low-titer analytes in order to boost the capture efficiency of biosensor surfaces (**Figure 4**) [47,48,56,68,69,89,103,104]. Briefly, phages specific to a given bacterial strain are immobilized on the beads, which are then mixed with a sample and bind to the target analyte (**Figure 5**). Application of a magnetic field can then be used to concentrate and confine the captured analyte to a given region, for example on the surface of a biosensor. Phage immobilization has been shown for magnetic beads with a variety of surface chemistries including tosyl [68,69], carboxyl [47,49,69,103], streptavidin [48,83,89,105], azide [81], and isothiocyanate-terminated coatings [104].

Carbon allotropes

Carbon allotropes (e.g. graphene, nanotubes) and glassy/vitreous carbon are common components of inks used to fabricate screen-printed electrodes (SPEs). Electrode screen-printing enables cheap, versatile electrodes for use in clinical assays[106], food processing[107], and environmental monitoring [108]. Such electrodes can also be composed of gold, silver, or platinum; but carbon is more typical due to its relatively low cost [109]. The versatility and easy manufacture of SPEs has led to carbon allotropes becoming a target for phage immobilization for the fabrication of biosensors specific to various bacterial strains [54,55,65,110,111], and in one paper a biosensor for West Nile virus-specific IgG [29]. Carbon nanotubes can also be used as an

intermediate structure for the immobilization of phages on different substrates, as was demonstrated by Farooq *et al.* for bacterial cellulose matrices for ultra-sensitive and selective electrochemical detection of *Staphylococcus aureus* [112]. Carbon allotrope-specific binding peptides have been discovered that may enable recombinant phage immobilization on such substrates [113–116] (see Polymer and other binding domains below).

Polymers

Phage-functionalization of polymers is of interest since such materials can be formed into antimicrobial wound dressing [41,117], food packaging [20], and biocontrol surfaces resistant to biofilm formation [118]. They also form the coating of many commercially available magnetic beads [47,49,68,69,103]. Polymers that have been successfully conjugated or co-polymerized with phages include polycaprolactone [41], polymethyl methacrylate (PMMA) [86], polyethersulfone [118], polystyrene [119], polyhydroxyalkanoates [40], polyethylene [120], and poly(3,4-ethylenedioxythiophene) (PEDOT) [33,121,122].

It is interesting to note that a large number of peptides have been discovered that have high binding affinities for specific polymers [123–129], and that such proteins have been expressed on the capsids of recombinant phages to facilitate immobilization [83,86,89].

Cellulose-based materials

A particularly important subcategory of polymers is cellulose and cellulose-derived materials. As the most abundant natural polymer on Earth [130], cellulose features in the phage-functionalization literature because it forms the principal component of paper. With its high porosity, hydrophilicity, chemically inert character, and slight negative charge at neutral pH [42,53], paper lends itself to the fabrication of cheap, mass-produced devices for healthcare [131] and environmental monitoring [132].

Phage-functionalization of paper and cellulose-derived polymers is motivated by the development of antimicrobial food packaging materials [19,20,39], and low cost biosensors [53,133,134]. Phage-containing bio-inks can be printed onto paper substrates, and it has been shown that T4 phages are capable of resisting the shear stress and drying processes involved in industrial printing [135]. It has also been demonstrated that careful consideration of the bio-ink constituents can enable production of bioactive paper that is stable for several days after printing [136]. Anany *et al.* have demonstrated a dipstick assay based on inkjet-printed phages that efficiently captured and infected *E. coli* and *Salmonella* Newport in broth and food matrices [53]. Farooq *et al.* demonstrated phage-functionalization of bacteria-derived cellulose fibers, but *via* intermediate multi-walled carbon nanotubes [112].

There is ample precedent for lateral flow devices that rely on capillary action along capillary beds to channel fluid for the purposes of biochemical analysis, the most well-known of which is probably modern pregnancy tests [137] and covid-19 antigen tests. Such microfluidic paper-based devices may also be combined with electrode screen printing for more elaborate microfluidic electrochemical sensors [137,138]. Phage-derived proteins [139] have been incorporated into lateral flow assays, but to our knowledge in all cases have been immobilized onto intermediate supports (e.g. nanoparticles) rather than the polymer substrate of the device itself. The ability to reliably immobilize phages directly on paper substrates would open new avenues for the development of low-cost, mass-produced bioassays [134].

Some evidence suggests immobilization is more successful if paper has been precoated with polydiallyldimethylammonium chloride (polyDADMAC), a cationic polyelectrolyte which imparts a positive charge to the cellulose fibers and thus electrostatically binding the phage heads [134]. Phage resistance to dry environments can be improved by incorporating gelatin into the deposition ink [136]

When considering cellulose-based substrates, of note is the existence of cellulose binding modules (CBMs) – polypeptides that bind strongly to cellulose [140] and which can be expressed by genetically-engineered phages to facilitate their immobilization on such substrates [83,89].

Silicon-based materials

In this review, phage-functionalization of several materials including silicon nitride [37], optical fibers [141–143], atomic force microscopy probes [144], silica nanoparticles [60,62], and glass [50,51,67,79,80] are all grouped into the category of silicon-based substrates. Such surfaces are typically rendered reactive for immobilization chemistry through amino-silanization [37,46,50,51,60,62,67,79,80,95,141,142,144–148].

Optical fiber biosensing is of particular interest since it can exploit the properties of optical biosensing techniques (e.g. SPR), while avoiding drawbacks associated with bulky equipment [141]. Using a smaller sensing element and sample volume can be advantageous in the analysis of small amounts of precious analytes, and can accommodate multiple parallel measurements on adjacent bundled optical fibers [149].

Since the fiber-optic material itself is cheap, this may offer the possibility of disposable, single-use sensors [150,151]. Finally, since the nature of optical fiber geometry means that signal transduction can take place at a physically remote location relative to the optical setup, this form of biosensing enables remote detecting and monitoring capabilities in potentially harsh environments [149], allowing one to bring the sensor to the sample rather than bring the sample to the sensor. Phage-functionalized optical fibers have been demonstrated for the specific detection of E. coli [141–143].

Covalent methods

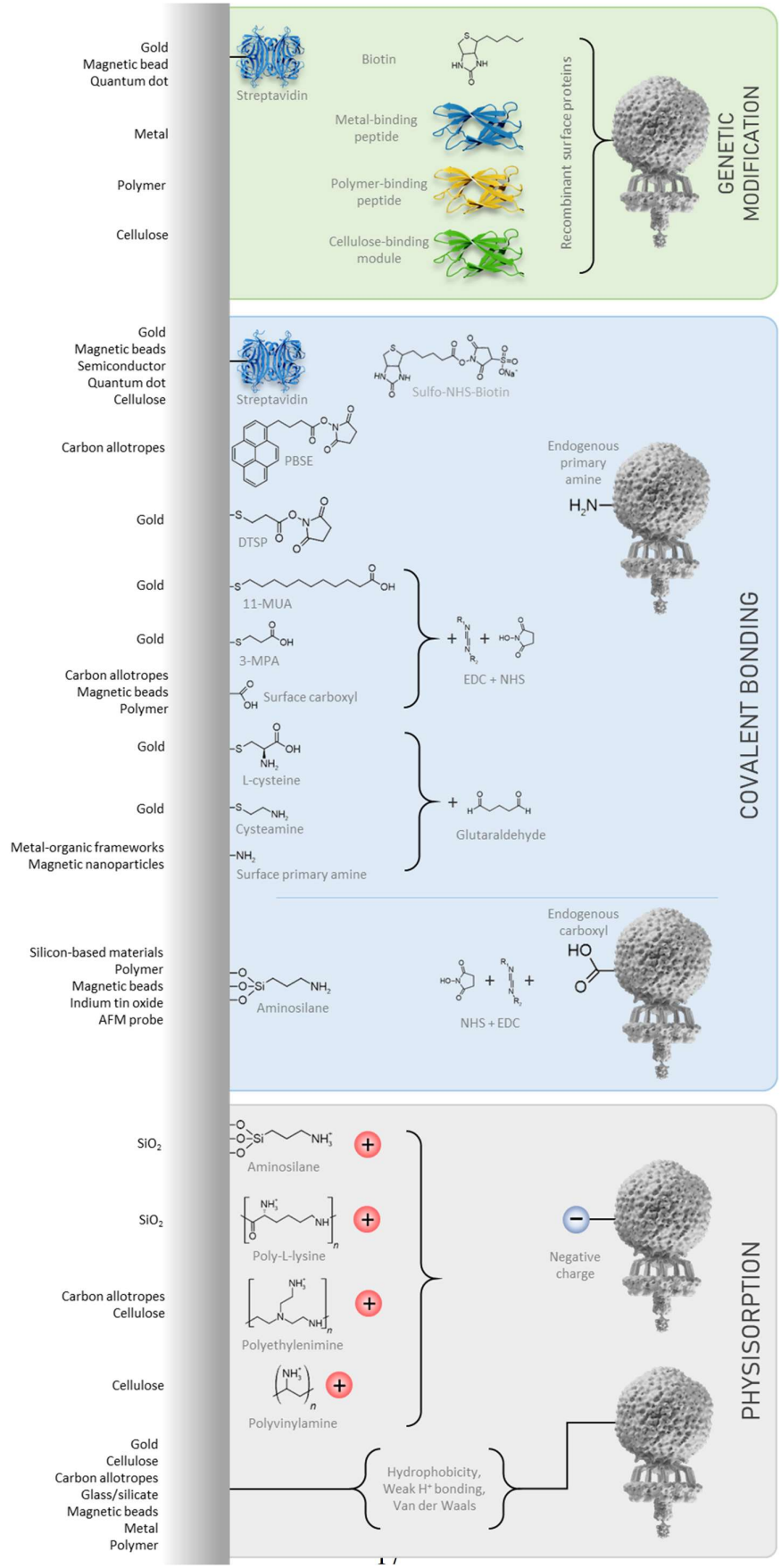
Gold
Magnetic bead
Quantum dot
Metal
Polymer
Cellulose
Streptavidin
Biotin
Metal-binding peptide
Polymer-binding peptide
Cellulose-binding module
Recombinant surface proteins
GENETIC MODIFICATION
Gold
Magnetic beads
Semiconductor
Quantum dot
Cellulose
Carbon allotropes
Gold
Gold
Gold
Carbon allotropes
Magnetic beads
Polymer
Gold
Gold
Metal-organic frameworks
Magnetic nanoparticles
Streptavidin
Sulfo-NHS-Biotin
PBSE
DTSP
11-MUA
3-MPA
Surface carboxyl
EDC + NHS
Endogenous primary amine
L-cysteine
Cysteamine
Surface primary amine
Glutaraldehyde
Silicon-based materials
Polymer
Magnetic beads
Indium tin oxide
AFM probe
Aminosilane
NHS + EDC
Endogenous carboxyl
COVALENT BONDING
SiO2
SiO2
Carbon allotropes
Cellulose
Cellulose
Gold
Cellulose
Carbon allotropes
Glass/silicate
Magnetic beads
Metal
Polymer
Aminosilane
Poly-L-lysine
Polyethylenimine
Polyvinylamine
Negative charge
Hydrophobicity, Weak H+ bonding, Van der Waals
PHYSISORPTION

Figure 3. Schematic representation of a selection of the most popular bacteriophage immobilization strategies, broadly grouped into covalent bonding, physisorption, and genetic modification. At left, the substrates that have been demonstrated in the literature with the adjacent immobilization method. Note: bacteriophages are represented by a generic *Podoviridae* but in most cases represent other phage morphologies

EDC/NHS Chemistry

For substrates presenting carboxyl (−COOH) groups – be they endogenous or introduced – a common covalent conjugation method involves the use of the carbodiimide EDC (1-Ethyl-3-(3-dimethylaminopropyl)carbodiimide) to activate the carboxyl groups, creating an unstable ester intermediate [152]. Typically, a separate molecule containing a succinimidal group in the form of NHS (N-hydroxysuccinimide) is then introduced to the surface and supplants the carbodiimide, which is released into the solution. This stabilizes the activated carboxyl group and forms a second NHS-ester intermediate which is more vulnerable to nucleophilic attack from amino groups, in turn priming the NHS to be supplanted by the primary amine of an amino acid [67,152].

When a suspension of amine-containing ligands – such as phages or proteins – is introduced to the sensor surface, a primary amine of the ligand reacts with the NHS (the leaving group) and is then covalently bonded to the surface while the succinimidal group is released into the solution. After ligand binding is complete, the surface may be washed with ethanolamine whose amine groups will react with the remaining activated carboxyl “sites”, which blocks further binding.[152]. In this way, the EDC/NHS solution facilitates amide bonding between carboxyl groups of the surface and amine groups of the ligand [67].

Such EDC/NHS coupling is extremely popular for surface functionalization of gold following introduction of exogenous carboxyl groups (for example by formation of an

alkanethiol self-assembled monolayer) [34,57,153–158], but has also been demonstrated for a variety of carboxylated substrates including glassy carbon electrodes [55], glass [50], magnetic beads [103], and polymers [40,159].

The creation of the second NHS-ester intermediate is not obligatory and in cases where a high yield of conjugated ligands is not crucial, the use of NHS may be omitted entirely. Such EDC-mediated binding has been used to covalently immobilize phages on glassy carbon electrodes [110,111], magnetic microbeads [103], and carboxyl-polystyrene latex beads [119]. However, the addition of even small amount of NHS to an EDC coupling reaction can boost the yield of conjugated ligand by a factor of 20 [160]. NHS activation decreases the water-solubility of the activated carboxylate molecule and for this reason is often instead sold as sulfo-NHS, wherein the charged sulfonate group preserves or increases water-solubility.

One paper made a rigorous comparison of the surface density of immobilized phage BP14 on gold that resulted from different combinations of EDC/NHS with L-cysteine, 11-MUA, and glutaraldehyde cross-linking; finding that cysteine – when combined with 11-MUA and ECD/NHS – gives an incredible 10^3 improvement in phage activity (measured by bacterial lysis) compared to simple physisorption [72].

EDC/NHS can also be used in the other direction: activating the surface carboxyl groups of the phages themselves in order to facilitate grafting to substrates featuring primary amines – be they endogenous or introduced (e.g. *via* aminosilanization) [67,144,146,161,162]. However, this approach is believed by some researchers to lead to increased blocking of the phage receptors responsible for bacterial capture [50], which seems to have been confirmed in experiment [95,146].

One feature of amide binding is the non-uniform nature of the ligand orientation. Since a ligand typically displays several primary amines, any one of which may react with the activated substrate carboxyl group, this allows a variety of ligand orientations during immobilization. This issue is compounded for very large molecules. On the scale of a bacteriophage, the large

number of available primary amines means orientation may be effectively random unless effective mitigation strategies are employed, as discussed below.

Some substrates will already feature carboxyl groups, without the need to introduce a carboxyl intermediate. Such is the case for polyhydroxyalkanoate (PHA), a bacterially produced biopolymer [163] that is currently under investigation as a biodegradable food-packaging. Wang *et al.* have demonstrated that plasma treatment of PHA films results in surface carboxyl groups which can be activated and bound to phages using EDC/NHS, for the purposes of selective bioburden reduction in foodstuffs [40].

Carboxyl-activated magnetic beads are commercially available, for example *Dynabeads MyOne™ Carboxylic Acid* magnetic beads from Invitrogen. Although of proprietary formulation, the manufacturer describes these beads as having a coating of glycidyl ether and a core of highly cross-linked polystyrene with ferromagnetic inclusions. These beads have been employed for the detection of *E. coli* with an LOD as low as 10^3 colony-forming units/milliliter (CFU/mL) by impedimetric [49,103] and linear sweep voltammetry assays [49], as well as a colorimetric scheme based on release of endemic β-galactosidase from lysed analyte cells [47].

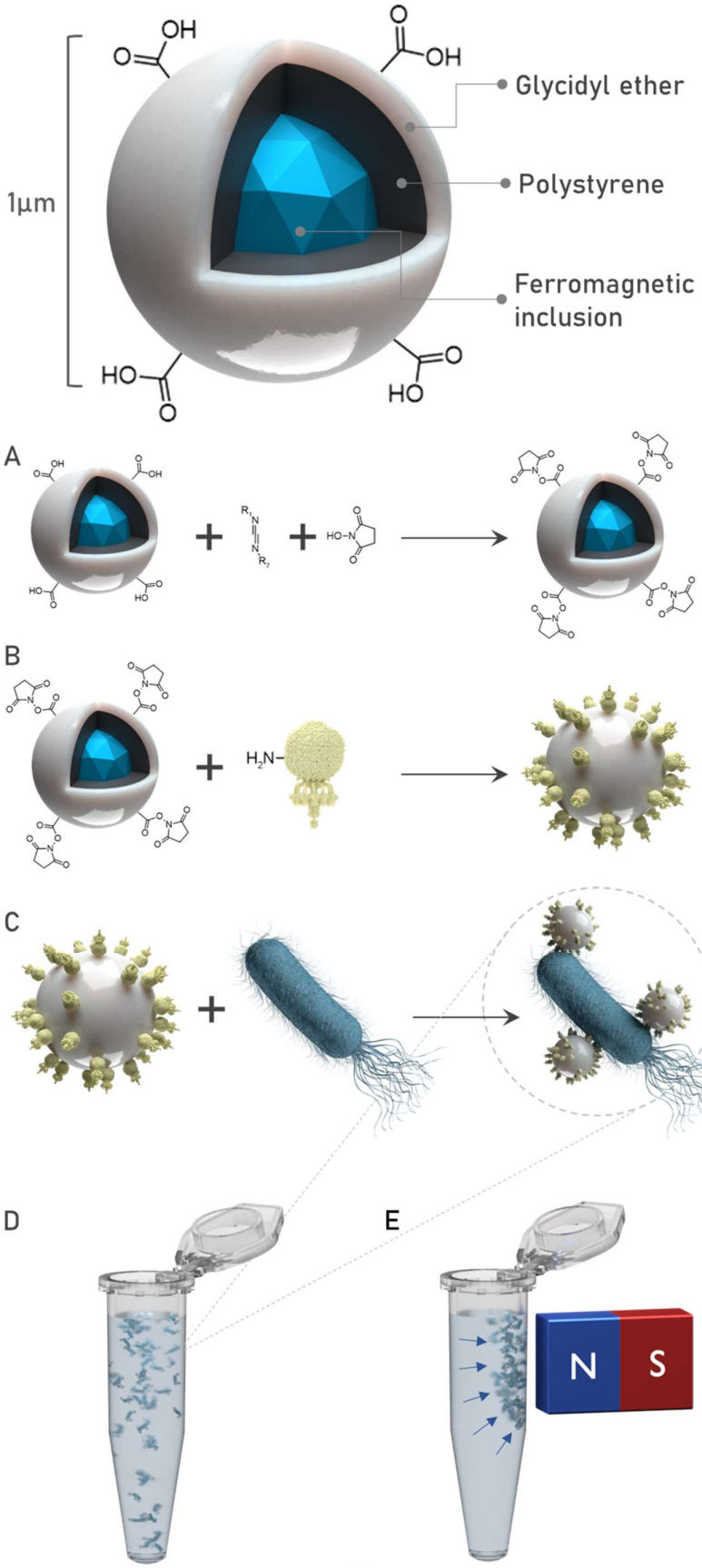
1µm
Glycidyl ether
Polystyrene
Ferromagnetic inclusion
A
B
C
D
E
N
S

Figure 4. Schematic representation of a typical magnetic bead and its use for phagomagnetic separation. (A) A carboxyl-terminated magnetic bead is activated with EDC and NHS, priming it for conjugation. (B) A ligand bearing primary amines, in this case a phage, is mixed with the beads and is conjugated to the bead surface through amide bonding. (C) Mixing the functionalized beads with bacteria causes the beads to bind to the surface of any bacteria present. (D) and (E) The bacteria can now be retained in a standard tube while the supernatant is removed, or concentrated near a biosensor transducer surface, by the application of a magnetic field.

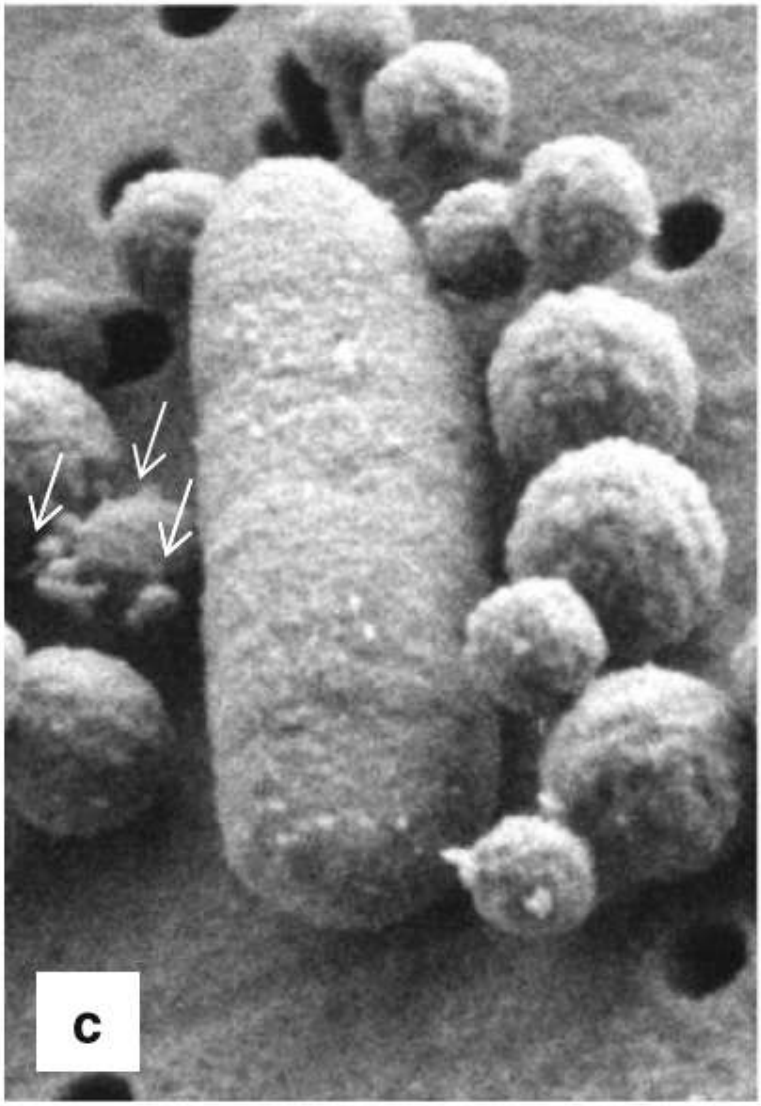

Figure 5. Scanning electron micrograph of P22 phages immobilized on carboxyl-activated magnetic beads following magnetic capture of a *Salmonella* bacterium. Reproduced from Laube *et al.* (2014) [69].

A similar product is that of Ademtech SA, in the form of *Carboxyl-Adembeads* which feature a superparamagnetic core of magnetite, covered with a proprietary styrene-based copolymer which presents carboxyl groups to the solution.† Regardless of the magnetic bead product used,

† Personal communication

in all cases in the literature reviewed, the particles' carboxyl groups are activated by EDC/NHS, exposed to the phage for immobilization, and used for the magneto-separation and subsequent detection of bacteria (*e.g. Salmonella* [69] or *E. coli* [47,49,103]) by varying detection mechanisms (**Scheme 1**).

Alternatively, carboxyl groups may be grafted to the substrate. This has been shown for graphene which can be electrochemically oxidized to produce carboxyl sites, allowing phage-functionalization of glassy [110] and screen-printed carbon electrodes [111]. A similar process has been demonstrated for carboxylated multi-walled carbon nanotubes for the phage-mediated detection of *S. aureus* [112].There are many advantages of EDC/NHS chemistry that have led to it becoming a staple in the bioconjugation literature. Both EDC and the resultant isourea formed after binding are water soluble, meaning one can avoid organic solvents which could otherwise harm the ligand. The carbodiimide reaction occurs with high yield up to pH 7.5, allowing conjugation at physiological pH which is well-tolerated by most biological ligands. Since carbodiimides such as EDC are what is known as zero-length crosslinkers, no additional chemical structure is introduced between the conjugated molecules after cross-linking [90].

Self-assembled monolayers of thiolated molecules

No discussion of surface immobilization techniques would be complete without mention of thiol-gold bonding, a workhorse of surface chemistry. Also known as sulfhydryl groups, thiol moieties are widely exploited for the formation of self-assembled monolayers (SAMs) on soft metal substrates [98], and are regularly employed in the functionalization of planar and nanoparticulate metals – gold in particular – with proteins, antibodies, and DNA. The most popular thiol-containing molecules are the alkanethiols which feature a sulfhydryl headgroup, an alkane chain of specified length, and a terminal functional group which can be used to

introduce carboxyl sites to the substrate, for example (Figure 6). This stereotypical structure serves as a good model for a brief discussion of SAM formation.

In a classical SAM formation model, a soft metal surface is incubated with a solution of alkanethiol molecules. The strong affinity of the sulfur headgroup for the metal surface leads to an initial "lying-down" configuration of the alkanethiol molecules, chemisorbed to the surface strongly by the metal-sulfur bond of the headgroup but also lightly physisorbed *via* van der Waals interactions between the surface and the alkane chain [164].

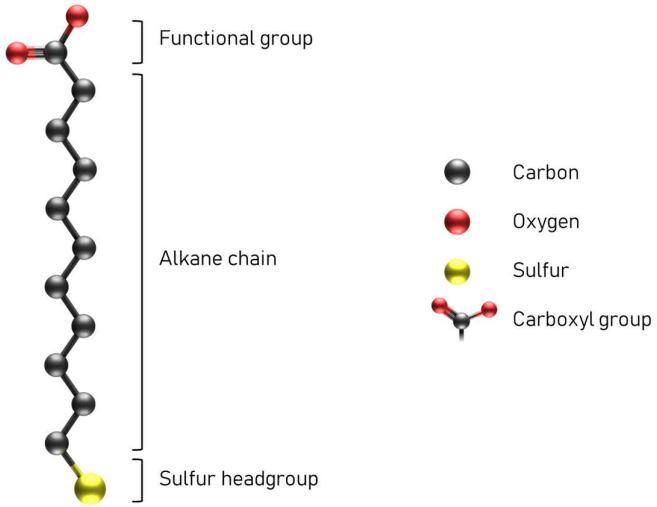

Figure 6. Structure of a typical alkanethiol, in this case 11-mercaptoundecanoic acid (11-MUA). Hydrogens have been omitted for simplicity.

Since the sulfur headgroups of arriving conjugate molecules have a higher affinity for the metal surface compared to the hydrocarbon chains, over time the latter are displaced from the surface as more alkanethiol molecules diffuse to and bind with the substrate (**Figure 7**). This gives rise to a phase transition to a "standing up" configuration with a strong entropic preference for upright orientation of the conjugated molecules relative to the surface. Mutual intramolecular van der Waals interactions between the alkane chains stabilize the SAM, resulting in the formation of a closely packed (surface coverage ≈1/3), crystalline monolayer of alkanethiolate molecules [164].

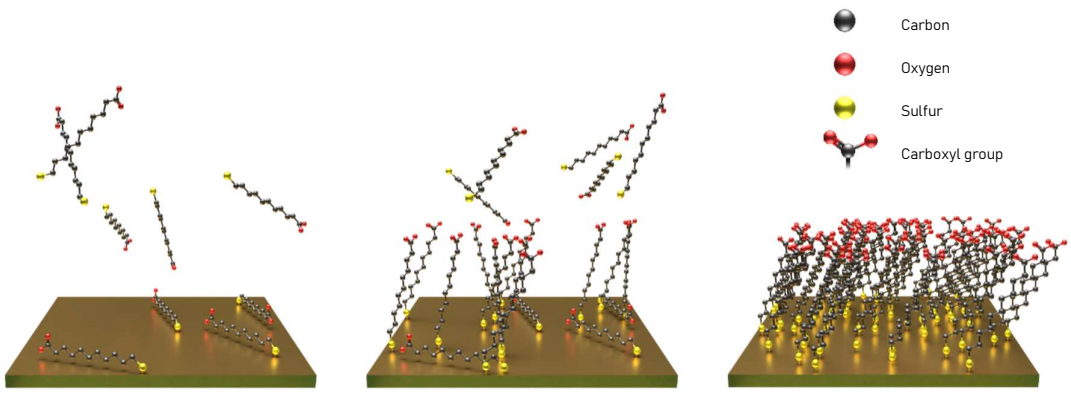

Figure 7. Progressive formation of an alkanethiol self-assembled monolayer (SAM) on a gold substrate. Diffusion of alkanethiol from the solution to the surface is followed by binding of the molecule to the gold surface through a strong gold-sulfur bond and also by interactions with the alkane chain, leading to a "lying down" configuration. With increasing incubation duration, more of the molecule diffuses to the surface. As surface density increases, arriving sulfur headgroups compete with and displace the alkane chains on the surface, leading to a standing-up configuration. Finally, above a threshold density, intra-molecular forces between the alkane chains stabilize the SAM with the functional groups presented to the solution above

While thiols exhibit high binding affinity for a variety of transition metals (Au, Ag, Cu, Pt, Pd, Ni)[98] and metal alloys, gold's other advantageous properties make it the *de facto* standard substrate for SAM formation and bioconjugation, for reasons discussed above [98].

An advantage of thiol-based immobilization is that the thiol groups readily displace biological contaminants and interferents during adsorption [98]. Thiol-based SAMs are known to be stable for periods from days to weeks even in the presence of complex liquid media, as is often the case in biological experiments [98].

Cross-linking molecules containing thiol moieties have been used to immobilize phages of various morphologies on gold surfaces [72,95,153], nanoparticles [158], and plasmonic quasicrystals [70].

Both cysteamine and the amino acid L-cysteine bind to gold through a strong thiol linkage while presenting an amine group which can be cross-linked to primary amines *via* glutaraldehyde (**Erreur ! Source du renvoi introuvable.**) [66,72,165]. In the case of L-cysteine, a carboxyl group is also present and is available for activation, for example by EDC/NHS [57,66].

11-mercapto-undecanoic acid (11-MUA) is an example of an alkanethiol featuring a long alkane chain terminated at one end by a thiol moiety and on the other end by a carboxyl group (**Erreur ! Source du renvoi introuvable.**). Mutual van der Waals interactions between the alkane chains and the high affinity of the sulfur headgroup for the gold surface leads 11-MUA to readily form SAMs on gold surfaces, presenting abundant carboxyl groups to the solution which may be activated by EDC/NHS [164].

11-MUA has been used as a tether molecule to functionalize gold substrates with phages such as M13 to detect peptides by SPR [153]; T4 and BP14 to detect *E. coli* and *S. aureus* by SPR and impedance measurements [57]; T4 to detect *E. coli* by differential pulse voltammetry (DPV) [157]; and various phages for the detection of *S. aureus* by SPR, and *Bacillus cereus* by ferromagnetoelasticity [155].

As mentioned above, by combining 11-MUA with L-cysteine, Tawil *et al.* were able to achieve a 10^3-fold increase in phage activity relative to simple physisorption [72].

The authors attributed this improvement to the creation of uniform, regularly interspaced depressions in the L-cysteine / 11-MUA monolayer, with a length scale similar to that of the phage head of 36 ± 2 nm, permitting uniform and oriented immobilization of the phages.

Another example of a thiol-based linker is 3-mercaptopropionic acid (3-MPA) (**Erreur ! Source du renvoi introuvable.**). 3-MPA has a similar structure to 11-MUA, featuring terminal carboxyl and thiol moieties, but with a much shorter carbon chain linking them. Sedki *et al.* functionalized glassy carbon electrodes by coating them with 3-MPA-functionalized gold

nanoparticles which were then activated with EDC/NHS and conjugated to M13 phages, forming an electrochemical impedance-based bacterial biosensor which achieved an impressive LOD of just 14 CFU/mL [158]. Han *et al.* used a SAM of 3-MPA to immobilize fd phage for DPV-based detection of prostate specific antigen at concentrations as low as 3 pg/mL [34].

While 11-MUA and 3-MPA are both examples of monothiols, there also exist dithiol linkers such as dithiobis(succinimidyl propionate), also known as Lomant's reagent, DTSP, or sometimes DSP [90]. DTSP is a homobifunctional NHS ester crosslinking agent, in the form of a homodimer exhibiting both thiol and succinimide moieties, linked by a disulfide bridge allowing SAM-formation on clean gold substrates (**Erreur ! Source du renvoi introuvable.**). Upon introduction to a gold surface, DTSP cleaves at the disulfide bridge, resulting in two thiolate moieties bonded to the surface, each bound *via* a carboxyl group to a terminal succinimidyl group that is exposed to the solution. This succinimidyl group is thus available as a binding site for primary amines of a target ligand, as with the EDC/NHS method [166]. Following conjugation, rinsing with ethanolamine blocks further binding of primary amines.

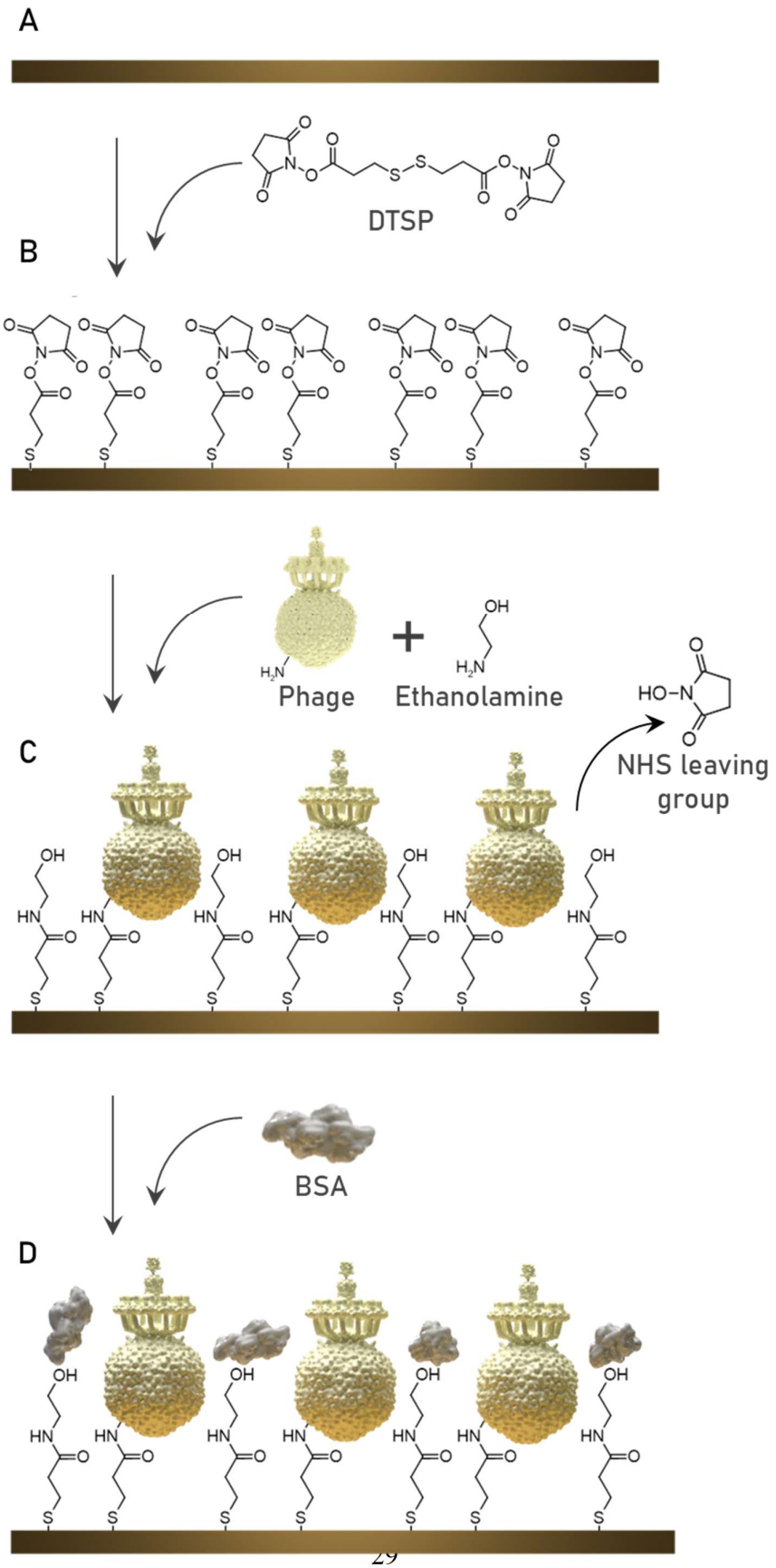
A
DTSP
B
Phage
Ethanolamine
HO-N
NHS leaving group
C
BSA
D

Figure 8. Schematic of a generalized protocol for DTSP functionalization and phage-conjugation, followed by surface blocking with bovine serum albumin (BSA). (A) A bare gold substrate is cleaned by plasma or otherwise. (B) After incubation on the gold surface, DTSP cleaves at the disulfide bridge and forms a monolayer on the substrate. (C) Sequential introduction of the ligand (phage) followed by ethanolamine results in conjugation of the phage to the surface and blocking of the remaining activated carboxyl sites by ethanolamine. (D) The surface is then incubated with BSA in order to reduce non-specific binding. Not to scale. Note that immobilization will not always result in a tail-upward orientation as shown.

Arya *et al.* first proposed DTSP for the immobilization of phages in 2011 [166]. By 2012, Naidoo *et al.* were able to leverage DTSP to reach an incredible surface density of 199±2 phages/μm^2. However, they found a threshold surface coverage of 18.9±0.8 phages/μm^2, beyond which higher phage density led to a reduction in total bacterial capture [58]. This result was influential and is widely cited in the phage immobilization literature, with many subsequent papers quoting their results with reference to this "jamming effect". Notable subsequent research by Richter *et al.* combined DTSP with application of an alternating electric field during immobilization to "bake in" a tail-upward orientation of T4 phage as a surface density of 13.64 phages/μm^2 [167]. DTSP has also been used to immobilize T4 [166] and P22 [58] bacteriophages on gold surfaces for detection of *E. coli* [58,166,167] and *Salmonella* Typhimurium [58].

4-amino-thiophenol (4-ATP) is an aromatic thiol featuring a primary amine moiety (**Erreur ! Source du renvoi introuvable.**). 4-ATP has been used to immobilize T4 phages on nano-sculptured thin films of silver for detection of *E. coli* by surface-enhanced Raman scattering (SERS) with an LOD of 1.5×10^2 CFU/mL [168]. In this method, glutaraldehyde is used to cross-link primary amines present both on 4-ATP and on the phage capsid.

In a different approach, Rippa *et al.* deposited and diazotized an SAM of 4-ATP on plasmonic quasicrystals of gold [70]. The diazonium moieties were then available for covalent linkage to the histidyl groups of bacteriophage *Tbilisi*. This SERS-based sensor was capable of detecting femtomolar concentration of immobilized phages, but this work did not extend the method for the detection of an analyte. The choice of plasmonic quasicrystals is motivated, among other considerations, by the higher spatial density and larger field strengths of electromagnetic hot-spots, enhancing SPR and SERS effect and thus the sensitivity of the sensor.

Horikawa *et al.* made a comparison between carboxy-terminated, aldehyde-terminated, and methyl-terminated SAMs for immobilization of filamentous fd phages on the gold surface of magnetoelastic sensors [169]. The resultant phage surface coverage was found to be 46.8%, 49.4%, 4.2%, and 5.2% for bare gold, carboxy-, aldehyde-, and methyl-functionalized resonators, respectively. This paper is notable in its findings that physisorption can be as performant as activated carboxyl-mediated immobilization. The authors propose that the aldehyde and methyl surface treatments were so effective in *reducing* phage adsorption that they may be employed as "anti-phage surfaces", which may provide the possibility of negative surface patterning using these surface treatments as a form of negative resist.

Glutaraldehyde

Glutaraldehyde – a symmetrical, bireactive compound with an aldehyde (−CHO) at each end – is frequently used as a cross-linker (**Erreur ! Source du renvoi introuvable.**). The aldehydes can react with an amine to form an imine – a group with a carbon-nitrogen double bond. In this way, glutaraldehyde cross-links amine groups.

Singh *et al.* immobilized L-cysteine and cysteamine on a gold surface *via* their thiol side-chains, and then cross-linked the amine groups of these immobilized species to those exposed on the capsids of wild type T4 phages. The surfaces were then used for the specific capture of *E. coli* EC12 bacteria, as confirmed by scanning electron microscopy (SEM) and X-ray

photoelectron spectroscopy (XPS) [165]. Compared to simple physisorption, they found a 37-fold improvement of phage immobilization at 18±0.15 phages/μm^2, resulting in a 9-fold higher bacterial capture density of 11.9±0.2 bacteria/100μm^2.

Similarly, He *et al.* coated interdigitated gold electrodes with L-cysteine before crosslinking *via* glutaraldehyde to phage D29, to form an impedimetric sensor of *Mycobacterium smegmatis* and *Mycobacterium tuberculosis* [66].

Richter *et al.* further developed this technique to achieve some of the most convincing evidence for oriented immobilization in the literature. By combining an alternating electric field with glutaraldehyde cross-linking to a gold substrate, the authors leveraged the permanent dipole moment of T4 phages to yield a tail-outward orientation that is "baked in" at the time of immobilization [167]. This allowed the authors to achieve immobilized phage densities on gold of 13.64 phage/μm^2 and 17.32 phage/μm^2 for oriented and non-oriented layers, respectively. The same paper demonstrated a very low LOD of 10^2 CFU/mL *E. coli* without any pre-enrichment step.

Immobilization chemistries featuring glutaraldehyde have been demonstrated for phage-functionalization of silica-based materials such as optical fibers [141], silicon nitride [37], and silica nanoparticles [62] for the purposes of biodetection and biocontrol, respectively. A widely-cited paper demonstrated glutaraldehyde cross-linking of T4 phages onto long-period gratings etched into optical fiber for the specific detection of *E. coli* with an LOD of 10^3 CFU/mL [141].

Glutaraldehyde has also been used for the creation of bacteriophage-functionalized metal-organic frameworks (MOFs). MOFs – coordination networks with organic ligands [170] – are characterized by an easily tunable size (nano- to micron scale depending on synthesis parameters) [171] and potentially large surface area [63]. An area of active research is the use of MOFs as fluorescent probes for molecular sensing. Bharwaj *et al.* have used glutaraldehyde to create bacteriophage-functionalized MOFs for the detection of *Staphylococcus arlettae* [63] by

means of fluorescence and *S. aureus* [64] by photoluminescence-based biodetection. Very low LODs were demonstrated of 10^2 CFU/mL for *S. arlettae* and 31 CFU/mL for *S. aureus*.

In a different approach, Yoo *et al.* demonstrated a variation of glutaraldehyde cross-linking whereby a solution of M13 phages was simply drop cast and allowed to dry on a cysteamine monolayer on gold, then exposed to a glutaraldehyde vapor for three days in order to cross-link the phages [147]. This allowed the study of mouse fibroblast proliferation under the influence of growth factors immobilized to the phages themselves, taking advantage of the phages' self-assembled nanofibrous matrix structure.

In all cases, cross-linking with glutaraldehyde relies on the presence of amine groups on the substrate, which is typically achieved through amino-silanization of the surface, deposition of an intermediate molecule presenting both thiol and amine moieties (e.g. L-cysteine and cysteamine), or through electropolymerisation, for example of polytyramine [172].

Silane-based self-assembled monolayers

For immobilization on silicate-based materials, a preferred method is silanization of the substrate using alkoxysilanes which act as hetero-bifunctional crosslinkers between inorganic mineral surfaces and organic ligands [37,50,51,60,62,67,79,80,95,141,142,144–146,173,174].

Typically, the inorganic surface is treated with a strong oxidizer (e.g. piranha solution or aqua regia) or oxygen plasma to form surface silanol groups which feature dangling hydroxyl (-OH) groups. These hydroxyl groups will then condensate with the three alkoxy groups on the alkoxysilane*, leaving a primary amine bonded to the surface. One can then perform standard amine-immobilization chemistry with these amines, as above (Figure 3).

* In reality the hydroxy groups will replace between zero and three alkoxy groups in each alkoxysilane. One can even have the terminal amino ($-NH_2$) group bond with the surface hydroxyl group [257]. Recent research supports a model wherein the silane monolayer is in fact

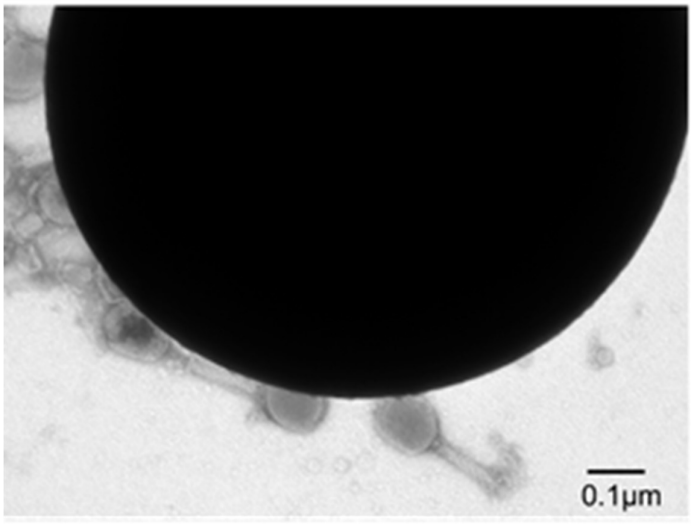

Figure 9. Transmission electron micrograph of T4 myovirus covalently immobilized on APTES-functionalized 1 µm diameter silica particles [146]. Reproduced with the permission.

The most popular alkoxysilanes for phage immobilization are (3-aminopropyl)triethoxysilane (APTES or APTS) and (3-aminopropyl)trimethoxysilane (APTMS) [90]. Alkoxysilanes can be used either for electrostatic or covalent immobilization of proteinaceous ligands (**Figure 3**). In covalent bonding, the amine groups of the alkoxysilane react with aldehyde either present on a cross-linker molecule such as glutaraldehyde [37,141,142], or on the phage itself after enzymatic modification to yield a reactive aldehyde as demonstrated by Kwak *et al*. [79]. Alternatively, the phage's endogenous carboxyl groups can be activated by EDC/NHS to facilitate amide bonding with the substrate aminosilane layer [67,144,146] (Figure 3), although – as explained above – activation of the phage by EDC/NHS can be detrimental to phage infectivity [50,95,146].

highly cross-linked *via* these remaining alkoxy groups, with only occasional bonds to the surface [258].

In contrast, electrostatic binding with alkoxysilanes relies on the differing isoelectric points of the ligand and the silanized surface, as discussed later in this work in the 'Electrostatic binding' subsection.

Hosseinidoust *et al.* demonstrated covalent immobilization of a variety of phage families through silanization of glass with APTES, achieving a consistent surface density of 4.5 +/- 0.7 phages/μm^2, as calculated from SEM imagery of the surface [50].

A modification of this strategy is to instead use EDC/NHS to activate the carboxyl groups of the phages themselves, which are then bound to the primary amines of an amino-silanized surface. Handa *et al.* used this technique to functionalize atomic force microscopy probes [144], and in a separate paper achieved 67% surface coverage of phage P22 on glass substrates [67]. However, EDC/NHS activation of the phage carboxyl groups is believed by some researchers to lead to increased blocking of the phage receptors [50,146].

An interesting application of organosilane grafting has been demonstrated for the phage-functionalization of indium tin oxide (ITO) [173,174]. ITO is the most well-known of all transparent conductors – exhibiting exceptional optical transmissivity combined with low electrical resistance [175] – and is seen as a promising material in biosensing technology [176]. In a pair of papers, Liana *et al.* investigate phage adsorption onto bare, amine, methyl, and carboxyl-functionalized planar and particulate ITO [173,174]. These comparative studies found divergent results between planar and particulate ITO, but a consistent drop in performance was observed with the introduction of amine groups on the substrate compared to carboxylic and hydroxyl groups, suggesting the latter as more promising routes for phage immobilization on ITO.

Miscellaneous covalent techniques

Isothiocyanate

Isothiocyanate compounds feature a terminal sulfur atom and a central electrophilic carbon which is susceptible to nucleophilic attack by the primary amines of amino acids, yielding a thiourea linkage with the latter, with no leaving group in the reaction [90]. Isothiocyanates react best at alkaline pH, and it has been demonstrated that by carefully controlling pH during conjugation, it is possible to modify only the N-terminal α-amines while leaving side-chain amines unmodified [177]. Zhang *et al.* functionalized isothiocyanate-terminated magnetic beads for the purposes of phagomagnetic separation in an enzymatic assay for the presence of *E. coli* O157:H7, with a comparatively poor LOD of 4.9×10^4 CFU/mL [104].

Electro-deposited polytyramine

Niyomdecha *et al.* demonstrated immobilization of M13 phages using glutaraldehyde cross-linking between primary amines on the phage capsid and the activated primary amine groups of an electrodeposited polytyramine layer on a gold surface, for use as a capacitive biosensor for *Salmonella* [172]. Rinsing with ethanolamine blocks any unoccupied aldehyde groups and reduces non-specific binding following functionalization. The use of electrodeposited polytyramine for immobilization of phages has some precedent, having been demonstrated for enzymes [178], myoglobin [179], and oligonucleotides [180].

However, a potential complication in the use of electropolymerisation for phage functionalization may lie in the necessity of an electric field during immobilization. Richter *et al.* have already demonstrated that application of an electric field during immobilization can influence the final orientation of the phages [78,167]. It is the opinion of the author that this effect may prove detrimental to phage infectivity since an anodic substrate may attract the positively charged phage tail fibers and result in head-outward immobilization.

Tosyl

A toluenesulfonyl (tosyl) is a molecule or group with the formula $CH_3C_6H_4SO_2$ (**Erreur ! Source du renvoi introuvable.**). Tosyl chloride is used to activate hydroxyl groups on a substrate in nonaqueous conditions, creating a tosyl ester. When subsequently placed in aqueous conditions, this ester can then react with sulfhydryls, amines, and hydroxyls to form thioether, secondary amine, and ether linkages, respectively. This allows the immobilization of proteins either through the primary amino group or sulfhydryl side-groups [90,181]. The tosyl group is an effective "leaving group", since it is easily released during the conjugation reaction.

Dynabeads M-280 from Invitrogen are tosyl-activated, 2.8 µm diameter polystyrene beads which feature superparamagnetic inclusions and an outer polyurethane coating. They have been demonstrated to be capable of immobilizing P22 *Podoviridae* for the purposes of phagomagnetic separation and detection of *Salmonella* in two papers [68,69]. Such methods were capable of reaching an impressive LOD of only 3 CFU/mL [68] and as low as 0.06 CFU/mL if combined with a pre-enrichment step [69].

Non-covalent & physical methods

Physisorption

Many papers make use of simple "physisorption" which is generally not considered to involve covalent bonding between the phage and the substrate. The simplicity of these methods is appealing since the functionalization operation can be as trivial as cleaning the substrate and then incubating it with a purified phage suspension [35,143,182–204]. However, physisorption yields a functionalization that is more variable and less robust since the physisorbed phage can detach following changes in ionic strength, temperature, pH, or even high fluid velocities at the substrate surface [92].

There appears to be no clear consensus on the physical mechanism behind physisorption, with many papers proposing several factors which could play a role such as van der Waals

forces, hydrophobic bonding, H^+ bonding, or weak covalent bonding between cysteine residues and gold surfaces [185,205].

Several papers present physisorption and electrostatic attachment as synonymous, attributing the binding to charge differences: positively charged surfaces attracting negatively charged phages [146]. Following this convention, electrostatic binding will be presented here as a subcategory of physisorption.

Electrostatic binding

The basis of electrostatic immobilization is to take advantage of the relative charges of the surface and of the ligand to be immobilized. Most phages have a net negative charge and permanent dipole moment at neutral pH [39,77,78]. In the case of T4 and T7 phages, the head acquires a negative charge above a pH of 4 and is thought to be responsible for the overall negative charge of the virion despite the positive charge on the tail fibers [39,94].

Electrostatic immobilization can be acheived by varying the pH of the aqueous environment to control the surface charge of the substrate and/or phage in order to produce favorable conditions for attraction between the two. If there exists a pH at which the surface species present a positive charge while the phage – or even just the phage head – presents a negative charge (i.e. if the isoelectric point of the surface is higher than that of the phage), then the pH of the solution can be tuned to facilitate electrostatic attraction of phage particles [93]. Alternatively, chemical modification of the substrate can also result in a positive surface charge, facilitating phage immobilization without recourse to tuning the pH.

Alkoxysilanes such as APTES and APTMS will present NH_3^+ groups – and thus a positive charge on the substrate – from a neutral pH [62] to as high as 9 [206,207]. This surface charge can then be used to electrostatically attract phages that display a negative charge at the same pH (Figure 13) [145], and indeed achieve oriented immobilization. Such oriented electrostatic

immobilization has been confirmed by transmission electron microscopy (TEM) microscopy (**Erreur ! Source du renvoi introuvable.**) [60].

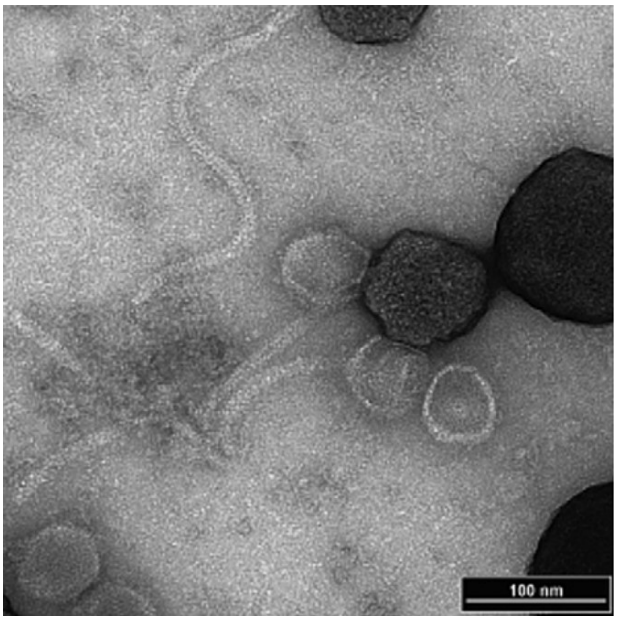

Figure 10. Transmission electron micrograph of the siphovirus VB_SenS-AG11 bacteriophages (active against *Salmonella)* electrostatically physisorbed by their heads on cationic, APTES-modified silica particles [60]. Reproduced with the permission.

Cademartiri *et al.* found a linear correlation between infective phage binding and the magnitude of positive surface charge resulting from chemical modification of silica beads (Figure 13) [60].

In 2011, Anany *et al.* developed a method for electrostatic immobilization of anti- *Listeria monocytogenes* phages on cellulose membranes that had been chemically modified with the cationic polymer polyvinylamine to present a positive surface charge (Figure 3) [39]. In 2016 Lone *et al.* employed this technique with anti-*E. coli* O104:H4 phages on alginate beads to produce a bioactive packaging prototype [20].

Similarly, Zhou *et al.* used polyethylenimine (PEI) to impart a positive surface charge to a carbon nanotube (CNT)-modified glassy carbon electrode, for the specific detection of *E. Coli* B [54]. In this case T2 phages were electrostatically oriented by the positive surface charge, while immobilization was achieved through PBSE-mediated conjugation (see π - π stacking). Vonasek *et al.* similarly used PEI to electrostatically immobilize T7 phages on electrospun cellulose microfibers for biocontrol in the context of food packaging and biomedical applications [42]. More recently, Farooq *et al.* used PEI to phage functionalize CNT-modified bacterial cellulose for the electrochemical detection of *S. aureus* [112].

Poly(diallyl dimethylammonium chloride) or polyDADMAC is a cationic polyelectrolyte that has been used to electrostatically bind T4 phages on paper [134], M13 phages on glass [208], and S13' phages on gold [71]; in the latter case for the specific detection of *S. aureus*.

An alternative strategy to impart a positive charge to the substrate was demonstrated by Richter et al. wherein a positive potential was applied to a gold substrate, yielding an oriented physisorbed layer of T4 phages with a density of 14.3 PFU/mL (Figure 11) [78].

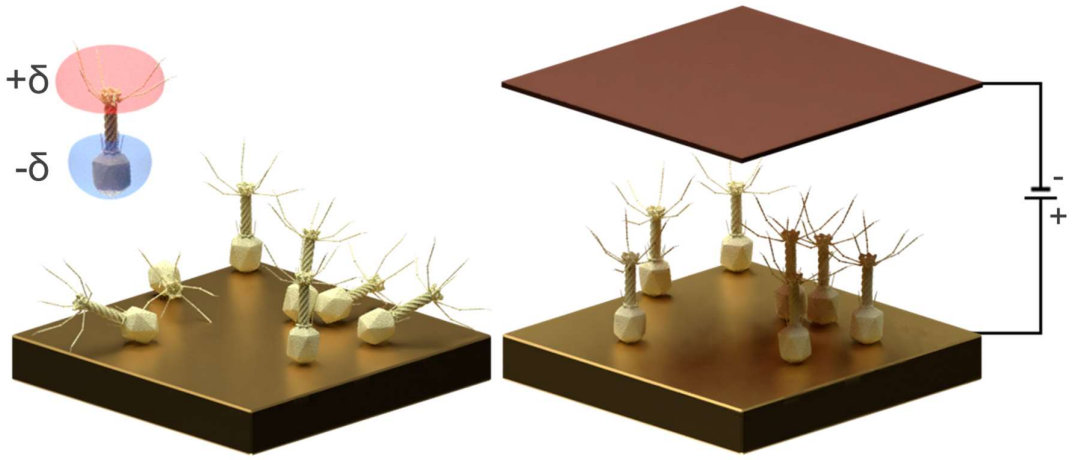

Figure 11. Due to the inherent dipole moment of T4 phage particles, an externally-applied electric field orients the phages such that their tail fibers point outward from the substrate. Such

an orientation is considered essential for increasing the immobilized phages' infectivity and host capture efficiency. Adapted from Richter et al. [78].

In the same paper, Richter *et al.* proposed a model of orientation of bacteriophages based on electrical screening of the substrate surface due to the formation of an electric double layer [78]. Briefly, the Debye length (denoted κ^{-1}) refers to the physical distance in an electrolyte solution over which an electrical potential will decrease by a factor of 1/e. This length is proportional to the inverse square root of the ionic strength of the solution, since it is the mobile charge carriers of the solution which form an electric double layer, screening the electric field that results from the substrate surface potential. Richter *et al.* proposed that when κ^{-1} is larger than the phage, they will align along electric field lines; whereas when κ^{-1} is smaller, the phage orientation occurs instead due to electrostatic interactions (**Figure 12**).

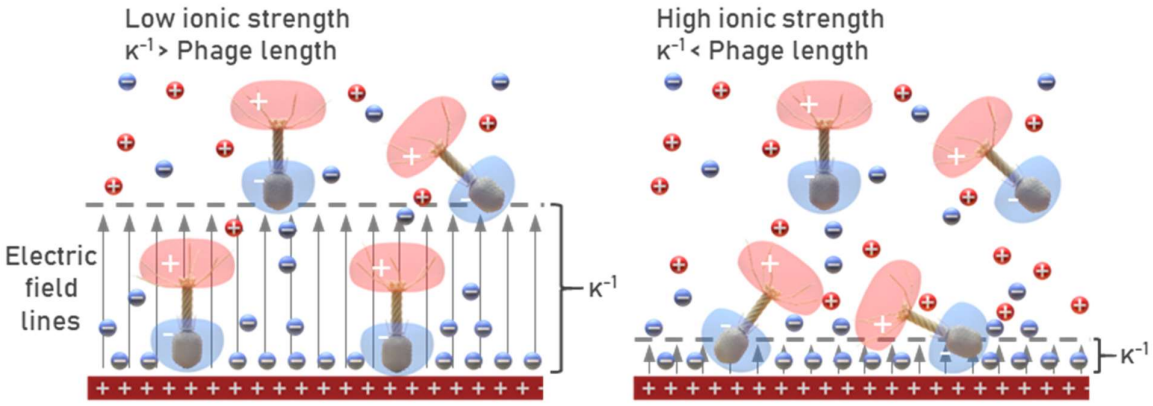

Figure 12. The electrostatic binding model proposed by Richter et al. [78]. At low ionic strength, fewer charge carriers are available to screen the surface charge. This leads to a larger Debye length of the same scale as a phage particle and thus oriented immobilization. Conversely, at high ionic strength the surface charge is more effectively screened, leading to a Debye length

smaller than the phage. In the latter case, the phages are still attracted to the substrate due to their overall negative charge, but the immobilization is not appreciably oriented.

The ionic strength also influences the stability of the phage solution and aggregation of the phages[73–75]. Archer and Liu reported that physisorbed T4 phages are susceptible to aggregation in high ionic strength solutions (>100mM) or low pH [93]. However, the same study observed phage immobilization even on negatively charged surfaces, indicating that interactions other than purely electrostatic attraction might be at play. Confusingly, a different paper found that a relatively high ionic strength of 420 mM NaCl gave the best surface coverage for physisorption of filamentous phage fd [26]. These seemingly contradictory results suggest that phage morphology may play a role in immobilization and aggregative effects of different ionic strengths.

Whatever the mechanism, while simple physisorption of phages has been demonstrated to enable bacterial capture [198], it is not sufficient to prevent phages from migrating on the substrate while in storage or during binding assays [166]. Covalent attachment of phages offers a much stronger bond than simple physisorption, yielding surface functionalization more resistant to phage detachment and resulting in a higher phage surface density [92].

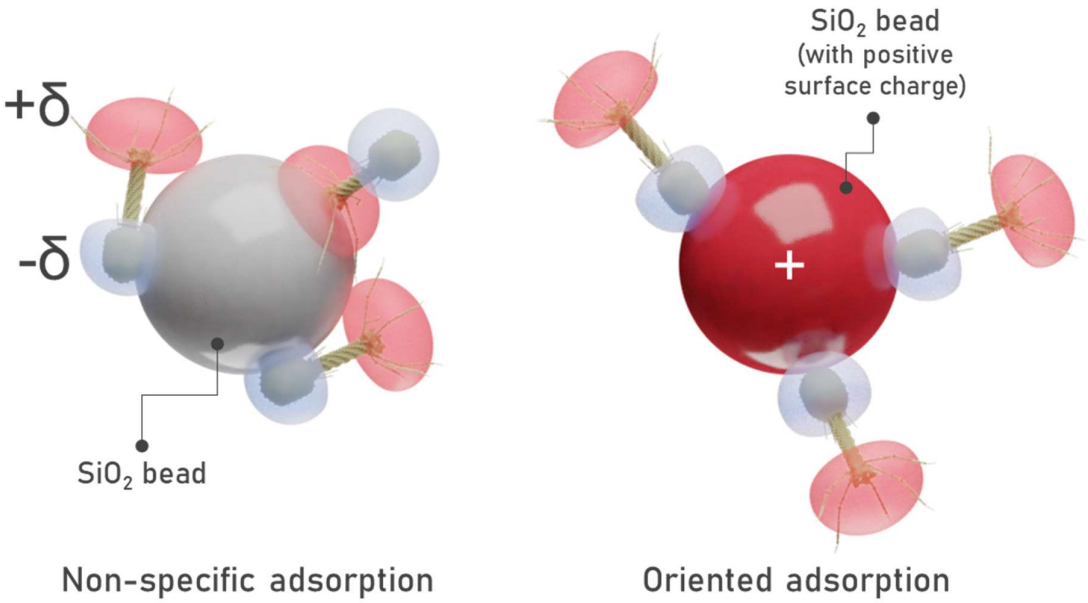

Figure 13. Left: A neutral surface charge leads to non-oriented adsorption of phages on silica particles. Right: A polymer layer (e.g. X or X) is protonated as neutral pH, electrostatically binding the phage head, leading to oriented immobilization. Adapted from Immobilization of bacteriophages on modified silica particles [60].

π - π stacking

Zhou *et al.* demonstrated a novel strategy for immobilization of T2 phages on multiwall carbon nanotubes (CNT) on glassy carbon electrodes [54]. First, the CNT are functionalized with polyethylenimine (PEI), which introduces a positive charge to the CNT surface, facilitating tail-outward phage orientation. A hetero-bifunctional molecular tethering agent, 1-pyrenebutanoic acid succinimidyl ester (PBSE) (**Erreur ! Source du renvoi introuvable.**), is then used to link the phages to the CNT. PBSE features four aromatic rings which interact with CNT sidewalls through π-π stacking [209], and a succinimidyl group which facilitates amide

bonding [54]. Application of a positive potential of +0.5 V *vs.* Ag/AgCl further facilitates oriented phage immobilization.

Kim *et al.* leveraged π- π stacking between the imidazole rings of recombinantly expressed histidine tags on M13 phages (see Genetic modification below) to achieve a nematically aligned unidirectional bundle structure on the surface of an SPR biosensor [210]. The resultant colorimetric sensor was capable of detecting streptavidin – a surrogate analyte in this work – down to femtomolar concentrations.

Biotinylation

The biotin-avidin bond is one of the strongest non-covalent bonds in nature, with a dissociation constant as low as 10^{-15} M [90]. The binding is also extremely stable, exhibiting high resistance to breakdown by extremes of pH, temperature, or the presence of denaturants or detergents [211]. Avidin is a tetrameric protein, binding up to four biotin molecules simultaneously. These qualities have made the avidin-biotin interaction particularly useful and widespread in bioconjugation chemistry, and it is frequently used to cross-link biotinylated ligands to one another as well as to substrates.

While avidin is a component of egg-whites, streptavidin is a similar biotin-binding protein of bacterial origin which exhibits superior properties to avidin. The main disadvantage of avidin is its high isoelectric point of 10, presenting a positive charge at neutral pH making it susceptible to non-specific binding to negatively charged components other than biotin, such as cell surfaces for example [90]. This problem is circumvented by instead using streptavidin which has a pI of 5-6, which greatly reduces nonspecific binding due to ionic interactions with non-analyte molecules. For this reason, streptavidin has largely replaced avidin in most (but not all) conjugation protocols.

The use of streptavidin-biotin heterobifunctional cross-linkers has been demonstrated for phage immobilization using sulfo-NHS-ss-biotin and sulfo-NHS-biotin (**Erreur ! Source du**

renvoi introuvable.). These molecules can participate in an amide bond with the phage capsid – facilitated by a terminal succinimidyl group on one end – tagging the phage with a terminal biotin group which can bind to a streptavidin-functionalized surface. Such covalent biotinylation of the phage was used by Sun *et al.* to immobilize of SJ2 phages on streptavidin-capped magnetic beads to create a biosorbent for the specific capture of *Salmonella* Enteritidis [105].

Sulfo-NHS-ss-biotin differs from sulfo-NHS-biotin in that the former features a spacer to mitigate steric hindrance effects, and a cleavable disulfide bon. This latter molecule has been used by Fernandes *et al.* to biotinylate a gold substrate, which was then crosslinked *via* streptavidin to genetically biotinylated T4 phages [61].

Despite the above successes seen with covalent biotinylation, all immobilization mediated by streptavidin-biotin since 2001 has instead made use of genetic biotinylation (see Genetic biotinylation)

Genetic modification

Genetic engineering can be used either as an alternative immobilization strategy in itself or to enhance the above chemi- and physisorption methods. A popular technique in the literature is site-directed mutagenesis, wherein a foreign coding sequence is spliced in-frame into bacteriophage capsid protein genes. This allows the targeted expression of "guest" peptides which are fused to the coat protein and which exhibit an affinity for a given substrate, or onto which a moiety can be conjugated [212]. Since filamentous phages in the Ff class (*e.g.* fd and M13) typically have several thousand identical, helically-tessellated copies of the pVIII coat protein [213], they are the most frequent examples of genetic modification for the purpose of immobilization [38,79,80,84–87,214], although examples of such modification of T4 [81,83,88,89] and T7 [215] phages are also found.

The popularity of this technique and of the filamentous phages M13 and fd, stems from the success of phage display-based selection and the closely related technique of biopanning [212]. While the 50-residue pVIII protein of filamentous phages are typically modified [212–214] (but also pIII [79]), in the case of phages T4 and T7 it is rather Soc and Hoc proteins of the phage head that are targeted for modification [81,216,217].

A drawback of genetic modification is that the expression of peptides, especially of large size, can interfere with phage assembly and hence its physical and infective properties [93]. Genetic modification can also prove laborious, time-consuming and expensive [88], and for these reasons genetic modification techniques are somewhat marginal compared to physisorption and covalent techniques.

Genetic biotinylation

Several papers demonstrate phage immobilization facilitated by streptavidin/biotin, wherein the biotinylation of the target phages is a result of recombinant expression of a biotin tag rather than the result of chemical modification.

In 2006, Edgar *et al.* genetically modified T7 bacteriophage to exhibit a small peptide on the major capsid protein, which is then post-translationally biotinylated at a specific lysine residue by the host bacterium's biotin-ligase protein during phage assembly [82]. This allows conjugation to streptavidin-coated quantum dots, resulting in a biosensor with a LOD of as low as 10 bacterial cells/mL.

Gervais et. al demonstrated an impedance-based biosensor by immobilizing T4 phages on streptavidin-coated gold at a density of 4.4 phage/μm^2, with tail-outward orientation enabled by the strategic genetic biotinylation of only the head capsid protein [88]. Phages were found to retain their infectivity, burst size and latent period compared to the wild-type. Attractive features of this method are the retention of infective activity after biotinylation, and the

localization of the modified tagged peptide exclusively on the phage head, leading to a 15-fold increase in phage attachment to the gold surface.

Wang *et al.* immobilized a genetically biotinylated T4 phage to streptavidin-terminated magnetic beads, calculating that each bead was on average conjugated to 248 ± 15 phages per 2.8 μm-diameter bead after 12 hours of incubation [48].

Formylglycine

Kwak *et al.* used genetic engineering to introduce a cysteine-containing peptide motif to the pIII coat protein of fd phage, which was converted to formylglycine by formylglycine-generating enzyme (FGE) (**Figure 14**). This yields a reactive aldehyde (-CHO) group that is then available for immobilization chemistry, for example to form a Schiff base with primary amines on a silanized substrate surface [79]. As with genetic biotinylation, an advantage of this technique is that the formylglycine modification is site-specific and can be targeted to exclusively modify the pIII coat protein which is displayed at one extremity of filamentous phage fd. This allows the pVIII coat protein to be preferentially presented to the solution, since the phage is immobilized in an upright orientation [79]. This method has been further developed to enable surface patterning of filamentous phages with 200μm spot size as a template for organic and inorganic materials [80].

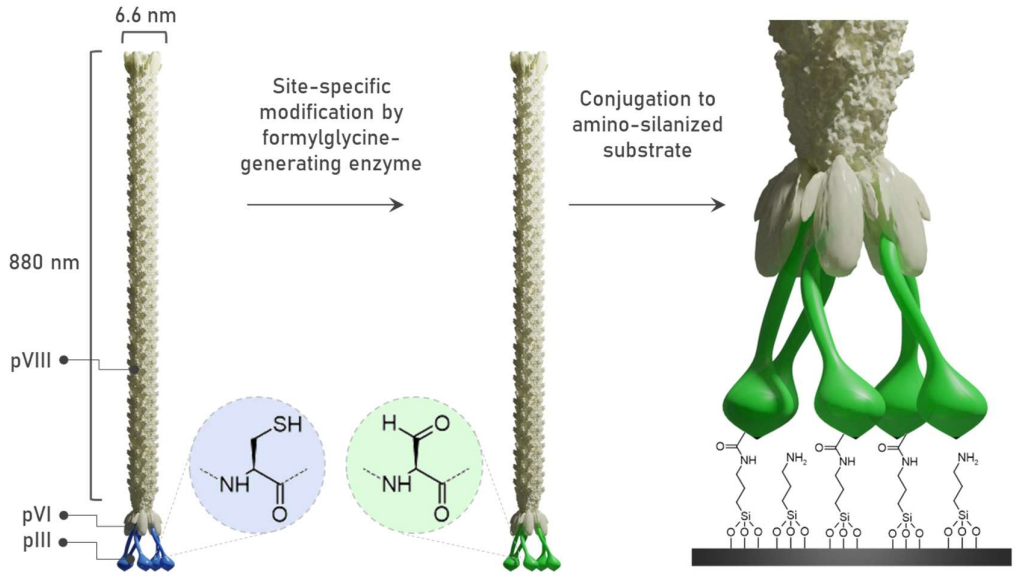

Figure 14. Recombinant expression of a specific peptide motif exclusively on the pIII coat protein of an M13 phage enables enzymatic modification of cysteine residues to yield formylglycine and its associated carboxyl side-chains. Formylglycine can then undergo amide bonding with an amino-silanized surface. This oriented immobilization yields a high density of pVIII coat proteins displayed at the surface. Adapted from Kwak et al. [79]. Not to scale

Carbohydrate-binding modules

Carbohydrate-binding modules, also known as cellulose-binding modules (CBM), are short protein domains normally found within carbohydrate-active enzymes, that exhibit high affinity for a given substrate. Fusion of phage capsid and CBM genes results in expression of recombinant CBM on the phage capsid. This allows oriented immobilization of the phages on cellulosic substrates such as paper or cellulose beads. Tolba *et al.* demonstrated such modification of T4 phages which, when combined with polymerase chain reaction (PCR), resulted in an assay with a LOD of 800 cells/mL [83]. A similar method allowed immobilization of T4 phages on microcrystalline cellulose beads [89].

Polymer and other binding domains

Short peptides have also been identified that exhibit highly specific affinities against a range of materials. Sawada *et al.* have demonstrated the immobilization of M13 phages on isotactic poly(methyl methacrylate) (it-PMMA) *via* an (it-PMMA)-binding terminal peptide expressed on the pIII coat protein [86]. This result is intriguing since it demonstrates a potentially fruitful avenue for further research. As the same authors point out in another paper [128], similar peptides have been identified that exhibit binding specificity towards targets as varied as metals (silver [218], titanium [219], platinum [220]), metal oxides (iron oxide [221], magnetite [222]), silica [223], semi-conductors [224,225], carbon allotropes (nanotubes [113,114], nanohorns [115], and fullerenes [116]), and various polymers (polystyrene and polyvinyl chloride [123], nano-imprinted methacrylate polymer [124], chlorine-doped polypyrrole [125], PMMA [126], syndiotactic PMMA [127], syndiotactic polystyrene [129]). Thus, the successful demonstration of one of these peptides as a strategy for M13 phage immobilization, presents a compelling case for the use of substrate-specific peptides as a general phage grafting strategy.

Click chemistry

An alterative class of reactions, thusfar seldom exploited for phage immobilization, is click chemistry. Click reactions proceeds quickly at room temperature, producing strongly stabalized products and either no byproducts or only water as a byproduct [226]. Furthermore, click reactions are highly tolerant to water and in some cases even accelrated in acqueous solutions.

Click chemistry is therefore a popular choice for making carbon−heteroatom−carbon bonds in aqueous solutions in a wide variety of chemical and biological applications in drug discovery, chemical biology, and proteomic applications[227].

An elegant method of phage capsid modification was recently demonstrated by Zurier *et al.* wherein a genetically engineered variant of T4 known as NRGp17 was decorated with a self-assembled cage of 870 small outer capsid (soc) proteins engineered with unnatural alkynylated amino acids [81]. These alkynes enable oriented immobilization of the phage heads on azide-

terminated magnetic beads[228,229] (TurboBeads, Zurich, SUI) *via* click chemistry, creating a biosorbent that can concentrate target bacteria from a very low initial concentration. NRGp17 causes expression of a nanoluciferase (Nluc) reporter enzyme fused to a cellulose-binding module (CBM) [230]. The bioluminescent activity of Nluc serves to transduce the presence of their host *E. coli* into a luminescence signal, while the fused CBM enables immobilization and concentration of the reporter enzyme on a nitrocellulose membrane to improve sensitivity. This assay presents an impressive LOD of <10 CFU *E. coli* in 100 mL of tap water

Optimization of the immobilized bacteriophage layer

In discussing the targeted immobilization of bacteriophage particles, we must also confront the issue of immobilization of undesirabe interferents which will have a significant impact on the quality of the immobilized layer both during preparation as well as in its final application, be it an immoblized interaction layer on a biosensor transducer or a biosorbent for bio-active food packaging. The purification protocol immediately preceding conjugation can have a large effect on the success, homogeneity, and overall quality of the immobilized phage layer [231], and is thus of critical importance and an integral part of any phage immobilizaiton protocol. In addition, following immobilization, an additional blocking step

Phage propagation and purification methods

The process of phage propogation (also referred to as phage amplification) necessarily generates large amounts of bacterial debris (e.g. DNA, peptidoglycan, lipopolsaccharide[232] etc.) which must be separated from the phage particles, since many immobilization techniques will equally – if not preferentially – bind these contaminants to the surface along with the phages of interest [231]. Furthermore, storage of phages in the presence of certain cellular debris can trigger premature ejection of phage genetic material[233–235], potentially rendering the phage

inactive. For these reasons, immobilization of phages requires first the isolation of a high-purity, high-titer phage suspension. Typical phage concentrations used for immobilizations range between 10^{10} and 10^{12} plaque-forming units per milliliter (PFU/mL), although some success has been seen with lower infective titers. The lower phage concentrations in this range tend to be biased towards myoviruses such as T4 and podoviruses such as P22, while the higher concentrations are almost exclusively seen in papers using the filamentous phages M13 and fd. The topic of phage purification necessitates a review in its own right, but the main methods will be outlined briefly here.

Dead-end filtration through 0.45µm and 0.2µm pore-size membranes is typically employed[†] – along with differential centrifugation[236] – as an initial first purification step to rid phage suspensions of the largest bacterial debris and leftover culture medium constituents. Differential centrifugation can be used to pellet contaminants brought out of solution using chemical precipitation (e.g. using PEG and/or NaCl)[236,237]. It is carried out at relatively low centrifugal force of ~5000g, in larger volumes (between 1 and 1000 mL), and in simple centrifugation media (typically simply the phage buffer) compared to ultracentrifugation.

In contrast, in density gradient ultracentrifugation (DGU) the components of a sample are fractionated based on their buoyant density. DGU necessitates centrifugation at very high acceleration (>70-80,000g for 4-6 hours is typical [238]), smaller volumes (~6 mL), and the careful selection and preparation of centrifugation media such as CsCl or sucrose[239]. DGU is performant enough to permit the separation of terminated viruses from empty ghost particles [240]. Potential drawbacks of DGU include the high cost of ultracentrifuge equipment, the potential for phage aggregation due to high ionic strength of centrifugation media [93], and the difficulty in harvesting the final product. DGU purification has also been found to lose un-

[†] Unfortunately, such filtration can immediately reduce the infectious titer by a factor of 10.

tailed phages [241] and can yield solutions contaminated by – for example – large quantities of host bacterium flagella fragments [58,67]. Despite these disadvantages, the use of DGU has become an established technique for the isolation and purification of virus particles [78,240,242,243].

PEG precipitation – either employed on its own or in conjunction with DGU [239] – is another popular method for concentration and purification of viruses [237,244–247]. PEG, a polymerized form of ethylene glycol (used at various molecular weights [238] but most often at 6 kD [237,248–250] for phage purification), is employed as a fractional precipitating agent which separates proteins by virtue of their solubility. PEG acts as an inert solvent sponge, reducing water availability. With increasing concentration of PEG the effective protein concentration is increased until solubility is exceeded and precipitation occurs. Thus, larger proteins will precipitate at lower concentrations of PEG and can be separated with differential centrifugation [251,252]. PEG precipitation is considered by some experts to be "*a crude and non-specific technique*" [252].

An increasingly popular suite of purification methods involve various forms of chromatography [253]. Boratynski *et al.* used size-exclusion chromatography (SEC) to produce phage suspensions with endotoxin levels low enough to permit intravenous administration [232]. SEC can also be used as part of a short-turnaround purification protocol, used by Naidoo *et al.* to avoid CsCl DGU and PEG precipitation, giving a total process time of only 3 hours [58]. Recombinant affinity tags expressed on T4 capsids have been used by Ceglarek *et al.* to facilitate affinity chromatography [253]. While elegant, this method relies on genetic modification of each host bacterial strain which may be infeasible for some researchers and applications. Adriaenssens *et al.* demonstrated anion-exchange chromatography (AEC) for the purification of eleven morphologically distinct phages. The authors concluded that although this method presents easier scalability for industrial-scale throughput compared to CsCl DGU, it requires more laborious optimization of purification at the outset [254].

Surface blocking

Due to their inherent charge – and often their hydrophobicity – proteins have a tendency to spontaneously adhere to surfaces in an aqueous environment. Extremely pure reagents and clean surfaces are a *sine qua non* for well-controlled and reproducible fabrication of biosensors and bioactive surfaces. However, a clean surface is also susceptible to non-specific binding of proteins in aqueous solutions. Non-specific binding of interferents can hinder specific biofunctionalization, obscure the transduction of specific interaction events and decrease the signal-to-noise ratio (SNR) in the case of biosensors, and generally compromise reproducibility, even when phage infectivity is not impacted [51].

For this reason, a common unit operation in phage-functionalization is to follow conjugation with a blocking step, whereby the surface is flooded with an amphiphilic biological species (*e.g.* casein, salmon sperm DNA, bovine serum albumin (BSA)) or synthetic polymer (*e.g.* PEG) that will occupy non-functionalized sites on the surface without impeding the sensitivity of the functionalized sites. In this way, the non-specific binding of proteins – and other components of the sample – is reduced, while specific reactions with the target analyte are (ideally) unaffected. If a researcher finds that they have trouble with non-specific binding to their phage-functionalized substrate, surface blocking may be an easy first step to boost performance.

PEG and casein have also been investigated for surface blocking and have in some cases been found to be more performant than BSA [192,255]. However, incubating with BSA remains – by a wide margin – the most popular strategy for passivation of biofunctionalized surfaces to reduce or even eliminate non-specific binding, due to its low cost and its ease of storage, preparation, and use.

Conclusion and Remarks

Since the first papers on phage immobilization began to appear at the turn of the century [105,256], a variety of strategies have been developed. By far the most popular single method relies on simple physisorption of phages to the substrate (usually a gold layer) without any chemical modification of the surface, with over one third of papers making use of this method. Although such easily implemented methods may be seductive, physisorbed phages have been shown to easily detach following changes in ionic strength, temperature, and pH at the substrate surface [92], when compared to covalent immobilization.

Covalent conjugation of phages has been demonstrated with a variety of techniques, but three surface modifications in particular dominate: carbodiimide activation of surface carboxyl moieties (i.e. by EDC and NHS); self-assembled monolayer formation of thiol linkers (e.g. 11-MUA, L-cysteine, and DTSP); and amino-silanization (e.g. APTES, APTMS). Together, these chemistries cover half of all the reviewed literature on phage conjugation, and each relies on heterofunctional linkers with at least one terminal functional group (carboxyl (-COOH), or primary amine ($-NH_2$)) that engages in amide bonding with the phage capsid.

Genetic modification-based methods compose a significant minority of the immobilization techniques demonstrated in the literature, being used in about 10% of all papers reviewed. Genetic engineering of phages may prove time-consuming and laborious compared to physisorption or covalent conjugation [88], but may prove practical in some instances. Nevertheless, new avenues for immobilization *via* display of recombinant phage coat proteins may be revealed as a result of the discovery of a plethora of peptides exhibiting binding specificity for a variety of substrates including metals[218–220] and their oxides[221,222], silica [223], semi-conductors [224,225], carbon allotropes [113–116], and several polymers [123–129].

The protocols presented in many papers omit a surface-blocking step to prevent non-specific binding, despite ample evidence in the literature that such a step increases sensitivity and overall performance in the case of biosensors. Surface blocking can be as simple as soaking a

substrate for 30 minutes in a 1% BSA solution, which is unlikely to prove too onerous to be incorporated into any workflow.

Regarding the purity of phage suspensions, since the purification protocol immediately preceding immobilization can have a large effect on the success, homogeneity, and overall quality of the immobilized phage layer, researchers may have difficulty replicating and comparing results in the literature where the purification protocol has not been stated explicitly. Many papers do not clearly describe the purification procedure for the bacteriophages used, particularly when these phages have been obtained from collaborators. Historically, a large impediment to the widespread adoption of phage therapy in the west was the lack of standardization of phage preparation procedures or the criteria for purity and potency [10]. In order to facilitate greater reproducibility of results and comparison between studies, the authors of this review would recommend inclusion of any purification procedures in future papers.

In conclusion, phage-functionalization of substrates presents many promising avenues for the development of both novel bioactive surfaces and specific interaction layers within biosensors. The performance of these phage-functionalized substrates depends on the production of high-purity phage suspensions and careful consideration of the immobilization technique employed. As the pernicious effects of antimicrobial resistance become more apparent in the 21st century, bacteriophages and adjacent research are well-placed to play an increasing role in biomedical, agricultural, and environmental monitoring applications for many years to come.

Schemes

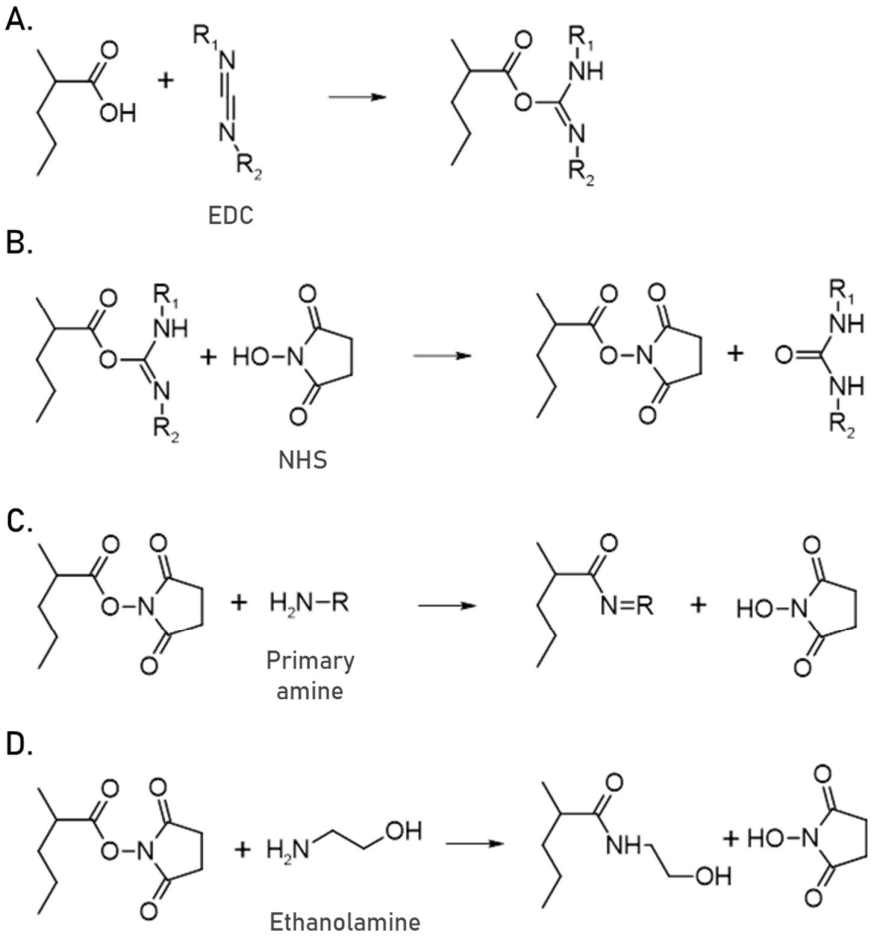

Scheme 1. The chemical reactions involved in EDC/NHS-mediated ligand conjugation. The carboxyl group (−COOH) is activated with EDC/NHS (A. and B.), and then covalently bonds to the primary amine of the target ligand (C.). The remaining NHS esters are blocked using ethanolamine (D.). Here, R represents any arbitrary radical, in this case a bacteriophage. The side group R_1 is $–CH_2CH_3$ and R_2 is $–(CH_2)_3N{+}H(CH_3)_2Cl–$. Adapted from Chapter 3 - Surface plasmon resonance, Phillips and Cheng [152].

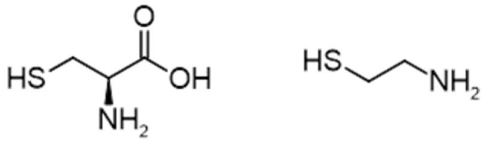

Scheme 2. Structural formulae of the amino acid L-cysteine (left) and cysteamine (right)

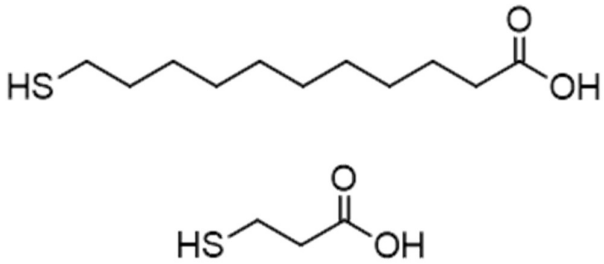

Scheme 3. Structural formulae of 11-mercapto-undecanoic acid (top) and 3-mercaptopropionic acid (bottom).

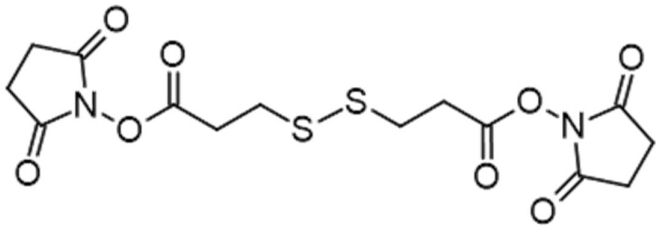

Scheme 4. Structural formula of dithiobis(succinimidyl propionate).

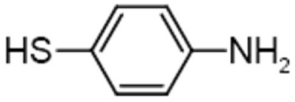

Scheme 5. Structural formula of 4-Aminothiophenol

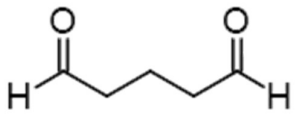

Scheme 6. Structural formula of glutaraldehyde

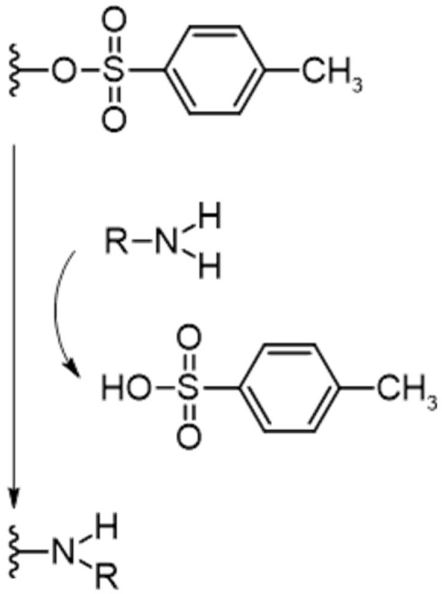

Scheme 7. Immobilization via a primary amine, facilitated by a tosyl leaving group.

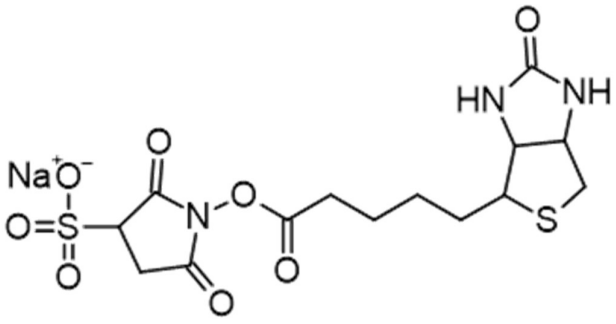

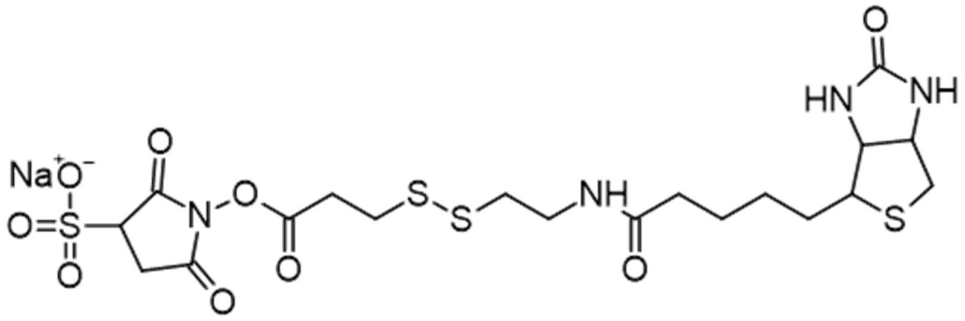

Scheme 8. Structural formulae of and sulfo-NHS-biotin (top) and sulfo-NHS-ss-biotin (bottom).

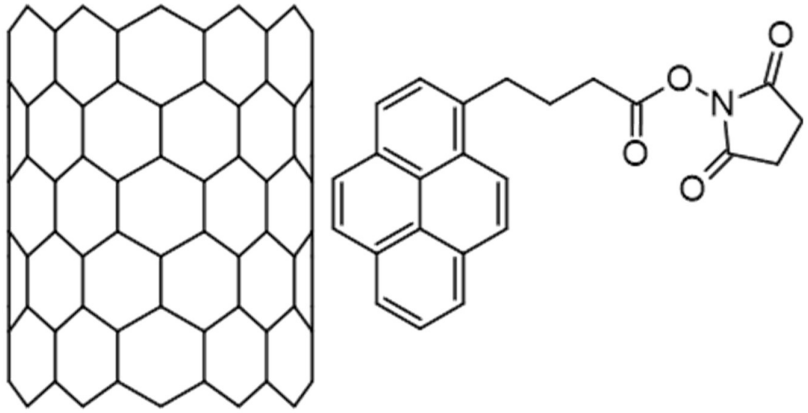

Scheme 9. Structural formula of 1-pyrenebutanoic acid succinimidyl ester (PBSE), illustrating pi-stacking interactions between the pyrene moiety and a carbon nanotube sidewall

Tables

Table 1

Covalent phage immobilization techniques

Table 2

Physisorptive phage immobilization techniques

Table 3

Phage immobilization techniques based on genetic engineering

								Purification										
Substrate	**Paper Category**	**Immobilization Category**	**Surface treatment**	**Phage**	**Phage morphology (geometry)**	**Analyte/Host**	**Detection scheme (if biosensor)**	**Centrifugation**	**Ultracentrifugation**	**Solvent precipitation**	**PEG precipitation**	**Filtration**	**Dialysis**	**Chromatography**	**Limit of detection (if biosensor)**	**Phage surface density**	**Reference**
AFM probe	Fundamental research	Amino-silanization	APTMS + EDC / NHS	P22	Podoviridae (Short-tailed)	N/A	AFM	✓	✓						N/A	40 PFU/μm^2	[144]
Cellulose Magnetic bead	Fundamental research, detection	Streptavidin / biotin*	Streptavidin / biotin Cellulose-binding module	T4†	Myoviridae (Long-tailed)	*E. coli*	Magnetic separation + qPCR								800 CFU/mL (with PCR)	84 - 98%	[80]
Glass/silicate	Biocontrol	Amino-silanization	APTES + EDC / NHS	PRD1 P22 PR772 MS2 T4	Tectiviridae, Podoviridae, Leviviridae, Myoviridae (Icosahedral, short-tailed, long-tailed)	*E. coli* *S.* Typhimurium	N/A	✓			✓				N/A	4.5 PFU/μm^2	[50]
Glass/silicate	Capture	Amino-silanization	APTES + EDC / NHS	PRD1 T4	Tectiviridae, Myoviridae (Icosahedral, long-tailed)	*S. enterica*	N/A	✓			✓	✓			N/A	?	[51]
Glass/silicate	Detection	Amino-silanization*	APTMS + EDC / NHS	P22	Podoviridae (Short-tailed)	*S.* Typhimurium	N/A	✓				✓			?	67%	[67]
Glass/silicate	Fundamental research	Amino-silanization, Amino-silanization + electrostatic physisorption*	APTES + EDC / NHS	T4	Myoviridae (Long-tailed)	*E. coli*	N/A	✓							N/A	16 PFU/particle	[146]
Glass/silicate	Structural	Amino-silanization	APTES	fd†	Inoviridae (Filamentous)	*E. coli*	N/A	✓			✓				N/A	?	[88]
Glass/silicate	Structural, detection	Electropolymerization	PEDOT	M13	Inoviridae (Filamentous)	Antibody	Resistive								20×10^-9 M	?	[121]
Glassy carbon electrode	Detection	Amide bond	EDC	T4	Myoviridae (Long-tailed)	*Salmonella*	EIS	✓				✓			10^4 CFU/mL	?	[110]
Glassy carbon electrode	Detection	Amide bond	EDC / NHS	PaP1	Myoviridae (Long-tailed)	*P. aeruginosa*	ECL								56 CFU/mL	?	[60]
Glassy carbon electrode	Detection	Electropolymerization	Pyrrole-alkyl ammonium	T7	Autographiviridae (Short-tailed)	Antibody	Amperometric	✓			✓				36 pg/mL	?	[29]
Gold	Capture, detection	Thiol SAM	DTSP	T4 P22 NCTC 12673	Myoviridae, Podoviridae (Long-tailed, short-tailed)	*E. coli* *S.* Typhimurium	SPR							✓	?	18.9 PFU/μm^2	[63]

Gold	Capture, detection	Thiol SAM + amide bond, Thiol SAM + crosslinker*	L-cysteine L-cysteine + gluteraldehyde 11-MUA 11-MUA + EDC/ NHS L-cysteine + 11-MUA + EDC/NHS	BP14	Podoviridae (Short-tailed)	*S. aureus*	SPR, SEM	✓		✓		N/A	19 ng/mm^2	[72]
Gold	Detection	Amide bond	Carboxymethylated dextran + EDC / NHS	M13	Inoviridae (Filamentous)	*E. coli* *Salmonella*	SPR		✓			1.3×10^7 CFU/mL	?	[154]
Gold	Detection	Electropolymerisation + crosslinking	Polytyramine + glutaraldehyde	M13	Inoviridae (Filamentous)	*Salmonella*	Capacitive					200 CFU/mL	?	[172]
Gold	Detection	Thiol SAM	DTSP	T4	Myoviridae (Long-tailed)	*E. coli*	SPR	✓	✓	✓	✓	7×10^2 CFU/mL	57 ng/mm^2	[166]
Gold	Detection	Thiol SAM	Sulfo-LC-SPDP	PVP-SE1	Myoviridae (Long-tailed)	*S.* Enteritidis	Magnetoresistive					3-4 cells/sensor	?	[55]
Gold	Detection	Thiol SAM + amide bond	11-MUA + EDC / NHS	BCP8-2	Herellevirida e (Long-tailed)	*Bacillus cereus*	Ferromagnetoelastic					?	5.51 phages/ µm^2	[155]
Gold	Detection	Thiol SAM + amide bond	11-MUA + EDC / NHS	M13	Inoviridae (Filamentous)	ET101 protein	SPR					?	?	[153]
Gold	Detection	Thiol SAM + amide bond	3-MPA + EDC / NHS	fd	Inoviridae (Filamentous)	Prostate-specific antigen	DPV					3 pg/mL	?	[34]
Gold	Detection	Thiol SAM + amide bond	3-MPA + EDC / NHS	M13	Inoviridae (Filamentous)	*E. coli*	EIS	✓		✓		14 CFU/mL	?	[158]
Gold	Detection	Thiol SAM + amide bond	L-cysteine + 11-MUA + EDC / NHS	T4 BP14	Myoviridae, Podoviridae (Long-tailed, short-tailed)	*E. coli* *S. aureus*	SPR, ECIS	✓		✓		10^3 CFU/mL	?	[62]
Gold	Detection	Thiol SAM + amide bond	NHS thioctic ester	M13	Inoviridae (Filamentous)	Antibody	EIS, QCM					6.6×10^-9 M	1100 PFU/µm^2	[30]
Gold	Detection	Thiol SAM + amide bond	NHS thioctic ester	M13	Inoviridae (Filamentous)	Antibody	EIS		✓			20×10^-9 M	?	[31]
Gold	Detection	Thiol SAM + amide bond	NHS thioctic ester	M13	Inoviridae (Filamentous)	Prostate-specific antigen Antibody	EIS, QCM					120×10^-9 M	?	[32]
Gold	Detection	Thiol SAM + amide bond*	11-MUA + EDC / NHS	T4	Myoviridae (Long-tailed)	*E. coli*	DPV	✓	✓			14 ± 5 CFU/mL	3.65 PFU/µm^2	[157]
Gold	Detection	Thiol SAM + crosslinker	L-cysteine + glutaraldehyde	D29	Siphoviridae (Long-tailed)	*M. tuberculosis*	Piezoelectric	✓	✓			10^3 CFU/mL	?	[66]
Gold	Detection	Thiol SAM + crosslinking	Cysteamine + glutaraldehyde	M13†	Inoviridae (Filamentous)	NIH3T3 mouse fibroblasts	SPR					1000 cells	?	[147]
Gold	Detection	Thiol SAM + crosslinking	L-cysteine + glutaraldehyde	D29	Siphoviridae (Long-tailed)	*M. smegmatis* *M. tuberculosis*	QCM	✓	✓			10^3 CFU/mL	?	[66]
Gold	Detection	Thiol SAM + crosslinking*	Cysteamine + 1,4-phenylene diisothiocyanate	T4	Myoviridae (Long-tailed)	*E. coli*	CV, LSV, EIS, LAMP					8×10^2 CFU/mL (impedimetric) 10^2 CFU/mL (LAMP)	?	[64]

Gold	Detection	Thiol SAM + crosslinking*	DTSP Cysteamine + glutaraldehyde	T4	Myoviridae (Long-tailed)	*E. coli*	Confocal microscopy	✓	✓		✓		✓		10^2 CFU/mL	13.64 - 17.32 PFU/μm²	[167]
Gold	Detection	Thiol SAM + streptavidin / biotin*	Sulfo-NHS-SS-biotin + streptavidin / biotin	T4†	Myoviridae (Long-tailed)	*E. coli*	ECIS	✓			✓				?	4.4 PFU/μm²	[85]
Gold	Detection, fundamental research	Thiol SAM	carboxy-terminated SAM aldehyde-terminated SAM methyl-terminated SAM	fd-tet	Inoviridae (Filamentous)	Microbeads	Magnetoelastic								3.6×10^5 beads/mL	5.2 - 49.4%	[169]
Gold	Fundamental research, capture	Thiol SAM + crosslinking	Histidine + glutaraldehyde L-cysteine + glutaraldehyde Cysteamine + glutaraldehyde	T4	Myoviridae (Long-tailed)	*E. coli*	SPR	✓	✓		✓		✓		N/A	18 PFU/μm²	[41]
Gold	Structural	Electropolymerization	PEDOT	M13	Inoviridae (Filamentous)	Prostate-specific antigen	N/A								N/A	7.2 μg/cm²	[33]
Gold (plasmonic quasicyrstal)	Fundamental research	Thiol SAM	4-ATP	Tbilisi	Podoviridae (Short-tailed)	*Brucella abortus*	SERS	✓		✓	✓	✓			?	?	[70]
Gold Glass/silicate	Fundamental research, biocontrol	Amino-silanization Thiol SAM + amide bond	11-MUA + EDC / NHS (on gold) APTES (on glass)	FL-1	Myoviridae (Long-tailed)	*Flavobacterium columnare*	N/A				✓	✓	✓		N/A	0.5 PFU/μm²	[95]
Indium tin oxide	Biocontrol	Amino-silanization	APTES APTES + succinic anhydride Octadecyltrimethoxy silane	T4	Myoviridae (Long-tailed)	*E. coli*	N/A								N/A	?	[174]
Indium tin oxide	Fundamental research	Amino-silanization	APTES APTES + succinic anhydride Octadecyltrimethoxy silane	T4	Myoviridae (Long-tailed)	*E. coli*	N/A								N/A	~25 - 200 PFU/μm²	[173]
Magnetic bead	Capture	Crosslinking*	Bissulfosuccinimidyl suberate	P100 (Listex)	Myoviridae (Long-tailed)	*L. monocytogenes*	N/A								N/A	?	[61]
Magnetic bead	Capture, detection	Amide bond	Carboxyl-activation + EDC / NHS Tosyl-activation	P22	Podoviridae (Short-tailed)	*Salmonella*	Magnetic separation + optical reporter	✓	✓		✓	✓			19 CFU/mL (without preenrichment) 0.06 CFU/mL (with pre-enrichment)	1650 PFU/bead	[69]
Magnetic bead	Capture, detection	Amide bond	EDC / NHS	T4	Myoviridae (Long-tailed)	*E. coli*	Magnetic separation + impedimetric	✓		✓	✓	✓			10^3 CFU/mL	?	[103]
Magnetic bead	Capture, detection	Amide bond	EDC / NHS	T7	Autographiviridae (Short-tailed)	*E. coli*	Magnetic separation + LSV								10^5 CFU/mL	?	[49]

Magnetic bead	Capture, detection	Amide bond	EDC / NHS	T7	Autographiviridae (Short-tailed)	*E. coli*	Colorimetric	✓						1×10^4 CFU/mL (without preenrichment) 10 CFU/mL (with pre-enrichment)	1871 PFU/bead	[47]
Magnetic bead	Capture, detection	Misc.*	Tosyl-activation	P22	Podoviridae (short-tailed)	*Salmonella*	Magnetic separation + PCR	✓	✓			✓	✓	3 CFU/mL (with PCR)	2000 PFU/bead	[68]
Magnetic bead	Capture, detection	Thiol SAM	Isothiocyanate	O157-IOV-4	?	*E. coli O157:H7*	Magnetic separation + colorimetric	✓	✓		✓	✓		4.9×10^4 CFU/mL	?	[104]
Metal-organic framework	Detection	Crosslinking	Glutaraldehyde	?	?	*S. arlettae*	Fluorescence	✓	✓			✓		10^2 CFU/mL	?	[57]
Metal-organic framework	Detection	Crosslinking*	Glutaraldehyde	?	Siphoviridae (Long-tailed)	*S. aureus*	Photoluminescence quenching	✓		✓	✓	✓		31 CFU/mL	?	[58]
Optical fiber	Detection	Amino-silanization + crosslinking	APTES + glutaraldehyde	T4	Myoviridae (Long-tailed)	*E. coli*	SPR	✓		✓				10^3 CFU/mL	?	[141]
Optical fiber	Detection	Amino-silanization + crosslinking	APTES + glutaraldehyde	T4	Myoviridae (Long-tailed)	*E. coli*	Optical mode interference	✓				✓		10^3 CFU/mL	?	[142]
Polycaprolactone	Biocontrol	Amide bond*		vB_Pae_Kakheti25	Siphoviridae (Long-tailed)	*P. aeruginosa*	N/A							N/A	1 phage per 118 nm	[41]
Polyethersulfone	Biocontrol	Amide bond*	EDC / NHS	T4	Myoviridae (Long-tailed)	*E. coli*	N/A	✓			✓			N/A	2 PFU/μm^2	[86]
Polyhydroxyalkanoate	Fundamental research, capture	Amide bond	EDC / NHS	T4	Myoviridae (Long-tailed)	*E. coli*	N/A	✓				✓		N/A	4.24 PFU/μm^2	[40]
Polystyrene latex beads	Detection	Amide bond	EDC / NHS	M13	Inoviridae (Filamentous)	*P. aeruginosa*	Micro-Raman spectroscopy							10^3 CFU/mL	?	[119]
Screen-printed carbon electrode	Detection	Amide bond	EDC	?	Siphoviridae (Long-tailed)	*S. arlettae*	EIS	✓				✓		2 CFU	?	[111]
Screen-printed carbon electrode	Detection	Crosslinking	Glutaraldehyde	Gamma phage	Siphoviridae (Long-tailed)	*B. anthracis spores*	Impedimetric							10^3 CFU/mL	?	[65]
Silica nanoparticle	Fundamental research, biocontrol	Amino-silanization + crosslinking Amino-silanization + electrostatic Physisorption*	APTMS AEAPTMS + glutaraldehyde	?	Siphoviridae (Long-tailed)	*S. aureus*	N/A	✓	✓			✓		N/A	?	[56]
Silicon Nitride (Si3N4)	Detection	Amino-silanization + crosslinking	APTES + glutaraldehyde	?	?	Cancer biomarkers	Potentiometric							?	?	[37]
Silver	Detection	Thiol SAM + crosslinking	4-ATP + glutaraldehyde	T4	Myoviridae (Long-tailed)	*E. coli*	SERS	✓				✓		1.5×10^2 CFU/mL	?	[168]

N/A Not applicable

% Surface coverage

† Phage was genetically engineered

* Oriented immobilization

									Purification								
Substrate	**Paper Category**	**Immobilization Category**	**Surface treatment**	**Phage**	**Phage morphology (geometry)**	**Analyte/Host**	**Detection scheme (if biosensor)**	**Centrifugation**	**Ultracentrifugation**	**Solvent precipitation**	**PEG precipitation**	**Filtration**	**Dialysis**	**Chromatography**	**Limit of detection (for biosensors)**	**Phage surfac densit**
Carbon nanotubes	Detection	Electrostatic Physisorption*	Polyethylenimine	?	?	*S. aureus*	CV, DPV	✓		✓					3 CFU/mL	11.7 PFU/µm
Carboxymethylcellulose (paper)	Detection	Amide bond*		StyM-AG6 SenS-AG11 LmoM-AG20 EcoM-AG10 T4 MS2 rV5 AG2A vB_SnwM CGG4-1	Myoviridae, Herelleviridae, Siphoviridae, Leviviridae, Podoviridae (Long-tailed, icosahedral, short-tailed)	*E. coli* O157:H7 *E. coli* O45:H2 *Salmonella* *L. monocytogenes*	qPCR	✓				✓			10–50 CFU/mL	0.01 PFU/µm
Cellulose	Biocontrol	Electrostatic Physisorption*	Cibacron Blue F3GA Polyethylenimine Chitan	T7	Autographiviridae (Short-tailed)	*E. coli*	N/A								N/A	?
Cellulose	Biocontrol	Electrostatic Physisorption*	Polyvinylamine	LinM-AG8 LmoM-AG13 LmoM-AG20 EcoM-HG2 EcoM-HG7 EcoM-HG8 (LISTEX P100 commercial cocktail)	Myoviridae (Long-tailed)	*L. monocytogenes* *E. coli* O104:H4	N/A								N/A	?
Cellulose	Biocontrol	Electrostatic Physisorption*	Polyvinylamine	T4 EcoM-AG2 SboM-AG3 LinM-AG8	Myoviridae, Siphoviridae (Long-tailed)	*L. monocytogenes* *E. coli* O157:H7	N/A	✓							N/A	?
Cellulose	Biocontrol	Physisorption		BFSE16 BFSE18 PaDTA1 PaDTA9 PaDTA10 PaDTA11	?	*S.* Typhimurium	N/A								N/A	?
Cellulose (paper)	Fundamental research	Physisorption		T4	Myoviridae (Long-tailed)	*E. coli*	N/A								N/A	?
Cellulose (paper)	Fundamental research	Physisorption		T4	Myoviridae (Long-tailed)	*E. coli*	Colorimetric								N/A	?

Glass/silicate	Detection	Electrostatic Physisorption	Poly-L-lysine	PRD1 E79	Tectiviridae, Myoviridae (Icosahedral, long-tailed)	*P. aeruginosa* *S.* Typhimurium	QCM w/ dissipation monitoring	✓		✓	✓		?	1.6 - 2.2 µg/cm
Glass/silicate	Fundamental research	Amino-silanization + electrostatic physisorption	APTES	fd-tet	Inoviridae (Filamentous)	*E. coli*	N/A			✓	✓	✓	N/A	?
Glass/silicate	Fundamental research	Amino-silanization + electrostatic physisorption	ED3A PEG APTS	VB EcoM-AG2 VB_LinM-AG8 VB_SenS-AG11 VB_SboM-AG3	Myoviridae, Myoviridae, Siphoviridae, Myoviridae (Long-tailed)	*E. coli* O126:H8 *L. innocua* *S.* Enteritidis *S. boydii*	N/A	✓			✓		N/A	?
Glass/silicate	Structural	Physisorption	PolyDADMAC	M13	Inoviridae (Filamentous)	*N/A*	SERS						N/A	N/A
Glassy carbon electrode	Detection	Electrostatic Physisorption*	Polyethylenimine + PBSE	T2	Myoviridae (Long-tailed)	*E. coli*	EIS	✓			✓		10^3 CFU/mL	?
Gold	Detection	Physisorption		1G40 fd	Inoviridae (Filamentous)	Beta-galactosidase	SPR						10^-12 M	3nm thick adlaye
Gold	Detection	Physisorption		bacteriophage 12600	?	*S. aureus*	SPR	✓		✓			10^4 CFU/mL	3.1 ng/mm
Gold	Detection	Physisorption		E2	Inoviridae (Filamentous)	*S. aureus*	Acoustic wave						10^2 CFU/mL	300 PFU/µm
Gold	Detection	Physisorption		E2	Inoviridae (Filamentous)	*S.* Typhimurium	Magnetoelastic						2.03 log CFU/mL	?
Gold	Detection	Physisorption		E2	Inoviridae (Filamentous)	*S.* Typhimurium	Magnetoelastic						5×10^3 CFU/mL	?
Gold	Detection	Physisorption		E2	Inoviridae (Filamentous)	*S.* Typhimurium	Magnetoelastic						10^3 CFU/mL	?
Gold	Detection	Physisorption		E2	Inoviridae (Filamentous)	*S.* Typhimurium	Magnetostrictive						?	?
Gold	Detection	Physisorption		E2	Inoviridae (Filamentous)	*S.* Typhimurium	Magnetoelastic						5×10^2 CFU/mL	?
Gold	Detection	Physisorption		E2	Inoviridae (Filamentous)	*S.* Typhimurium	Magnetoelastic			✓			?	?
Gold	Detection	Physisorption		E2	Inoviridae (Filamentous)	*S.* Typhimurium	Magnetoelastic						1.6 x 10^2 CFU/cm2	~50%
Gold	Detection	Physisorption		E2	Inoviridae (Filamentous)	*S.* Typhimurium	Magnetoelastic			✓			?	?
Gold	Detection	Physisorption		E2	Inoviridae (Filamentous)	*S.* Typhimurium	Magnetoelastic						?	?
Gold	Detection	Physisorption		E2	Inoviridae (Filamentous)	*S.* Typhimurium	Magnetoelastic			✓			1.94 log CFU/spinach	?
Gold	Detection	Physisorption		E2	Inoviridae (Filamentous)	*S.* Typhimurium	Magnetoelastic						?	?
Gold	Detection	Physisorption		E2	Inoviridae (Filamentous)	*S.* Typhimurium	Magnetoelastic						?	12.5%
Gold	Detection	Physisorption		E2	Inoviridae (Filamentous)	*S.* Typhimurium	Magnetoelastic						5×10^2 CFU/mL	?
Gold	Detection	Physisorption		E2	Inoviridae (Filamentous)	*S.* Typhimurium *B. anthracis* spores	Magnetoelastic						5×10^3 CFU/mL	?
Gold	Detection	Physisorption		fd	Inoviridae (Filamentous)	*B. anthracis* spores	Magnetoelastic						10^3 spores/mL	?
Gold	Detection	Physisorption		fd	Inoviridae (Filamentous)	*B. anthracis* spores	Magnetoelastic						5*10^3 CFU/mL	?
Gold	Detection	Physisorption		fd	Inoviridae (Filamentous)	*Beta-galactosidase*	QCM						10^-9 M	?

Gold	Detection	Physisorption		fd-tet	Inoviridae (Filamentous)	*B. anthracis* spores	Magnetoelastic							?	?
Gold	Detection	Physisorption		JRB7	Inoviridae (Filamentous)	*B. anthracis* spores	Magnetoelastic							10^2 CFU/mL	?
Gold	Detection	Physisorption		JRB7	Inoviridae (Filamentous)	*B. anthracis* spores	Magnetostrictive							10^4 spores/mL	?
Gold	Detection	Physisorption		JRB7	Inoviridae (Filamentous)	*B. anthracis Sterne* spores *Bacillus cereus* spores *Bacillus megaterium* spores	Magnetoelastic							10^3 CFU/mL	?
Gold	Detection	Physisorption		JRB7	Inoviridae (Filamentous)	*B. anthracis* spores	Magnetoelastic							10^3 spores/mL	?
Gold	Detection	Physisorption		Lm P4:A8 M13K07	Inoviridae (Filamentous)	*L. monocytogenes*	SPR							2×10^6 CFU/mL	?
Gold	Detection	Physisorption		M13	Inoviridae (Filamentous)	*S.* Typhimurium	Magnetoelastic	✓			✓			7.85×10^3 CFU/mm^2	?
Gold	Detection	Physisorption		bacteriophage 12600	?	*S. aureus*	Magnetoelastic							1.76 log CFU/25 mm^2	26 PFU/µm
Gold	Detection	Physisorption		T4	Myoviridae (Long-tailed)	*E. coli*	EIS	✓		✓				10^4 CFU/mL	?
Gold	Detection	Physisorption*	PolyDADMAC	S13′	Podoviridae (Short-tailed)	*S. aureus*	Dark-field microscopy							8×10^4 CFU/mL	?
Gold	Detection	Physisorption*		bacteriophage 12600	?	*S. aureus*	Magnetoelastic							10^3 CFU/mL	0.455 µm/phag
Gold	Detection	Physisorption*		T4	Myoviridae (Long-tailed)	*E. coli*	Confocal microscopy	✓	✓				✓	10^2 CFU/mL	14.3 PFU/µm
Gold	Detection	Physisorption*		T4	Myoviridae (Long-tailed)	*E. coli*	EIS	✓		✓		✓		10^3 CFU/mL	?
Gold	Fundamental research, detection	Physisorption		fd	Inoviridae (Filamentous)	*S.* Typhimurium	Flow cytometry				✓			?	?
Gold	Structural	Genetic engineering	methionine	fd†	Inoviridae (Filamentous)	*E. coli*	N/A				✓	✓	✓	N/A	?
Gold	Structural, detection	Physisorption*		M13	Inoviridae (Filamentous)	Streptavidin	SPR							10^-15 M	?
Magnetic bead	Capture, biocontrol	Streptavidin / biotin	Sulfo-NHS-biotin + Streptavidin / biotin	SJ2	?	*S.* Enteritidis	N/A							?	?
Magnetic bead Alumina nanofibers Cellulose	Capture, detection	Streptavidin / biotin*	Streptavidin / biotin Cellulose-binding module	T4†	Myoviridae (Long-tailed)	*E. coli* *S.* Typhimurium	Magnetic separation + ATP bioluminescence							6×10^3 CFU/mL	?
Metallic glass (Fe80B20 alloy)	Detection	Physisorption		E2	Inoviridae (Filamentous)	*S.* Typhimurium	Magnetoelastic							50 CFU/mL	?
Optical fiber	Detection	Physisorption		T4	Myoviridae (Long-tailed)	*E. coli*	Resonance wavelength shift							?	?
Organic-inorganic nanoflowers	Detection	Physisorption		T4	Myoviridae (Long-tailed)	*E. coli*	EIS	✓				✓		1 CFU/mL	?
Paper	Fundamental research	Physisorption	PolyDADMAC	T4	Myoviridae (Long-tailed)	*E. coli*	N/A							N/A	?
Polyethylene (optical fiber)	Detection	Physisorption		T4	Myoviridae (Long-tailed)	*E. coli*	Optical fiber transmission	✓		✓		✓		10^4 CFU/mL	10%

Silver	Detection	Physisorption		M13	Inoviridae (Filamentous)	Paraquat (herbicide)	SERS	N/A	?

N/A Not applicable

% Surface coverage

† Phage was genetically engineered

*** Oriented immobilization**

								Purification									
Substrate	**Paper Category**	**Immobilization Category**	**Surface treatment**	**Phage**	**Phage morphology (geometry)**	**Analyte /Host**	**Detection scheme (for biosensors)**	**Centrifugation**	**Ultracentrifugation**	**Solvent precipitation**	**PEG precipitation**	**Filtration**	**Dialysis**	**Chromatography**	**Limit of detection (for biosensors)**	**Phage surface density**	**Reference**
Cellulose Magnetic bead	Fundamental research, detection	Streptavidin / biotin*	Streptavidin / biotin Cellulose-binding module	T4†	Myoviridae (Long-tailed)	*E. coli*	Magnetic separation + qPCR								800 CFU/mL (with PCR)	84 - 98%	[80]
Glass/silicate	Structural	Amino-silanization	APTES	fd†	Inoviridae (Filamentous)	*E. coli*	N/A	✓			✓				N/A	?	[88]
Glass/silicate Magnetic bead	Fundamental research	Amino-silanization*	APTES + formylglycine	fd-tet†	Inoviridae (Filamentous)	*E. coli*	N/A	✓			✓				N/A	?	[87]
Gold	Detection	Genetic engineering	Peptide linkers	M13†	Inoviridae (Filamentous)	*E. coli*	SPR				✓				N/A	?	[81]
Gold	Detection	Thiol SAM + streptavidin / biotin*	Sulfo-NHS-SS-biotin + streptavidin / biotin	T4†	Myoviridae (Long-tailed)	*E. coli*	ECIS	✓				✓			?	4.4 PFU/μm^2	[85]
Gold	Structural	Genetic engineering	methionine	fd†	Inoviridae (Filamentous)	*E. coli*	N/A				✓	✓	✓		N/A	?	[82]
Magnetic bead	Capture, detection	Streptavidin / biotin	Streptavidin / biotin	T7†	Autographiviridae (Short-tailed)	*E. coli*	Magnetic separation + PCR	✓	✓			✓			10^2 CFU/mL (with PCR)	248 PFU/bead	[48]

Magnetic bead Alumina nanofibers Cellulose	Capture, detection	Streptavidin / biotin*	Streptavidin / biotin Cellulose-binding module	T4†	Myoviridae (Long-tailed)	*E. coli* *S.* Typhimurium	Magnetic separation + ATP bioluminescence	6×10^3 CFU/mL	?	[86]
Platinum	Fundamental research	Genetic engineering*		fd†	Inoviridae (Filamentous)	*E. coli*	CV, EIS	N/A	?	[44]
PMMA	Fundamental research	Genetic engineering*	PMMA-binding peptide	M13†	Inoviridae (Filamentous)	*E. coli*	N/A	N/A	?	[83]
Quantum dot	Detection	Streptavidin / biotin*	Streptavidin / biotin	T4†	Myoviridae (Long-tailed)	*E. coli*	Fluorescence	10 CFU/mL	?	[79]

N/A Not applicable

% Surface coverage

† Phage was genetically engineered

*** Oriented immobilization**

AUTHOR INFORMATION

Corresponding Author

*Correspondence: yoann.roupioz@cea.fr; Tel.:+33-4-38-78-98-79

Author Contributions

The manuscript was written through contributions of all authors. All authors have given approval to the final version of the manuscript.

Funding Sources

This work has been partially supported by Labex Arcane and CBH-EUR-GS (ANR-17-EURE-0003).

ACKNOWLEDGMENT

All image credits are to the author unless otherwise stated. The authors would like to acknowledge the contribution of the Blender project (www.blender.org), wtihout which the illustrations in this review would not have been possible.

References for protein structures used in illustrations:

Structural analysis of PRD1

PDB ID: 1W8X

Abrescia, N.G.A. et al. (2004) Insights Into Assembly from Structural Analysis of Bacteriophage Prd1. Nature 432: 68

PRD1 vertex protein P5

PDB ID: 1YQ8

Merckel, M.C. et al. (2005) The structure of the bacteriophage PRD1 spike sheds light on the evolution of viral capsid architecture. Mol Cell 18: 161-170

Atomic models of P1, P4 C-terminal fragment and P8 fitted in the bacteriophage phi6 nucleocapsid reconstructed with icosahedral symmetry

PDB ID: 6HY0

Ilca, S.L. et al. (2019) Multiple liquid crystalline geometries of highly compacted nucleic acid in a dsRNA virus. Nature 570: 252-256

Cryo-electron microscopy structure of the hexagonal pre-attachment T4 baseplate-tail tube complex

PDB ID: 5IV5

Taylor, N.M. et al. (2016) Structure of the T4 baseplate and its function in triggering sheath contraction. Nature 533: 346-352

CryoEM single particle reconstruction of prolate head of bacteriophage T4

EMD ID: 6323

Sun, L. et al. (2015) Cryo-EM structure of the bacteriophage T4 portal protein assembly at near-atomic resolution in Nat Commun 6, 7548

Fitting of gp18M crystal structure into 3D cryo-EM reconstruction of bacteriophage T4 extended tail PDB ID: 3FOH

Aksyuk et al. (2009) The tail sheath structure of bacteriophage T4: a molecular machine for infecting bacteria in EMBO J 28(7):821-9

Structure of native bacteriophage P68

PDB ID: 6Q3G

Hrebík et al. (2019) Structure and genome ejection mechanism of Staphylococcus aureus phage P68 in Sci Adv. 16;5(10):eaaw7414

Structure of the bacteriophage C1 tail knob protein, gp12

PDB ID: 4EO2

Aksyuk et al. (2012) Structural investigations of a Podoviridae streptococcus phage C1, implications for the mechanism of viral entry in Proc.Natl.Acad.Sci.USA 109: 14001-14006

Localized reconstruction of tail-spike of bacteriophage P68

PDBJ ID: EMD-4450

Hrebík et al. (2019) Structure and genome ejection mechanism of Staphylococcus aureus phage P68 in Sci Adv. 16;5(10):eaaw7414

Capsid model of M13 bacteriophage virus from Magic-angle spinning NMR and Rosetta modeling

PDB ID: 2mjz

Morag, O. et al. (2015) The NMR-Rosetta capsid model of M13 bacteriophage reveals a quadrupled hydrophobic packing epitope in Proc Natl Acad Sci USA 112: 971-976

Crystal structure of Bovine Serum Albumin

PDB ID: 3v03

Majorek et al. (2012) Structural and immunologic characterization of bovine, horse, and rabbit serum albumins in Mol. Immunol. 52: 174-182

REFERENCES

(1) Wommack, K. E.; Colwell, R. R. Virioplankton: Viruses in Aquatic Ecosystems. *Microbiol. Mol. Biol. Rev.* **2000**, *64* (1), 69–114. https://doi.org/10.1128/mmbr.64.1.69-114.2000.

(2) Chibani-Chennoufi, S.; Bruttin, A.; Brüssow, H.; Dillmann, M.; Bru, H. Phage-Host Interaction : An Ecological Perspective. *J. Bacteriol.* **2004**, *186* (12), 3677–3686. https://doi.org/10.1128/JB.186.12.3677.

(3) Suttle, C. A. The Significance of Viruses to Mortality in Aquatic Microbial Communities. *Microb. Ecol.* **1994**, *28* (2), 237–243. https://doi.org/10.1007/BF00166813.

(4) Prescott, J. M. W.; Sherwood, L.; Woolverton, C. J.; M, L. Chapter 17 - The Viruses: Viruses of Bacteria and Archaea. In *Microbiology*; McGraw-Hill, Ed.; 2008; pp 427–446.

(5) Richard Calendar. *The Bacteriophages*, 2nd ed.; Calendar, R., Ed.; Oxford University Press, 2006.

(6) Duckworth, D. H. Who Discovered Bacteriophage? *Bacteriol. Rev.* **1976**, *40* (4), 793–802.

(7) Żaczek, M.; Weber-Dąbrowska, B.; Międzybrodzki, R.; Łusiak-Szelachowska, M.; Górski, A. Phage Therapy in Poland – a Centennial Journey to the First Ethically Approved Treatment Facility in Europe. *Front. Microbiol.* **2020**, *11* (June). https://doi.org/10.3389/fmicb.2020.01056.

(8) Almeida, G. M. de F.; Sundberg, L. R. The Forgotten Tale of Brazilian Phage Therapy. *Lancet Infect. Dis.* **2020**, *20* (5), e90–e101. https://doi.org/10.1016/S1473-3099(20)30060-8.

(9) Myelnikov, D. An Alternative Cure: The Adoption and Survival of Bacteriophage Therapy in the USSR, 1922-1955. *J. Hist. Med. Allied Sci.* **2018**, *73* (4), 385–411. https://doi.org/10.1093/jhmas/jry024.

(10) Summers, W. C. Bacteriophage Therapy. *Annu. Rev. Microbiol.* **2001**, No. 55, 437–451.

(11) Ferry, T.; Kolenda, C.; Gustave, C.-A.; Lustig, S.; Josse, J.; Batailler, C.; Pirot, F.; Leboucher, G.; Laurent, F. Phage Therapy in Bone and Joint Infection: History, Scientific Basis, Feasibility and Perspectives in France. *Virologie* **2020**, *24* (1), 49–56. https://doi.org/10.1684/vir.2020.0808.

(12) Levy, S. B.; Bonnie, M. Antibacterial Resistance Worldwide: Causes, Challenges and Responses. *Nat. Med.* **2004**, *10* (12S), S122–S129. https://doi.org/10.1038/nm1145.

(13) Elhani, D. L'émergence de la résistance aux antibiotiques annonce-t-elle le retour des âges sombres ? *Ann. Biol. Clin. (Paris).* **2011**, *69* (6), 637–646. https://doi.org/10.1684/abc.2011.0632.

(14) *Antimicrobial Resistance Global Report on Surveillance*; 2014.

(15) Jim O'Neill. Antimicrobial Resistance : Tackling a Crisis for the Health and Wealth of Nations. *Rev. Antimicrob. Resist.* **2014**, No. December, 1–16. https://doi.org/10.1038/510015a.

(16) Projan, S. J. Why Is Big Pharma Getting out of Antibacterial Drug Discovery? *Curr. Opin. Microbiol.* **2003**, *6* (5), 427–430. https://doi.org/10.1016/j.mib.2003.08.003.

(17) Broughton, C. E.; Van Den Berg, H. A.; Wemyss, A. M.; Roper, D. I.; Rodger, A. Beyond the Discovery Void: New Targets for Antibacterial Compounds. *Sci. Prog.* **2016**, *99* (2), 153–182. https://doi.org/10.3184/003685016X14616130512308.

(18) Kakasis, A.; Panitsa, G. Bacteriophage Therapy as an Alternative Treatment for Human Infections. A Comprehensive Review. *Int. J. Antimicrob. Agents* **2019**, *53* (1), 16–21. https://doi.org/10.1016/j.ijantimicag.2018.09.004.

(19) Gouvêa, D. M.; Mendonça, R. C. S.; Soto, M. L.; Cruz, R. S. Acetate Cellulose Film with Bacteriophages for Potential Antimicrobial Use in Food Packaging. *LWT - Food Sci. Technol.* **2015**, 1–7. https://doi.org/10.1016/j.lwt.2015.03.014.

(20) Lone, A.; Anany, H.; Hakeem, M.; Aguis, L.; Avdjian, A. C.; Bouget, M.; Atashi, A.; Brovko, L.; Rochefort, D.; Griffiths, M. W. Development of Prototypes of Bioactive

Packaging Materials Based on Immobilized Bacteriophages for Control of Growth of Bacterial Pathogens in Foods. *Int. J. Food Microbiol.* **2016**, *217*, 49–58. https://doi.org/10.1016/j.ijfoodmicro.2015.10.011.

(21) Lee, J. H.; Warner, C. M.; Jin, H. E.; Barnes, E.; Poda, A. R.; Perkins, E. J.; Lee, S. W. Production of Tunable Nanomaterials Using Hierarchically Assembled Bacteriophages. *Nat. Protoc.* **2017**, *12* (9), 1999–2013. https://doi.org/10.1038/nprot.2017.085.

(22) Sorokulova, I. B.; Olsen, E. V.; Chen, I. H.; Fiebor, B.; Barbaree, J. M.; Vodyanoy, V. J.; Chin, B. A.; Petrenko, V. A. Landscape Phage Probes for Salmonella Typhimurium. *J. Microbiol. Methods* **2005**, *63* (1), 55–72. https://doi.org/10.1016/j.mimet.2005.02.019.

(23) Wan, J.; Johnson, M. L.; Guntupalli, R.; Petrenko, V. A.; Chin, B. A. Detection of Bacillus Anthracis Spores in Liquid Using Phage-Based Magnetoelastic Micro-Resonators. *Sensors Actuators, B Chem.* **2007**, *127* (2), 559–566. https://doi.org/10.1016/j.snb.2007.05.017.

(24) Chen, I. H.; Petrenkc, V. A.; Huang, S.; Chin, B. A. Phage-Based Magnetoelastic Wireless Biosensors for Detecting Bacillus Anthracis Spores. *IEEE Sens. J.* **2007**, *7* (3), 470–477. https://doi.org/10.1109/JSEN.2006.890135.

(25) Wan, J.; Johnson, M. L.; Horikawa, S.; Chin, B. A.; Petrenko, V. A. Characterization of Phage-Coupled Magnetoelastic Micro-Particles for the Detection of Bacillus Anthracis Sterne Spores. In *Proceedings of IEEE Sensors*; 2007; pp 1085–1088. https://doi.org/10.1109/ICSENS.2007.4388594.

(26) Huang, S.; Yang, H.; Lakshmanan, R. S.; Johnson, M. L.; Chen, I.; Wan, J.; Wikle, H. C.; Petrenko, V. A.; Barbaree, J. M.; Cheng, Z. Y.; Chin, B. A. The Effect of Salt and Phage Concentrations on the Binding Sensitivity of Magnetoelastic Biosensors for Bacillus Anthracis Detection. *Biotechnol. Bioeng.* **2008**, *101* (5), 1014–1021. https://doi.org/10.1002/bit.21995.

(27) Fu, L.; Li, S.; Zhang, K.; Chen, I. H.; Barbaree, J. M.; Zhang, A.; Cheng, Z. Detection of Bacillus Anthracis Spores Using Phage-Immobilized Magnetostrictive Milli/Micro Cantilevers. *IEEE Sens. J.* **2011**, *11* (8), 1684–1691. https://doi.org/10.1109/JSEN.2010.2095002.

(28) Johnson, M. L.; Wan, J.; Huang, S.; Cheng, Z.; Petrenko, V. A.; Kim, D. J.; Chen, I. H.; Barbaree, J. M.; Hong, J. W.; Chin, B. A. A Wireless Biosensor Using Microfabricated Phage-Interfaced Magnetoelastic Particles. *Sensors Actuators, A Phys.* **2008**, *144* (1), 38–47. https://doi.org/10.1016/j.sna.2007.12.028.

(29) Ionescu, R. E.; Cosnier, S.; Herrmann, S.; Marks, R. S. Amperometric Immunosensor for the Detection of Anti-West Nile Virus IgG. *Anal. Chem.* **2007**, *79* (22), 8662–8668. https://doi.org/10.1021/ac0707129.

(30) Yang, L. M. C.; Diaz, J. E.; McIntire, T. M.; Weiss, G. A.; Penner, R. M. Covalent Virus Layer for Mass-Based Biosensing. *Anal. Chem.* **2008**, *80* (4), 933–943. https://doi.org/10.1021/ac071470f.

(31) Yang, L. M. C.; Diaz, J. E.; McIntire, T. M.; Weiss, G. A.; Penner, R. M. Direct Electrical

Transduction of Antibody Binding to a Covalent Virus Layer Using Electrochemical Impedance. *Anal. Chem.* **2008**, *80* (15), 5695–5705. https://doi.org/10.1021/ac8008109.

(32) Yang, L. M. C.; Tam, P. Y.; Murray, B. J.; McIntire, T. M.; Overstreet, C. M.; Weiss, G. A.; Penner, R. M. Virus Electrodes for Universal Biodetection. *Anal. Chem.* **2006**, *78* (10), 3265–3270. https://doi.org/10.1021/ac052287u.

(33) Donavan, K. C.; Arter, J. A.; Weiss, G. A.; Penner, R. M. Virus-PEDOT Biocomposite Films. *Langmuir* **2012**, *28* (34), 12581–12587. https://doi.org/doi:10.1021/la302473j.

(34) Han, L.; Xia, H.; Yin, L.; Petrenko, V. A.; Liu, A. Selected Landscape Phage Probe as Selective Recognition Interface for Sensitive Total Prostate-Specific Antigen Immunosensor. *Biosens. Bioelectron.* **2018**, *106* (October 2017), 1–6. https://doi.org/10.1016/j.bios.2018.01.046.

(35) Nanduri, V.; Sorokulova, I. B.; Samoylov, A. M.; Simonian, A. L.; Petrenko, V. A.; Vodyanoy, V. Phage as a Molecular Recognition Element in Biosensors Immobilized by Physical Adsorption. *Biosens. Bioelectron.* **2007**, *22* (6), 986–992. https://doi.org/10.1016/j.bios.2006.03.025.

(36) Nanduri, V.; Balasubramanian, S.; Sista, S.; Vodyanoy, V. J.; Simonian, A. L. Highly Sensitive Phage-Based Biosensor for the Detection of β-Galactosidase. *Anal. Chim. Acta* **2007**, *589* (2), 166–172. https://doi.org/10.1016/j.aca.2007.02.071.

(37) Jia, Y.; Qin, M.; Zhang, H.; Niu, W.; Li, X.; Wang, L.; Li, X.; Bai, Y.; Cao, Y.; Feng, X. Label-Free Biosensor: A Novel Phage-Modified Light Addressable Potentiometric Sensor System for Cancer Cell Monitoring. *Biosens. Bioelectron.* **2007**, *22* (12), 3261–3266. https://doi.org/10.1016/j.bios.2007.01.018.

(38) Kang, Y. R.; Park, E. J.; Kim, J. H.; Min, N. K.; Kim, S. W. Development of Bio-Nanowire Networks Using Phage-Enabled Assembly for Biological Sensor Application. *Talanta* **2010**, *81* (4–5), 1425–1430. https://doi.org/10.1016/j.talanta.2010.02.047.

(39) Anany, H.; Chen, W.; Pelton, R.; Griffiths, M. W. Biocontrol of Listeria Monocytogenes and Escherichia Coli O157:H7 in Meat by Using Phages Immobilized on Modified Cellulose Membranes. *Appl. Environ. Microbiol.* **2011**, *77* (18), 6379–6387. https://doi.org/10.1128/AEM.05493-11.

(40) Wang, C.; Sauvageau, D.; Elias, A. Immobilization of Active Bacteriophages on Polyhydroxyalkanoate Surfaces. *ACS Appl. Mater. Interfaces* **2016**, *8* (2), 1128–1138. https://doi.org/10.1021/acsami.5b08664.

(41) Nogueira, F.; Karumidze, N.; Kusradze, I.; Goderdzishvili, M.; Teixeira, P.; Gouveia, I. C. Immobilization of Bacteriophage in Wound-Dressing Nanostructure. *Nanomedicine Nanotechnology, Biol. Med.* **2017**, *13* (8), 2475–2484. https://doi.org/10.1016/j.nano.2017.08.008.

(42) Vonasek, E.; Lu, P.; Hsieh, Y. Lo; Nitin, N. Bacteriophages Immobilized on Electrospun Cellulose Microfibers by Non-Specific Adsorption, Protein–Ligand Binding, and Electrostatic Interactions. *Cellulose* **2017**, *24* (10), 4581–4589.

https://doi.org/10.1007/s10570-017-1442-3.

(43) Chung, W. J.; Oh, J. W.; Kwak, K.; Lee, B. Y.; Meyer, J.; Wang, E.; Hexemer, A.; Lee, S. W. Biomimetic Self-Templating Supramolecular Structures. *Nature* **2011**, *478* (7369), 364–368. https://doi.org/10.1038/nature10513.

(44) Merzlyak, A.; Indrakanti, S.; Lee, S. W. Genetically Engineered Nanofiber-like Viruses for Tissue Regenerating Materials. *Nano Lett.* **2009**, *9* (2), 846–852. https://doi.org/10.1021/n18036728.

(45) Lee, B. Y.; Zhang, J.; Zueger, C.; Chung, W. J.; Yoo, S. Y.; Wang, E.; Meyer, J.; Ramesh, R.; Lee, S. W. Virus-Based Piezoelectric Energy Generation. *Nat. Nanotechnol.* **2012**, *7* (6), 351–356. https://doi.org/10.1038/nnano.2012.69.

(46) Oh, J. W.; Chung, W. J.; Heo, K.; Jin, H. E.; Lee, B. Y.; Wang, E.; Zueger, C.; Wong, W.; Meyer, J.; Kim, C.; Lee, S. Y.; Kim, W. G.; Zemla, M.; Auer, M.; Hexemer, A.; Lee, S. W. Biomimetic Virus-Based Colourimetric Sensors. *Nat. Commun.* **2014**, *5*, 1–8. https://doi.org/10.1038/ncomms4043.

(47) Chen, J.; Alcaine, S. D.; Jiang, Z.; Rotello, V. M.; Nugen, S. R. Detection of Escherichia Coli in Drinking Water Using T7 Bacteriophage-Conjugated Magnetic Probe. *Anal. Chem.* **2015**, *87* (17), 8977–8984. https://doi.org/10.1021/acs.analchem.5b02175.

(48) Wang, Z.; Wang, D.; Chen, J.; Sela, D. A.; Nugen, S. R. Development of a Novel Bacteriophage Based Biomagnetic Separation Method as an Aid for Sensitive Detection of Viable Escherichia Coli. *Analyst* **2016**, *141* (3), 1009–1016. https://doi.org/10.1039/c5an01769f.

(49) Wang, D.; Hinkley, T.; Chen, J.; Talbert, J. N.; Nugen, S. R. Phage Based Electrochemical Detection of: Escherichia Coli in Drinking Water Using Affinity Reporter Probes. *Analyst* **2019**, *144* (4), 1345–1352. https://doi.org/10.1039/c8an01850b.

(50) Hosseinidoust, Z.; Van De Ven, T. G. M.; Tufenkji, N. Bacterial Capture Efficiency and Antimicrobial Activity of Phage-Functionalized Model Surfaces. *Langmuir* **2011**, *27* (9), 5472–5480. https://doi.org/10.1021/la200102z.

(51) Dixon, D. V.; Hosseinidoust, Z.; Tufenkji, N. Effects of Environmental and Clinical Interferents on the Host Capture Efficiency of Immobilized Bacteriophages. *Langmuir* **2014**, *30* (11), 3184–3190. https://doi.org/10.1021/la500059u.

(52) Olsson, A. L. J.; Wargenau, A.; Tufenkji, N. Optimizing Bacteriophage Surface Densities for Bacterial Capture and Sensing in Quartz Crystal Microbalance with Dissipation Monitoring. *ACS Appl. Mater. Interfaces* **2016**, *8* (22), 13698–13706. https://doi.org/10.1021/acsami.6b02227.

(53) Anany, H.; Brovko, L.; El Dougdoug, N. K.; Sohar, J.; Fenn, H.; Alasiri, N.; Jabrane, T.; Mangin, P.; Monsur Ali, M.; Kannan, B.; Filipe, C. D. M.; Griffiths, M. W. Print to Detect: A Rapid and Ultrasensitive Phage-Based Dipstick Assay for Foodborne Pathogens. *Anal. Bioanal. Chem.* **2018**, *410* (4), 1217–1230. https://doi.org/10.1007/s00216-017-0597-y.

(54) Zhou, Y.; Marar, A.; Kner, P.; Ramasamy, R. P. Charge-Directed Immobilization of Bacteriophage on Nanostructured Electrode for Whole-Cell Electrochemical Biosensors. *Anal. Chem.* **2017**, *89* (11), 5734–5741. https://doi.org/10.1021/acs.analchem.6b03751.

(55) Yue, H.; He, Y.; Fan, E.; Wang, L.; Lu, S.; Fu, Z. Label-Free Electrochemiluminescent Biosensor for Rapid and Sensitive Detection of Pseudomonas Aeruginosa Using Phage as Highly Specific Recognition Agent. *Biosens. Bioelectron.* **2017**, *94* (November 2016), 429–432. https://doi.org/10.1016/j.bios.2017.03.033.

(56) Zhou, Y.; Ramasamy, R. P. Isolation and Separation of Listeria Monocytogenes Using Bacteriophage P100-Modified Magnetic Particles. *Colloids Surfaces B Biointerfaces* **2019**, *175*, 421–427. https://doi.org/10.1016/j.colsurfb.2018.12.007.

(57) Tawil, N.; Sacher, E.; Mandeville, R.; Meunier, M. Surface Plasmon Resonance Detection of E. Coli and Methicillin-Resistant S. Aureus Using Bacteriophages. *Biosens. Bioelectron.* **2012**, *37* (1), 24–29. https://doi.org/10.1016/j.bios.2012.04.048.

(58) Naidoo, R.; Singh, A.; Arya, S. K.; Beadle, B.; Glass, N.; Tanha, J.; Szymanski, C. M.; Evoy, S. Surface-Immobilization of Chromatographically Purified Bacteriophages for the Optimized Capture of Bacteria. *Bacteriophage* **2012**, *2* (1), 15–24. https://doi.org/10.4161/bact.19079.

(59) Tlili, C.; Sokullu, E.; Safavieh, M.; Tolba, M.; Ahmed, M. U.; Zourob, M. Bacteria Screening, Viability, And Confirmation Assays Using Bacteriophage-Impedimetric/Loop-Mediated Isothermal Amplification Dual-Response Biosensors. *Anal. Chem.* **2013**.

(60) Cademartiri, R.; Anany, H.; Gross, I.; Bhayani, R.; Griffiths, M.; Brook, M. A. Immobilization of Bacteriophages on Modified Silica Particles. *Biomaterials* **2010**, *31* (7), 1904–1910. https://doi.org/10.1016/j.biomaterials.2009.11.029.

(61) Fernandes, E.; Martins, V. C.; Nóbrega, C.; Carvalho, C. M.; Cardoso, F. A.; Cardoso, S.; Dias, J.; Deng, D.; Kluskens, L. D.; Freitas, P. P.; Azeredo, J. A Bacteriophage Detection Tool for Viability Assessment of Salmonella Cells. *Biosens. Bioelectron.* **2014**, *52*, 239–246. https://doi.org/10.1016/j.bios.2013.08.053.

(62) Bhardwaj, N.; Bhardwaj, S.; Devi, P.; Dahiya, S.; SingLa, M. L.; Ghanshyam, C.; Prasad, M. Phage Immobilized Antibacterial Silica Nanoplatform: Application against Bacterial Infections. *Adv. Anim. Vet. Sci.* **2015**, *3* (1s), 1–9. https://doi.org/10.14737/journal.aavs/2015/3.1s.1.9.

(63) Bhardwaj, N.; Bhardwaj, S. K.; Mehta, J.; Nayak, M. K.; Deep, A. Bacteriophage Conjugated IRMOF-3 as a Novel Opto-Sensor for S. Arlettae. *New J. Chem.* **2016**, *40* (9), 8068–8073. https://doi.org/10.1039/c6nj00899b.

(64) Bhardwaj, N.; Bhardwaj, S. K.; Mehta, J.; Kim, K. H.; Deep, A. MOF-Bacteriophage Biosensor for Highly Sensitive and Specific Detection of Staphylococcus Aureus. *ACS Appl. Mater. Interfaces* **2017**, *9* (39), 33589–33598. https://doi.org/10.1021/acsami.7b07818.

(65) Shabani, A.; Marquette, C. A.; Mandeville, R.; Lawrence, M. F. Carbon Microarrays for

the Direct Impedimetric Detection of Bacillus Anthracis Using Gamma Phages as Probes. *Analyst* **2013**, *138* (5), 1434–1440. https://doi.org/10.1039/c3an36830k.

(66) He, F.; Xiang, M.; Mi, X. A New Bacteriophage-Modified Piezoelectric Sensor for Rapid and Specific Detection of Mycobacterium. *Anal. Lett.* **2012**, *45* (10), 1242–1253. https://doi.org/10.1080/00032719.2012.673106.

(67) Handa, H.; Gurczynski, S.; Jackson, M. P.; Auner, G.; Walker, J.; Mao, G. Recognition of Salmonella Typhimurium by Immobilized Phage P22 Monolayers. *Surf. Sci.* **2008**, *602* (7), 1392–1400. https://doi.org/10.1016/j.susc.2008.01.036.

(68) Liébana, S.; Spricigo, D. A.; Cortés, M. P.; Barbé, J.; Llagostera, M.; Alegret, S.; Pividori, M. I. Phagomagnetic Separation and Electrochemical Magneto-Genosensing of Pathogenic Bacteria. *Anal. Chem.* **2013**, *85* (6), 3079–3086. https://doi.org/10.1021/ac3024944.

(69) Laube, T.; Cortés, P.; Llagostera, M.; Alegret, S.; Pividori, M. I. Phagomagnetic Immunoassay for the Rapid Detection of Salmonella. *Appl. Microbiol. Biotechnol.* **2014**, *98* (4), 1795–1805. https://doi.org/10.1007/s00253-013-5434-4.

(70) Rippa, M.; Castagna, R.; Zhou, J.; Paradiso, R.; Borriello, G.; Bobeico, E.; Petti, L. Dodecagonal Plasmonic Quasicrystals for Phage-Based Biosensing. *Nanotechnology* **2018**, *29* (40). https://doi.org/10.1088/1361-6528/aad2f5.

(71) Imai, M.; Mine, K.; Tomonari, H.; Uchiyama, J.; Matuzaki, S.; Niko, Y.; Hadano, S.; Watanabe, S. Dark-Field Microscopic Detection of Bacteria Using Bacteriophage-Immobilized SiO2@AuNP Core-Shell Nanoparticles. *Anal. Chem.* **2019**, *91* (19), 12352–12357. https://doi.org/10.1021/acs.analchem.9b02715.

(72) Tawil, N.; Sacher, E.; Mandeville, R.; Meunier, M. Strategies for the Immobilization of Bacteriophages on Gold Surfaces Monitored by Surface Plasmon Resonance and Surface Morphology. *J. Phys. Chem. C* **2013**, *117* (13), 6686–6691. https://doi.org/10.1021/jp400565m.

(73) Szermer-Olearnik, B.; Drab, M.; Makosa, M.; Zembala, M.; Barbasz, J.; Dabrowska, K.; Boratyński, J. Aggregation/Dispersion Transitions of T4 Phage Triggered by Environmental Ion Availability. *J. Nanobiotechnology* **2017**, *15* (1), 1–15. https://doi.org/10.1186/s12951-017-0266-5.

(74) Langlet, J.; Gaboriaud, F.; Duval, J. F. L.; Gantzer, C. Aggregation and Surface Properties of F-Specific RNA Phages: Implication for Membrane Filtration Processes. *Water Res.* **2008**, *42* (10–11), 2769–2777. https://doi.org/10.1016/j.watres.2008.02.007.

(75) Langlet, J.; Gaboriaud, F.; Gantzer, C. Effects of PH on Plaque Forming Unit Counts and Aggregation of MS2 Bacteriophage. *J. Appl. Microbiol.* **2007**, *103* (5), 1632–1638. https://doi.org/10.1111/j.1365-2672.2007.03396.x.

(76) Ackermann, H. W. Bacteriophage Observations and Evolution. *Res. Microbiol.* **2003**, *154* (4), 245–251. https://doi.org/10.1016/S0923-2508(03)00067-6.

(77) Baran, G. J.; Bloomfield, V. A. Tail-Fiber Attachement in Bacteriophage T4D Studied by

Quasielastic Light Scattering–Band Electrophoresis. *Biopolymers* **1978**, *17* (8), 2015–2028. https://doi.org/10.1002/bip.1978.360170815.

(78) Richter, Ł.; Matuła, K.; Leśniewski, A.; Kwaśnicka, K.; Łoś, J.; Łoś, M.; Paczesny, J.; Hołyst, R. Ordering of Bacteriophages in the Electric Field: Application for Bacteria Detection. *Sensors Actuators B Chem.* **2016**, *224*, 233–240. https://doi.org/10.1016/j.snb.2015.09.042.

(79) Kwak, E. A.; Jaworski, J. Controlled Surface Immobilization of Viruses via Site-Specific Enzymatic Modification. *J. Mater. Chem. B* **2013**, *1* (28), 3486–3493. https://doi.org/10.1039/c3tb20526f.

(80) Ahn, S.; Jeon, S.; Kwak, E. A.; Kim, J. M.; Jaworski, J. Virus-Based Surface Patterning of Biological Molecules, Probes, and Inorganic Materials. *Colloids Surfaces B Biointerfaces* **2014**, *122*, 851–856. https://doi.org/10.1016/j.colsurfb.2014.08.019.

(81) Zurier, H. S.; Duong, M. M.; Goddard, J. M.; Nugen, S. R. Engineering Biorthogonal Phage-Based Nanobots for Ultrasensitive, in Situ Bacteria Detection. *ACS Appl. Bio Mater.* **2020**, *3* (9), 5824–5831. https://doi.org/10.1021/acsabm.0c00546.

(82) Edgar, R.; McKinstry, M.; Hwang, J.; Oppenheim, A. B.; Fekete, R. A.; Giulian, G.; Merril, C.; Nagashima, K.; Adhya, S. High-Sensitivity Bacterial Detection Using Biotin-Tagged Phage and Quantum-Dot Nanocomplexes. *Proc. Natl. Acad. Sci. U. S. A.* **2006**, *103* (13), 4841–4845. https://doi.org/10.1073/pnas.0601211103.

(83) Tolba, M.; Minikh, O.; Brovko, L. Y.; Evoy, S.; Griffiths, M. W.; Tolba, M.; Brovko, L. Y.; Minikh, O. Oriented Immobilization of Bacteriophages for Biosensor Applications. *Appl. Environ. Microbiol.* **2010**, *76* (2), 528–535. https://doi.org/10.1128/AEM.02294-09.

(84) White, S. J.; Johnson, S.; Szymonik, M.; Wardingley, R. A.; Pye, D.; Giles Davies, A.; Wälti, C.; Stockley, P. G. Directed Surface Attachment of Nanomaterials via Coiled-Coil-Driven Self-Assembly. *Nanotechnology* **2012**, *23* (49). https://doi.org/10.1088/0957-4484/23/49/495304.

(85) Korkmaz, N. Recombinant Bacteriophages as Gold Binding Bio-Templates. *Colloids Surfaces B Biointerfaces* **2013**, *112*, 219–228. https://doi.org/10.1016/j.colsurfb.2013.07.063.

(86) Sawada, T.; Serizawa, T. Immobilization of Highly Oriented Filamentous Viruses onto Polymer Substrates. *J. Mater. Chem. B* **2013**, *1* (2), 149–152. https://doi.org/10.1039/c2tb00066k.

(87) Kim, Y. J.; Jin, Y. H.; Salieb-Beugelaar, G. B.; Nam, C. H.; Stieglitz, T. Genetically Engineered Bacteriophage Delivers a Tumor Necrosis Factor Alpha Antagonist Coating on Neural Electrodes. *Biomed. Mater.* **2014**, *9* (1). https://doi.org/10.1088/1748-6041/9/1/015009.

(88) Gervais, L.; Gel, M.; Allain, B.; Tolba, M.; Brovko, L.; Zourob, M.; Mandeville, R.; Griffiths, M.; Evoy, S. Immobilization of Biotinylated Bacteriophages on Biosensor Surfaces. *Sensors Actuators, B Chem.* **2007**, *125* (2), 615–621.

https://doi.org/10.1016/j.snb.2007.03.007.

(89) Minikh, O.; Tolba, M.; Brovko, L. Y.; Griffiths, M. W. Bacteriophage-Based Biosorbents Coupled with Bioluminescent ATP Assay for Rapid Concentration and Detection of Escherichia Coli. *J. Microbiol. Methods* **2010**, *82* (2), 177–183. https://doi.org/10.1016/j.mimet.2010.05.013.

(90) Hermanson, G. T. *Bioconjugate Techniques*, 3rd ed.; Elsevier, 2013.

(91) *Phage Display: Methods and Protocols*, 1st ed.; Hust, M., Lim, T. S., Eds.; Humana Press, 2018.

(92) Hosseinidoust, Z.; Olsson, A. L. J.; Tufenkji, N. Going Viral: Designing Bioactive Surfaces with Bacteriophage. *Colloids Surfaces B Biointerfaces* **2014**, *124*, 2–16. https://doi.org/10.1016/j.colsurfb.2014.05.036.

(93) Archer, M. J.; Liu, J. L. Bacteriophage T4 Nanoparticles as Materials in Sensor Applications: Variables That Influence Their Organization and Assembly on Surfaces. *Sensors* **2009**, *9* (8), 6298–6311. https://doi.org/10.3390/s90806298.

(94) Serwer, P.; Hayes, S. J. Agarose Gel Electrophoresis of Bacteriophages and Related Particles. I. Avoidance of Binding to the Gel and Recognizing of Particles with Packaged DNA. *Electrophoresis* **1982**, *3* (2), 76–80. https://doi.org/10.1002/elps.1150030203.

(95) Leppänen, M.; Maasilta, I. J.; Sundberg, L. R. Antibacterial Efficiency of Surface-Immobilized Flavobacterium-Infecting Bacteriophage. *ACS Appl. Bio Mater.* **2019**, *2* (11), 4720–4727. https://doi.org/10.1021/acsabm.9b00242.

(96) Busch, R. T.; Karim, F.; Weis, J.; Sun, Y.; Zhao, C.; Vasquez, E. S. Optimization and Structural Stability of Gold Nanoparticle-Antibody Bioconjugates. *ACS omega* **2019**, *4* (12), 15269–15279. https://doi.org/10.1021/acsomega.9b02276.

(97) Couto, C.; Vitorino, R.; Daniel-da-silva, A. L. Gold Nanoparticles and Bioconjugation : A Pathway for Proteomic Applications Applications. *Crit. Rev. Biotechnol.* **2016**, *8551* (February). https://doi.org/10.3109/07388551.2016.1141392.

(98) Love, J. C.; Estroff, L. A.; Kriebel, J. K.; Nuzzo, R. G.; Whitesides, G. M. *Self-Assembled Monolayers of Thiolates on Metals as a Form of Nanotechnology*; 2005; Vol. 105. https://doi.org/10.1021/cr0300789.

(99) Huang, S.; Hu, J.; Wan, J.; Johnson, M. L.; Shu, H.; Chin, B. A. The Effect of Annealing and Gold Deposition on the Performance of Magnetoelastic Biosensors. *Mater. Sci. Eng. C* **2008**, *28*, 380–386. https://doi.org/10.1016/j.msec.2007.04.006.

(100) Janshoff, A.; Galla, H.; Steinem, C. Piezoelectric Mass-Sensing Devices as Biosensors: An Alternative to Optical Biosensors? *Angew Chem Int Ed Engl.* **2000**, *39* (22), 4004–4032. https://doi.org/10.1002/1521-3773(20001117)39:22<4004::aid-anie4004>3.0.co;2-2.

(101) Amendola, V.; Pilot, R.; Frasconi, M. Surface Plasmon Resonance in Gold Nanoparticles : A Review. *J. Phys. Condens. Matter* **2017**, *29* (20). https://doi.org/10.1088/1361-

648X/aa60f3.

(102) Schasfoort, R. B. M. *Handbook of Surface Plasmon Resonance*, 2nd ed.; Schasfoort, R. B. M., Ed.; Royal Society of Chemistry, 2017. https://doi.org/10.1039/9781788010283.

(103) Shabani, A.; Marquette, C. A.; Mandeville, R.; Lawrence, M. F. Magnetically-Assisted Impedimetric Detection of Bacteria Using Phage-Modified Carbon Microarrays. *Talanta* **2013**, *116*, 1047–1053. https://doi.org/10.1016/j.talanta.2013.07.078.

(104) Zhang, Y.; Yan, C.; Yang, H.; Yu, J.; Wei, H. Rapid and Selective Detection of E. Coli O157:H7 Combining Phagomagnetic Separation with Enzymatic Colorimetry. *Food Chem.* **2017**, *234*, 332–338. https://doi.org/10.1016/j.foodchem.2017.05.013.

(105) Sun, W.; Brovko, L.; Griffiths, M. Use of Bioluminescent Salmonella for Assessing the Efficiency of Constructed Phage-Based Biosorbent. *J. Ind. Microbiol. Biotechnol.* **2001**, *27* (2), 126–128. https://doi.org/10.1038/sj.jim.7000198.

(106) Lee, P. T.; Goncalves, L. M.; Compton, R. G. Electrochemical Determination of Free and Total Glutathione in Human Saliva Samples. *Sensors Actuators B Chem.* **2015**, *221*, 962–968. https://doi.org/https://doi.org/10.1016/j.snb.2015.07.050.

(107) Filik, H.; Aslıhan Avan, A. Conducting Polymer Modified Screen-Printed Carbon Electrode Coupled with Magnetic Solid Phase Microextraction for Determination of Caffeine. *Food Chem.* **2018**, *242*, 301–307. https://doi.org/https://doi.org/10.1016/j.foodchem.2017.09.068.

(108) Hayat, A.; Marty, J. Disposable Screen Printed Electrochemical Sensors: Tools for Environmental Monitoring. *Sensors* **2014**, *14* (6), 10432–10453. https://doi.org/10.3390/s140610432.

(109) González-Sánchez, M. I.; Gómez-Monedero, B.; Agrisuelas, J.; Iniesta, J.; Valero, E. Highly Activated Screen-Printed Carbon Electrodes by Electrochemical Treatment with Hydrogen Peroxide. *Electrochem. commun.* **2018**, *91* (February), 36–40. https://doi.org/10.1016/j.elecom.2018.05.002.

(110) Shabani, A.; Zourob, M.; Allain, B.; Marquette, C. A.; Lawrence, M. F.; Mandeville, R. Bacteriophage-Modified Microarrays for the Direct Impedimetric Detection of Bacteria. *Anal. Chem.* **2008**, *80* (24), 9475–9482.

(111) Bhardwaj, N.; Bhardwaj, S. K.; Mehta, J.; Mohanta, G. C.; Deep, A. Bacteriophage Immobilized Graphene Electrodes for Impedimetric Sensing of Bacteria (Staphylococcus Arlettae). *Anal. Biochem.* **2016**, *505*, 18–25. https://doi.org/10.1016/j.ab.2016.04.008.

(112) Farooq, U.; Ullah, M. W.; Yang, Q.; Aziz, A.; Xu, J.; Zhou, L.; Wang, S. High-Density Phage Particles Immobilization in Surface-Modified Bacterial Cellulose for Ultra-Sensitive and Selective Electrochemical Detection of Staphylococcus Aureus. *Biosens. Bioelectron.* **2020**, *157* (March), 112163. https://doi.org/10.1016/j.bios.2020.112163.

(113) Wang, S.; Humphreys, E. S.; Chung, S. Y.; Delduco, D. F.; Lustig, S. R.; Wang, H.; Parker, K. N.; Rizzo, N. W.; Subramoney, S.; Chiang, Y. M.; Jagota, A. Peptides with Selective

Affinity for Carbon Nanotubes. *Nat. Mater.* **2003**, *2* (3), 196–200. https://doi.org/10.1038/nmat833.

(114) Li, X.; Chen, W.; Zhan, Q.; Dai, L.; Sowards, L.; Pender, M.; Naik, R. R. Direct Measurements of Interactions between Polypeptides and Carbon Nanotubes. *J. Phys. Chem. B* **2006**, *110* (25), 12621–12625. https://doi.org/10.1021/jp061518d.

(115) Kase, D.; Kulp, J. L.; Yudasaka, M.; Evans, J. S.; Iijima, S.; Shiba, K. Affinity Selection of Peptide Phage Libraries against Single-Wall Carbon Nanohorns Identifies a Peptide Aptamer with Conformational Variability. *Langmuir* **2004**, *20* (20), 8939–8941. https://doi.org/10.1021/la048968m.

(116) Morita, Y.; Ohsugi, T.; Iwasa, Y.; Tamiya, E. A Screening of Phage Displayed Peptides for the Recognition of Fullerene (C60). *J. Mol. Catal. B Enzym.* **2004**, *28* (4–6), 185–190. https://doi.org/10.1016/j.molcatb.2004.01.018.

(117) Sulakvelidze, A.; Markoishvili, K.; Tsitlanadze, G.; Katsarava, R.; Morris Jr., J. G. A Novel Sustained-Release Matrix Based on Biodegradable Poly(Ester Amide)s and Impregnated with Bacteriophages and an Antibiotic Shows Promise in Management of Infected Venous Stasis Ulcers and Other Poorly Healing Wounds. *Int. J. Dermatol.* **2002**, *41* (7), 453–458. https://doi.org/10.1046/j.1365-4362.2002.01451.x.

(118) Ma, W.; Panecka, M.; Tufenkji, N.; Rahaman, M. S. Bacteriophage-Based Strategies for Biofouling Control in Ultrafiltration: In Situ Biofouling Mitigation, Biocidal Additives and Biofilm Cleanser. *J. Colloid Interface Sci.* **2018**, *523*, 254–265. https://doi.org/10.1016/j.jcis.2018.03.105.

(119) Lentini, G.; Franco, D.; Fazio, E.; De Plano, L. M.; Trusso, S.; Carnazza, S.; Neri, F.; Guglielmino, S. P. P. Rapid Detection of Pseudomonas Aeruginosa by Phage-Capture System Coupled with Micro-Raman Spectroscopy. *Vib. Spectrosc.* **2016**, *86*, 1–7. https://doi.org/10.1016/j.vibspec.2016.05.003.

(120) Mazhorova, A.; Markov, A.; Ung, B.; Ng, A.; Chinnappan, R.; Zourob, M.; Skorobogatiy, M. Label-Free Bacteria Detection Using Evanescent Mode of a Suspended Core Terahertz Fiber. *2012 Conf. Lasers Electro-Optics, CLEO 2012* **2012**, *20* (5), 20675–20683. https://doi.org/10.1364/oe.20.005344.

(121) Arter, J. A.; Taggart, D. K.; McIntire, T. M.; Penner, R. M.; Weiss, G. A. Virus-PEDOT Nanowires for Biosensing. *Nano Lett.* **2010**, *10* (12), 4858–4862. https://doi.org/10.1021/nl1025826.

(122) Donavan, K. C.; Arter, J. A.; Weiss, G. A.; Penner, R. M. Virus-Poly(3,4-Ethylenedioxythiophene) Biocomposite Films. *Langmuir* **2012**, *28* (34), 12581–12587. https://doi.org/10.1021/la302473j.

(123) Adey, N. B.; Mataragnon, A. H.; Rider, J. E.; Carter, J. M.; Kay, B. K. Characterization of Phage That Bind Plastic from Phage-Displayed Random Peptide Libraries. *Gene* **1995**, *156* (1), 27–31. https://doi.org/10.1016/0378-1119(95)00058-E.

(124) Berglund, J.; Lindbladh, C.; Nicholls, I. A.; Mosbach, K. Selection of Phage Display

Combinatorial Library Peptides with Affinity for a Yohimbine Imprinted Methacrylate Polymer. *Anal. Commun.* **1998**, *35* (January), 3–7. https://doi.org/10.1039/A708046H.

(125) Sanghvi, A. B.; Miller, K. P.; Belcher, A. M.; Schmidt, C. E. Biomaterials Functionalization Using a Novel Peptide That Selectively Binds to a Conducting Polymer. *Nat. Mater.* **2005**, *4* (June). https://doi.org/10.1038/nmat1397.

(126) Serizawa, T.; Sawada, T.; Matsuno, H.; Matsubara, T.; Sato, T. A Peptide Motif Recognizing a Polymer Stereoregularity. *J. Am. Chem. Soc.* **2005**, *127* (40), 13780–13781. https://doi.org/10.1021/ja054402o.

(127) Serizawa, T.; Sawada, T.; Kitayama, T. Peptide Motifs That Recognize Differences in Polymer-Film Surfaces. *Angew. Chemie* **2007**, *46* (5), 723–726. https://doi.org/10.1002/anie.200603212.

(128) Serizawa, T.; Sawada, T.; Matsuno, H. Highly Specific Affinities of Short Peptides against Synthetic Polymers. *Langmuir* **2007**, *23* (11), 11127–11133. https://doi.org/10.1021/la701822n.

(129) Serizawa, T.; Techawanitchai, P. Isolation of Peptides That Can Recognize Syndiotactic Polystyrene. *ChemBioChem* **2007**, *8* (9), 989–993. https://doi.org/10.1002/cbic.200700133.

(130) Kamide, K. *Cellulose and Cellulose Derivatives*; Kamide, K. B. T.-C. and C. D., Ed.; Elsevier: Amsterdam, 2005. https://doi.org/https://doi.org/10.1016/B978-044482254-3/50003-5.

(131) Kamel, S.; Ali, N.; Jahangir, K.; Shah, S. M. Pharmaceutical Significance of Cellulose : A Review. **2008**, *2* (11), 758–778. https://doi.org/10.3144/expresspolymlett.2008.90.

(132) Dincer, C.; Bruch, R.; Costa-rama, E.; Fernández-abedul, M. T.; Merkoçi, A.; Manz, A.; Urban, G. A.; Güder, F. Disposable Sensors in Diagnostics , Food , and Environmental Monitoring. **2019**, *1806739*. https://doi.org/10.1002/adma.201806739.

(133) Links, D. A. Portable Self-Contained Cultures for Phage and Bacteria Made of Paper and Tape. *Lab Chip* **2012**. https://doi.org/10.1039/c2lc40391a.

(134) Jabrane, T.; Dubé, M.; Mangin, P. J. Bacteriophage Immobilization on Paper Surface: Effect of Cationic Pre-Coat Layer. **2009**.

(135) Jabrane, T.; Jeaidi, J.; Dubé, M.; Mangin, P. J. Gravure Printing of Enzymes and Phages. *Adv Print Media Technol* **2008**, *35* (January), 279–288.

(136) Jabrane, T.; Laloi, M.; Dubé, M.; Mangin, P. Printing and Coating of T4 Phage Based Bioactive Paper. *Adv. Print. Media Technol.* **2010**, *37* (November 2014), 351–358.

(137) Yetisen, A. K.; Akram, M. S.; Lowe, C. R. Paper-Based Microfluidic Point-of-Care Diagnostic Devices. *Lab Chip* **2013**, 8–15. https://doi.org/10.1039/c3lc50169h.

(138) Tortorich, R. P.; Shamkhalichenar, H.; Choi, J. Inkjet-Printed and Paper-Based Electrochemical Sensors. **2018**. https://doi.org/10.3390/app8020288.

(139) Kong, M.; Shin, J. H.; Heu, S.; Park, J.-K.; Ryu, S. Lateral Flow Assay-Based Bacterial Detection Using Engineered Cell Wall Binding Domains of a Phage Endolysin. *Biosens. Bioelectron.* **2017**, *96*, 173–177. https://doi.org/10.1016/j.bios.2017.05.010.

(140) Shoseyov, O.; Shani, Z.; Levy, I. Carbohydrate Binding Modules : Biochemical Properties and Novel Applications. **2006**, *70* (2), 283–295. https://doi.org/10.1128/MMBR.00028-05.

(141) Tripathi, S. M.; Bock, W. J.; Mikulic, P.; Chinnappan, R.; Ng, A.; Tolba, M.; Zourob, M. Long Period Grating Based Biosensor for the Detection of Escherichia Coli Bacteria. *Biosens. Bioelectron.* **2012**, *35* (1), 308–312. https://doi.org/10.1016/j.bios.2012.03.006.

(142) Li, Y.; HuiMa; Gan, L.; Gong, A.; Zhang, H.; Liu, D.; Sun, Q. Immobilized Optical Fiber Microprobe for Selective and Sensitive Escherichia Coli Detection. *J. Biophotonics* **2017**. https://doi.org/10.1002/jbio.201700162.

(143) Smietana, M.; Bock, W. J.; Mikulic, P.; Ng, A.; Chinnappan, R.; Zourob, M. Detection of Bacteria Using Bacteriophages as Recognition Elements Immobilized on Long-Period Fiber Gratings. *Opt. Express* **2011**, *19* (9), 7971. https://doi.org/10.1364/oe.19.007971.

(144) Handa, H.; Gurczynski, S.; Jackson, M. P.; Mao, G. Immobilization and Molecular Interactions between Bacteriophage and Lipopolysaccharide Bilayers. *Langmuir* **2010**, *26* (14), 12095–12103. https://doi.org/10.1021/la1013413.

(145) Jeon, D. Y.; Hwang, K. H.; Park, S. J.; Kim, Y. J.; Joo, M. K.; Ahn, S. E.; Kim, G. T.; Nam, C. H. Controlled Surface Adsorption of Fd Filamentous Phage by Tuning of the PH and the Functionalization of the Surface. *J. Appl. Phys.* **2011**, *109* (6). https://doi.org/10.1063/1.3549113.

(146) Bone, S.; Alum, A.; Markovski, J.; Hristovski, K.; Bar-Zeev, E.; Kaufman, Y.; Abbaszadegan, M.; Perreault, F. Physisorption and Chemisorption of T4 Bacteriophages on Amino Functionalized Silica Particles. *J. Colloid Interface Sci.* **2018**, *532*, 68–76. https://doi.org/10.1016/j.jcis.2018.07.107.

(147) Yoo, S. Y.; Oh, J. W.; Lee, S. W. Phage-Chips for Novel Optically Readable Tissue Engineering Assays. *Langmuir* **2012**, *28* (4), 2166–2172. https://doi.org/10.1021/la203840n.

(148) Koh, E. H.; Mun, C.; Kim, C.; Park, S. G.; Choi, E. J.; Kim, S. H.; Dang, J.; Choo, J.; Oh, J. W.; Kim, D. H.; Jung, H. S. M13 Bacteriophage/Silver Nanowire Surface-Enhanced Raman Scattering Sensor for Sensitive and Selective Pesticide Detection. *ACS Appl. Mater. Interfaces* **2018**, *10* (12), 10388–10397. https://doi.org/10.1021/acsami.8b01470.

(149) Chen, C.; Wang, J. Optical Biosensors: An Exhaustive and Comprehensive Review. *Analyst* **2020**, *145* (5), 1605–1628. https://doi.org/10.1039/c9an01998g.

(150) Pinet, E.; Pham, A.; Rioux, S. Miniature Fiber Optic Pressure Sensor for Medical Applications: An Opportunity for Intra-Aortic Balloon Pumping (IABP) Therapy. *17th Int. Conf. Opt. Fibre Sensors* **2005**, *5855* (418), 234. https://doi.org/10.1117/12.623806.

(151) Hamel, C.; Pinet, É. Temperature and Pressure Fiber-Optic Sensors Applied to Minimally

Invasive Diagnostics and Therapies. *Opt. Fibers Sensors Med. Diagnostics Treat. Appl. VI* **2006**, *6083*, 608306. https://doi.org/10.1117/12.659935.

(152) Phillips, K. S.; Cheng, Q. J. *Surface Plasmon Resonance*; Mol, N. J. de, Fischer, M. J. E., Eds.; Humana Press, 2008. https://doi.org/10.1007/978-1-60327-375-6_46.

(153) Liu, F.; Luo, Z.; Ding, X.; Zhu, S.; Yu, X. Phage-Displayed Protein Chip Based on SPR Sensing. *Sensors Actuators, B Chem.* **2009**, *136* (1), 133–137. https://doi.org/10.1016/j.snb.2008.11.031.

(154) Karoonuthaisiri, N.; Charlermroj, R.; Morton, M. J.; Oplatowska-Stachowiak, M.; Grant, I. R.; Elliott, C. T. Development of a M13 Bacteriophage-Based SPR Detection Using Salmonella as a Case Study. *Sensors Actuators, B Chem.* **2014**, *190*, 214–220. https://doi.org/10.1016/j.snb.2013.08.068.

(155) Choi, I. Y.; Park, J. H.; Gwak, K. M.; Kim, K. P.; Oh, J. H.; Park, M. K. Studies on Lytic, Tailed Bacillus Cereus-Specific Phage for Use in a Ferromagnetoelastic Biosensor as a Novel Recognition Element. *J. Microbiol. Biotechnol.* **2018**, *28* (1), 87–94. https://doi.org/10.4014/jmb.1710.10033.

(156) Xu, J. Bacteriophage Based Micro Electrochemical Sensors and Extended Gate FET Sensors for Bacteria Detection. **2019**.

(157) Xu, J.; Zhao, C.; Chau, Y.; Lee, Y. K. The Synergy of Chemical Immobilization and Electrical Orientation of T4 Bacteriophage on a Micro Electrochemical Sensor for Low-Level Viable Bacteria Detection via Differential Pulse Voltammetry. *Biosens. Bioelectron.* **2020**, *151* (June 2019), 111914. https://doi.org/10.1016/j.bios.2019.111914.

(158) Sedki, M.; Chen, X.; Chen, C.; Ge, X.; Mulchandani, A. Non-Lytic M13 Phage-Based Highly Sensitive Impedimetric Cytosensor for Detection of Coliforms. *Biosens. Bioelectron.* **2020**, *148* (September 2019), 111794. https://doi.org/10.1016/j.bios.2019.111794.

(159) Ma, L.; Green, S. I.; Trautner, B. W.; Ramig, R. F.; Maresso, A. W. Metals Enhance the Killing of Bacteria by Bacteriophage in Human Blood. *Sci. Rep.* **2018**, *8* (1), 1–11. https://doi.org/10.1038/s41598-018-20698-2.

(160) Grabarek, Z.; Gergely, J. Zero-Length Crosslinking Procedure with the Use of Active Esters. *Anal. Biochem.* **1990**, *185* (1), 131–135. https://doi.org/https://doi.org/10.1016/0003-2697(90)90267-D.

(161) Singh, A.; Arya, S. K.; Glass, N.; Hanifi-Moghaddam, P.; Naidoo, R.; Szymanski, C. M.; Tanha, J.; Evoy, S. Bacteriophage Tailspike Proteins as Molecular Probes for Sensitive and Selective Bacterial Detection. *Biosens. Bioelectron.* **2010**, *26* (1), 131–138. https://doi.org/10.1016/j.bios.2010.05.024.

(162) Peng, H.; Chen, I. A. Rapid Colorimetric Detection of Bacterial Species through the Capture of Gold Nanoparticles by Chimeric Phages. *ACS Nano* **2019**, *13* (2), 1244–1252. https://doi.org/10.1021/acsnano.8b06395.

(163) Lenz, R. W.; Marchessault, R. H. Bacterial Polyesters: Biosynthesis, Biodegradable Plastics and Biotechnology. *Biomacromolecules* **2005**, *6* (1), 1–8. https://doi.org/10.1021/bm049700c.

(164) Vericat, C.; Vela, M. E.; Benitez, G.; Carro, P.; Salvarezza, R. C. Self-Assembled Monolayers of Thiols and Dithiols on Gold: New Challenges for a Well-Known System. *Chem. Soc. Rev.* **2010**, *39* (5), 1805–1834. https://doi.org/10.1039/b907301a.

(165) Singh, A.; Glass, N.; Tolba, M.; Brovko, L.; Griffiths, M.; Evoy, S. Immobilization of Bacteriophages on Gold Surfaces for the Specific Capture of Pathogens. *Biosens. Bioelectron.* **2009**, *24* (12), 3645–3651. https://doi.org/10.1016/j.bios.2009.05.028.

(166) Arya, S. K.; Singh, A.; Naidoo, R.; Wu, P.; McDermott, M. T.; Evoy, S. Chemically Immobilized T4-Bacteriophage for Specific Escherichia Coli Detection Using Surface Plasmon Resonance. *Analyst* **2011**, *136* (3), 486–492. https://doi.org/10.1039/c0an00697a.

(167) Richter, Ł.; Bielec, K.; Leśniewski, A.; Łoś, M.; Paczesny, J.; Hołyst, R. Dense Layer of Bacteriophages Ordered in Alternating Electric Field and Immobilized by Surface Chemical Modification as Sensing Element for Bacteria Detection. *ACS Appl. Mater. Interfaces* **2017**, *9* (23), 19622–19629. https://doi.org/10.1021/acsami.7b03497.

(168) Srivastava, S. K.; Hamo, H. Ben; Kushmaro, A.; Marks, R. S.; Grüner, C.; Rauschenbach, B.; Abdulhalim, I. Highly Sensitive and Specific Detection of E. Coli by a SERS Nanobiosensor Chip Utilizing Metallic Nanosculptured Thin Films. *Analyst* **2015**, *140* (9), 3201–3209. https://doi.org/10.1039/c5an00209e.

(169) Horikawa, S.; Bedi, D.; Li, S.; Shen, W.; Huang, S.; Chen, I. H.; Chai, Y.; Auad, M. L.; Bozack, M. J.; Barbaree, J. M.; Petrenko, V. A.; Chin, B. A. Effects of Surface Functionalization on the Surface Phage Coverage and the Subsequent Performance of Phage-Immobilized Magnetoelastic Biosensors. *Biosens. Bioelectron.* **2011**, *26* (5), 2361–2367. https://doi.org/10.1016/j.bios.2010.10.012.

(170) Batten, S. R.; Champness, N. R.; Chen, X.; Garcia-martinez, J.; Kitagawa, S.; Öhrström, L.; Keeffe, M. O.; Suh, M. P.; Reedijk, J. Terminology of Metal–Organic Frameworks and Coordination Polymers (IUPAC Recommendations 2013). *Pure Appl. Chem.* **2013**, *85* (8), 1715–1724. https://doi.org/10.1351/PAC-REC-12-11-20.

(171) Li, P.; Klet, R. C.; Moon, S. Y.; Wang, T. C.; Deria, P.; Peters, A. W.; Klahr, B. M.; Park, H. J.; Al-Juaid, S. S.; Hupp, J. T.; Farha, O. K. Synthesis of Nanocrystals of Zr-Based Metal-Organic Frameworks with Csq-Net: Significant Enhancement in the Degradation of a Nerve Agent Simulant. *Chem. Commun.* **2015**, *51* (54), 10925–10928. https://doi.org/10.1039/c5cc03398e.

(172) Niyomdecha, S.; Limbut, W.; Numnuam, A.; Kanatharana, P.; Charlermroj, R.; Karoonuthaisiri, N.; Thavarungkul, P. Phage-Based Capacitive Biosensor for Salmonella Detection. *Talanta* **2018**, *188* (April), 658–664. https://doi.org/10.1016/j.talanta.2018.06.033.

(173) Liana, A. E.; Chia, E. W.; Marquis, C. P.; Gunawan, C.; Gooding, J. J.; Amal, R. Adsorption

of T4 Bacteriophages on Planar Indium Tin Oxide Surface via Controlled Surface Tailoring. *J. Colloid Interface Sci.* **2016**, *468*, 192–199. https://doi.org/10.1016/j.jcis.2016.01.052.

(174) Liana, A. E.; Marquis, C. P.; Gunawan, C.; Justin Gooding, J.; Amal, R. Antimicrobial Activity of T4 Bacteriophage Conjugated Indium Tin Oxide Surfaces. *J. Colloid Interface Sci.* **2018**, *514*, 227–233. https://doi.org/10.1016/j.jcis.2017.12.029.

(175) Ginley, D.; Hosono, H.; Paine, D. C. *Handbook of Transparent Conductors*; Springer, 2010.

(176) Aydın, E. B.; Sezgintürk, M. K. Indium Tin Oxide (ITO): A Promising Material in Biosensing Technology. *Trends Anal. Chem.* **2017**, *97*, 309–315. https://doi.org/https://doi.org/10.1016/j.trac.2017.09.021.

(177) Rana, T. M.; Meares, C. F. N-Terminal Modification of Immunoglobulin Polypeptide Chains Tagged with Isothiocyanato Chelates. *Bioconjug. Chem.* **1990**, *1* (5), 357–362. https://doi.org/10.1021/bc00005a010.

(178) Situmorang, M.; Gooding, J. J.; Hibbert, D. B.; Barnett, D. Electrodeposited Polytyramine as an Immobilisation Matrix for Enzyme Biosensors. *Biosens. Bioelectron.* **1998**, *13* (9), 953–962. https://doi.org/10.1016/S0956-5663(98)00033-5.

(179) Vilian, A. T. E.; Veeramani, V.; Chen, S.-M.; Madhu, R.; Kwak, C. H.; Huh, Y. S.; Han, Y.-K. Immobilization of Myoglobin on Au Nanoparticle-Decorated Carbon Nanotube/Polytyramine Composite as a Mediator-Free H2O2 and Nitrite Biosensor. *Sci. Rep.* **2015**, *5* (1), 18390. https://doi.org/10.1038/srep18390.

(180) Tran, L. D.; Piro, B.; Pham, M. C.; Ledoan, T.; Angiari, C.; Dao, L. H.; Teston, F. A Polytyramine Film for Covalent Immobilization of Oligonucleotides and Hybridization. *Synth. Met.* **2003**, *139* (2), 251–262. https://doi.org/https://doi.org/10.1016/S0379-6779(03)00131-0.

(181) Surface-Activated Dynabeads: Product Portfolio. Life Technologies 2010.

(182) Huang, S.; Yang, H.; Lakshmanan, R. S.; Johnson, M. L.; Wan, J.; Chen, I. H.; Wikle, H. C.; Petrenko, V. A.; Barbaree, J. M.; Chin, B. A. Sequential Detection of Salmonella Typhimurium and Bacillus Anthracis Spores Using Magnetoelastic Biosensors. *Biosens. Bioelectron.* **2009**, *24* (6), 1730–1736. https://doi.org/10.1016/j.bios.2008.09.006.

(183) Shen, W.; Lakshmanan, R. S.; Mathison, L. C.; Petrenko, V. A.; Chin, B. A. Phage Coated Magnetoelastic Micro-Biosensors for Real-Time Detection of Bacillus Anthracis Spores. *Sensors Actuators, B Chem.* **2009**, *137* (2), 501–506. https://doi.org/10.1016/j.snb.2009.01.027.

(184) Li, S.; Li, Y.; Chen, H.; Horikawa, S.; Shen, W.; Simonian, A.; Chin, B. A. Direct Detection of Salmonella Typhimurium on Fresh Produce Using Phage-Based Magnetoelastic Biosensors. *Biosens. Bioelectron.* **2010**, *26* (4), 1313–1319. https://doi.org/10.1016/j.bios.2010.07.029.

(185) Park, M. K.; Oh, J. H.; Chin, B. A. The Effect of Incubation Temperature on the Binding of Salmonella Typhimurium to Phage-Based Magnetoelastic Biosensors. *Sensors Actuators,*

B Chem. **2011**, *160* (1), 1427–1433. https://doi.org/10.1016/j.snb.2011.10.003.

(186) Chai, Y.; Li, S.; Horikawa, S.; Park, M.-K.; Vodyanoy, V.; Chin, B. A. Rapid and Sensitive Detection of Salmonella Typhimurium on Eggshells by Using Wireless Biosensors. *J. Food Prot.* **201AD**, *75* (4), 631–636.

(187) Park, M. K.; Wikle, H. C.; Chai, Y.; Horikawa, S.; Shen, W.; Chin, B. A. The Effect of Incubation Time for Salmonella Typhimurium Binding to Phage-Based Magnetoelastic Biosensors. *Food Control* **2012**, *26* (2), 539–545. https://doi.org/10.1016/j.foodcont.2012.01.061.

(188) Chai, Y.; Wikle, H. C.; Wang, Z.; Horikawa, S.; Best, S.; Cheng, Z.; Dyer, D. F.; Chin, B. A. Design of a Surface-Scanning Coil Detector for Direct Bacteria Detection on Food Surfaces Using a Magnetoelastic Biosensor. *J. Appl. Phys.* **2013**, *114* (10). https://doi.org/10.1063/1.4821025.

(189) Park, M. K.; Park, J. W.; Wikle, H. C.; Chin, B. A. Evaluation of Phage-Based Magnetoelastic Biosensors for Direct Detection of Salmonella Typhimurium on Spinach Leaves. *Sensors Actuators, B Chem.* **2013**, *176*, 1134–1140. https://doi.org/10.1016/j.snb.2012.10.084.

(190) Park, M. K.; Li, S.; Chin, B. A. Detection of Salmonella Typhimurium Grown Directly on Tomato Surface Using Phage-Based Magnetoelastic Biosensors. *Food Bioprocess Technol.* **2013**, *6* (3), 682–689. https://doi.org/10.1007/s11947-011-0708-2.

(191) Chen, I. H.; Horikawa, S.; Bryant, K.; Riggs, R.; Chin, B. A.; Barbaree, J. M. Bacterial Assessment of Phage Magnetoelastic Sensors for Salmonella Enterica Typhimurium Detection in Chicken Meat. *Food Control* **2017**, *71*, 273–278. https://doi.org/10.1016/j.foodcont.2016.07.003.

(192) Park, M.-K.; Chin, B. A. Novel Approach of a Phage-Based Magnetoelastic Biosensor for the Detection of Salmonella Enterica Serovar Typhimurium in Soil. *J. Microbiol. Biotechnol.* **2016**, *26* (12), 2051–2059. https://doi.org/10.4014/jmb.1609.09062.

(193) Wang, F.; Horikawa, S.; Hu, J.; Wikle, H. C.; Chen, I. H.; Du, S.; Liu, Y.; Chin, B. A. Detection of Salmonella Typhimurium on Spinach Using Phage-Based Magnetoelastic Biosensors. *Sensors* **2017**, *17* (2), 1–9. https://doi.org/10.3390/s17020386.

(194) Mejri, M. B.; Baccar, H.; Baldrich, E.; Del Campo, F. J.; Helali, S.; Ktari, T.; Simonian, A.; Aouni, M.; Abdelghani, A. Impedance Biosensing Using Phages for Bacteria Detection: Generation of Dual Signals as the Clue for in-Chip Assay Confirmation. *Biosens. Bioelectron.* **2010**, *26* (4), 1261–1267. https://doi.org/10.1016/j.bios.2010.06.054.

(195) Moghtader, F.; Congur, G.; Zareie, H. M.; Erdem, A.; Piskin, E. Impedimetric Detection of Pathogenic Bacteria with Bacteriophages Using Gold Nanorod Deposited Graphite Electrodes. *RSC Adv.* **2016**, *6* (100), 97832–97839. https://doi.org/10.1039/c6ra18884b.

(196) Li, S.; Horikawa, S.; Park, M. K.; Chai, Y.; Vodyanoy, V. J.; Chin, B. A. Amorphous Metallic Glass Biosensors. *Intermetallics* **2012**, *30*, 80–85. https://doi.org/10.1016/j.intermet.2012.03.030.

(197) Li, Y.; Xie, G.; Qiu, J.; Zhou, D.; Gou, D.; Tao, Y.; Li, Y.; Chen, H. A New Biosensor Based on the Recognition of Phages and the Signal Amplification of Organic-Inorganic Hybrid Nanoflowers for Discriminating and Quantitating Live Pathogenic Bacteria in Urine. *Sensors Actuators, B Chem.* **2018**, *258*, 803–812. https://doi.org/10.1016/j.snb.2017.11.155.

(198) Balasubramanian, S.; Sorokulova, I. B.; Vodyanoy, V. J.; Simonian, A. L. Lytic Phage as a Specific and Selective Probe for Detection of Staphylococcus Aureus — A Surface Plasmon Resonance Spectroscopic Study. *Biosens. Bioelectron.* **2007**, *22* (6), 948–955. https://doi.org/10.1016/j.bios.2006.04.003.

(199) Hiremath, N.; Guntupalli, R.; Vodyanoy, V.; Chin, B. A.; Park, M. K. Detection of Methicillin-Resistant Staphylococcus Aureus Using Novel Lytic Phage-Based Magnetoelastic Biosensors. *Sensors Actuators, B Chem.* **2015**, *210*, 129–136. https://doi.org/10.1016/j.snb.2014.12.083.

(200) Byeon, H. M.; Vodyanoy, V. J.; Oh, J.-H.; Kwon, J.-H.; Park, M.-K. Lytic Phage-Based Magnetoelastic Biosensors for On-Site Detection of Methicillin-Resistant Staphylococcus Aureus on Spinach Leaves. *J. Electrochem. Soc.* **2015**, *162* (8), B230–B235. https://doi.org/10.1149/2.0681508jes.

(201) Nanduri, V.; Bhunia, A. K.; Tu, S. I.; Paoli, G. C.; Brewster, J. D. SPR Biosensor for the Detection of L. Monocytogenes Using Phage-Displayed Antibody. *Biosens. Bioelectron.* **2007**, *23* (2), 248–252. https://doi.org/10.1016/j.bios.2007.04.007.

(202) Lakshmanan, R. S.; Guntupalli, R.; Hu, J.; Petrenko, V. A.; Barbaree, J. M.; Chin, B. A. Detection of Salmonella Typhimurium in Fat Free Milk Using a Phage Immobilized Magnetoelastic Sensor. *Sensors Actuators, B Chem.* **2007**, *126* (2), 544–550. https://doi.org/10.1016/j.snb.2007.04.003.

(203) Lakshmanan, R. S.; Guntupalli, R.; Hu, J.; Kim, D. J.; Petrenko, V. A.; Barbaree, J. M.; Chin, B. A. Phage Immobilized Magnetoelastic Sensor for the Detection of Salmonella Typhimurium. *J. Microbiol. Methods* **2007**, *71* (1), 55–60. https://doi.org/10.1016/j.mimet.2007.07.012.

(204) Fu, L.; Li, S.; Zhang, K.; Chen, I. H.; Petrenko, V. A.; Cheng, Z. Magnetostrictive Microcantilever as an Advanced Transducer for Biosensors. *Sensors* **2007**, *7* (11), 2929–2941. https://doi.org/10.3390/s7112929.

(205) Olsen, E. V.; Sorokulova, I. B.; Petrenko, V. A.; Chen, I. H.; Barbaree, J. M.; Vodyanoy, V. J. Affinity-Selected Filamentous Bacteriophage as a Probe for Acoustic Wave Biodetectors of Salmonella Typhimurium. *Biosens. Bioelectron.* **2006**, *21* (8), 1434–1442. https://doi.org/10.1016/j.bios.2005.06.004.

(206) Kim, Y.-K.; Park, S. J.; Koo, J. P.; Kim, G. T.; Hong, S.; Ha, J. S. Control of Adsorption and Alignment of V2O5nanowires via Chemically Functionalized Patterns. *Nanotechnology* **2006**, *18* (1), 15304. https://doi.org/10.1088/0957-4484/18/1/015304.

(207) Gu, G.; Schmid, M.; Chiu, P.-W.; Minett, A.; Fraysse, J.; Kim, G.-T.; Roth, S.; Kozlov, M.;

Muñoz, E.; Baughman, R. H. V2O5 Nanofibre Sheet Actuators. *Nat. Mater.* **2003**, *2* (5), 316–319. https://doi.org/10.1038/nmat880.

(208) Devaraj, V.; Han, J.; Kim, C.; Kang, Y. C.; Oh, J. W. Self-Assembled Nanoporous Biofilms from Functionalized Nanofibrous M13 Bacteriophage. *Viruses* **2018**, *10* (6), 1–11. https://doi.org/10.3390/v10060322.

(209) Chen, R. J.; Zhang, Y.; Wang, D.; Dai, H. Noncovalent Sidewall Functionalization of Single-Walled Carbon Nanotubes for Protein Immobilization. *J. Am. Chem. Soc.* **2001**, *123* (16), 3838–3839. https://doi.org/10.1021/ja010172b.

(210) Kim, W.; Song, H.; Kim, C.; Moon, J.; Kim, K.; Lee, S.; Oh, J. Biomimetic Self-Templating Optical Structures Fabricated by Genetically Engineered M13 Bacteriophage. *Biosens. Bioelectron.* **2016**, *85*, 853–859. https://doi.org/10.1016/j.bios.2016.05.099.

(211) Sherman E. Ross, Steven D. Carson, L. M. F. Effects of Detergents on Avidin–Biotin Interaction. *Biotechniques* **1986**, *4* (4), 350–353.

(212) Petrenko, V. A.; Sorokulova, I. B. Detection of Biological Threats. A Challenge for Directed Molecular Evolution. *J. Microbiol. Methods* **2004**, *58* (2), 147–168. https://doi.org/10.1016/j.mimet.2004.04.004.

(213) Mao, C.; Liu, A.; Cao, B. Virus-Based Chemical and Biological Sensing. *Angew Chem Int Ed Engl* **2009**, *48* (37), 6790–6810. https://doi.org/10.1002/anie.200900231.

(214) Kim, I.; Moon, J.-S.; Oh, J.-W. Recent Advances in M13 Bacteriophage-Based Optical Sensing Applications. *Nano Converg.* **2016**, *3* (1). https://doi.org/10.1186/s40580-016-0087-5.

(215) Wu, L.; Song, Y.; Luan, T.; Ma, L.; Su, L.; Wang, S.; Yan, X. Specific Detection of Live Escherichia Coli O157: H7 Using Tetracysteine-Tagged PP01 Bacteriophage. *Biosens. Bioelectron.* **2016**, *86*, 102–108. https://doi.org/10.1016/j.bios.2016.06.041.

(216) Li, Q.; Shivachandra, S. B.; Zhang, Z.; Rao, V. B.; Ave, M. Assembly of the Small Outer Capsid Protein , Soc , on Bacteriophage T4 : A Novel System for High Density Display of Multiple Large Anthrax Toxins and Foreign Proteins on Phage Capsid. **2007**, 1006–1019. https://doi.org/10.1016/j.jmb.2007.05.008.

(217) Ren, Z.; Black, L. W. Phage T4 SOC and HOC Display of Biologically Active , Full-Length Proteins on the Viral Capsid. *Gene* **1998**, *215* (2), 439–444. https://doi.org/10.1016/s0378-1119(98)00298-4.

(218) Naik, R. R.; Stringer, S. J.; Agarwal, G.; Jones, S. E.; Stone, M. O. Biomimetic Synthesis and Patterning of Silver Nanoparticles. *Nat. Mater.* **2002**, *1* (3), 169–172. https://doi.org/10.1038/nmat758.

(219) Sano, K. I.; Shiba, K. A Hexapeptide Motif That Electrostatically Binds to the Surface of Titanium. *J. Am. Chem. Soc.* **2003**, *125* (47), 14234–14235. https://doi.org/10.1021/ja038414q.

(220) Seker, U. O. S.; Wilson, B.; Dincer, S.; Kim, I. W.; Oren, E. E.; Evans, J. S.; Tamerler, C.; Sarikaya, M. Adsorption Behavior of Linear and Cyclic Genetically Engineered Platinum Binding Peptides. *Langmuir* **2007**, *23* (15), 7895–7900. https://doi.org/10.1021/la700446g.

(221) Brown, S. Engineered Iron Oxide-Adhesion Mutants of the Escherichia Coli Phage λ Receptor. *Proc. Natl. Acad. Sci. U. S. A.* **1992**, *89* (18), 8651–8655. https://doi.org/10.1073/pnas.89.18.8651.

(222) Barbas, C. F.; Rosenblum, J. S.; Lerner, R. A. Direct Selection of Antibodies That Coordinate Metals from Semisynthetic Combinatorial Libraries. *Proc. Natl. Acad. Sci. U. S. A.* **1993**, *90* (14), 6385–6389. https://doi.org/10.1073/pnas.90.14.6385.

(223) Naik, R. R.; Brott, L. L.; Clarson, S. J.; Stone, M. O. Silica-Precipitating Peptides Isolated from a Combinatorial Phage Display Peptide Library. *J. Nanosci. Nanotechnol.* **2002**, *2* (1), 95–100. https://doi.org/10.1166/jnn.2002.074.

(224) Whaley, S. R.; Belcher, A. M. Borrowing Ideas from Nature: Peptide Specific Binding to Gallium Arsenide. In *Materials Research Society Symposium - Proceedings*; 2000; Vol. 599, pp 189–199. https://doi.org/10.1557/proc-599-189.

(225) Whaley, S. R.; English, D. S.; Hu, E. L.; Barbara, P. F.; Belcher, A. M. Selection of Peptides with Semiconductor Binding Specificity for Directed Nanocrystal Assembly. *Nature* **2000**, *405* (6787), 665–668. https://doi.org/10.1038/35015043.

(226) Thirumurugan, P.; Matosiuk, D.; Jozwiak, K. Click Chemistry for Drug Development and Diverse Chemical-Biology Applications. *Chem. Rev* **2013**, *113* (7), 4905–4979. https://doi.org/10.1021/cr200409f.

(227) Kolb, H. C.; Sharpless, K. B. The Growing Impact of Click Chemistry on Drug Discovery. *Drug Discovery Today*. Elsevier Current Trends December 15, 2003, pp 1128–1137. https://doi.org/10.1016/S1359-6446(03)02933-7.

(228) Grass, R. N.; Athanassiou, E. K.; Stark, W. J. Covalently Functionalized Cobalt Nanoparticles as a Platform for Magnetic Separations in Organic Synthesis. *Angew. Chemie - Int. Ed.* **2007**, *46* (26), 4909–4912. https://doi.org/10.1002/anie.200700613.

(229) Schätz, A.; Grass, R. N.; Stark, W. J.; Reiser, O. TEMPO Supported on Magnetic C/Co-Nanoparticles: A Highly Active and Recyclable Organocatalyst. *Chemistry (Easton).* **2008**, *14* (27), 8262–8266. https://doi.org/10.1002/chem.200801001.

(230) Duong, M. M.; Carmody, C. M.; Ma, Q.; Peters, J. E.; Nugen, S. R. Optimization of T4 Phage Engineering via CRISPR/Cas9. *Sci. Rep.* **2020**, *10* (1), 18229. https://doi.org/10.1038/s41598-020-75426-6.

(231) Singh, A.; Arutyunov, D.; Szymanski, C. M.; Evoy, S. Bacteriophage Based Probes for Pathogen Detection. *Analyst* **2012**, *137* (15), 3405–3421. https://doi.org/10.1039/c2an35371g.

(232) Boratýnski, J.; Syper, D.; Weber-Dąbrowska, B.; Łusiak-Szelachowska, M.; Poźniak, G.; Górski, A. Preparation of Endotoxin-Free Bacteriophages. *Cell. Mol. Biol. Lett.* **2004**, *9*

(November 2003), 253–259.

(233) Broeker, N. K.; Kiele, F.; Casjens, S. R.; Gilcrease, E. B.; Thalhammer, A.; Koetz, J.; Barbirz, S. In Vitro Studies of Lipopolysaccharide-Mediated DNA Release of Podovirus HK620. *Viruses* **2018**, *10* (6). https://doi.org/10.3390/v10060289.

(234) Andres, D.; Roske, Y.; Doering, C.; Heinemann, U.; Seckler, R.; Barbirz, S. Tail Morphology Controls DNA Release in Two Salmonella Phages with One Lipopolysaccharide Receptor Recognition System. *Mol. Microbiol.* **2012**, *83* (6), 1244–1253. https://doi.org/10.1111/j.1365-2958.2012.08006.x.

(235) Andres, D.; Hanke, C.; Baxa, U.; Seul, A.; Barbirz, S.; Seckler, R. Tailspike Interactions with Lipopolysaccharide Effect DNA Ejection from Phage P22 Particles in Vitro. *J. Biol. Chem.* **2010**, *285* (47), 36768–36775. https://doi.org/10.1074/jbc.M110.169003.

(236) Lawrence, J. E.; Steward, G. F. Purification of Viruses by Centrifugation. *Man. Aquat. Viral Ecol.* **2010**, *2* (2), 166–181. https://doi.org/10.4319/mave.2010.978-0-9845591-0-7.166.

(237) Yamamoto, R.; Alberts, M. Rapid Bacteriophage Glycol Sedimentation Its Application in the to Virus of Polyethylene Purification. *Virology* **1970**, *40* (3), 734–744. https://doi.org/10.1016/0042-6822(70)90218-7.

(238) Clokie, M. R. J.; Kropinski, A. M. *Bacteriophages - Methods and Protocols, Volume 1: Isolation, Characterization, and Interactions*; Clokie, M. R. J., Kropinski, A., Eds.; Humana Press, 2009. https://doi.org/10.1007/978-1-60327-164-6.

(239) Thurber, R. V.; Haynes, M.; Breitbart, M.; Wegley, L.; Rohwer, F. Laboratory Procedures to Generate Viral Metagenomes. *Nat. Protoc.* **2009**, *4* (4), 470–483. https://doi.org/10.1038/nprot.2009.10.

(240) Bachrach, U.; Friedmann, A. Practical Procedures for the Purification of Bacterial Viruses. *Appl. Microbiol.* **1971**, *22* (4), 706–715.

(241) Holmfeldt, K.; Solonenko, N.; Shah, M.; Corrier, K.; Riemann, L.; VerBerkmoes, N. C.; Sullivan, M. B. Twelve Previously Unknown Phage Genera Are Ubiquitous in Global Oceans. *Proc. Natl. Acad. Sci.* **2013**, *110* (31), 12798–12803. https://doi.org/10.1073/pnas.1305956110.

(242) Akhwale, J. K.; Rohde, M.; Rohde, C.; Bunk, B.; Spröer, C.; Boga, H. I.; Klenk, H. P.; Wittmann, J. Isolation, Characterization and Analysis of Bacteriophages from the Haloalkaline Lake Elmenteita, Kenya. *PLoS One* **2019**, *14* (4), 1–19. https://doi.org/10.1371/journal.pone.0215734.

(243) Clokie, M. R. J.; Kropinski, A. M. *Bacteriophages - Methods and Protocols, Volume 2: Molecular and Applied Aspects*; Clokie, M. R. J., Kropinski, A., Eds.; 2009. https://doi.org/10.1007/978-1-60327-565-1.

(244) Kohno, T.; Mohan, S.; Goto, T.; Morita, C.; Nakano, T.; Hong, W.; Sangco, J. C. E.; Morimatsu, S.; Sano, K. A New Improved Method for the Concentration of HIV-1 Infective Particles. *J. Virol. Methods* **2002**, *106* (2), 167–173. https://doi.org/10.1016/S0166-

0934(02)00162-3.

(245) Vajda, B. P. Concentration and Purification of Viruses and Bacteriophages with Polyethylene Glycol. *Folia Microbiol. (Praha).* **1978**, *23* (1), 88–96. https://doi.org/10.1007/BF02876605.

(246) Kanarek, A. D.; Tribe, G. W. Concentration of Certain Myxoviruses with Polyethylene Glycol. *Nature* **1967**, *214* (5091), 927–928. https://doi.org/10.1038/214927a0.

(247) Warner, C. M.; Barker, N.; Lee, S. W.; Perkins, E. J. M13 Bacteriophage Production for Large-Scale Applications. *Bioprocess Biosyst. Eng.* **2014**, *37* (10), 2067–2072. https://doi.org/10.1007/s00449-014-1184-7.

(248) Lane, J. R. Quantitation of Cell-Free HIV by Reverse Transcriptase Activity. In *HIV Protocols*; Michael, N. L., Kim, J. H., Eds.; Humana Press, 1999; pp 17–22.

(249) Greene, R. A.; Japour, A. J.; Brewster, F.; Joseph, R. A.; Chung, P. H.; Kasila, P. A.; Chatis, P. A. Determination of HIV-1 Susceptibility to Reverse Transcriptase (RT) Inhibitors by a Quantitative Cell-Free RT Assay. *Clin. Diagn. Virol.* **1996**, *7* (2), 111–119.

(250) Sarmati, L.; Ercoli, L.; Parisi, S. G.; Rocchi, G.; Giannini, G.; Galluzzo, C.; Vella, S.; Andreoni, M. High Rate of HIV Isolation from Plasma of Asymptomatic Patients through Polyethylene Glycol (PEG) Treatment. *J. Acquir. Immune Defic. Syndr.* **1994**, *7* (1), 10–14.

(251) Atha, D. H.; Inghamg, K. C. Mechanism of Precipitation of Proteins by Polyethylene Glycols. *J. Biol. Chem.* **1981**, *256* (23), 12108–12117.

(252) Fahie-Wilson, M.; Halsall, D. Polyethylene Glycol Precipitation: Proceed with Care. *Ann. Clin. Biochem.* **2008**, *45* (3), 233–235. https://doi.org/10.1258/acb.2008.007262.

(253) Ceglarek, I.; Piotrowicz, A.; Lecion, D.; Miernikiewicz, P.; Owczarek, B.; Da, K. A Novel Approach for Separating Bacteriophages from Other Bacteriophages Using Affinity Chromatography and Phage Display. *Sci. Rep.* **2013**, 1–6. https://doi.org/10.1038/srep03220.

(254) Adriaenssens, E. M.; Lehman, S. M.; Vandersteegen, K. CIM Monolithic Anion-Exchange Chromatography as a Useful Alternative to CsCl Gradient Purification of Bacteriophage Particles. *Virology* **2015**, *434* (2), 265–270. https://doi.org/10.1016/j.virol.2012.09.018.CIM.

(255) Mack, J. D.; Yehualaeshet, T.; Park, M. K.; Tameru, B.; Samuel, T.; Chin, B. A. Phage-Based Biosensor and Optimization of Surface Blocking Agents to Detect Salmonella Typhimurium on Romaine Lettuce. *J. Food Saf.* **2017**, *37* (2). https://doi.org/10.1111/jfs.12299.

(256) Bennett, A. R.; Davids, F. G. C.; Vlahodimou, S.; Banks, J. G.; Betts, R. P. The Use of Bacteriophage-Based Systems for the Separation and Concentration of Salmonella. *J. Appl. Microbiol.* **1997**, *83* (2), 259–265. https://doi.org/10.1046/j.1365-2672.1997.00257.x.

(257) Kyaw, H. H.; Al-Harthi, S. H.; Sellai, A.; Dutta, J. Self-Organization of Gold Nanoparticles

on Silanated Surfaces. *Beilstein J. Nanotechnol.* **2015**, *6* (1), 2345–2353. https://doi.org/10.3762/bjnano.6.242.

(258) Naik, V. V.; Crobu, M.; Venkataraman, N. V.; Spencer, N. D. Multiple Transmission-Reflection Ir Spectroscopy Shows That Surface Hydroxyls Play Only a Minor Role in Alkylsilane Monolayer Formation on Silica. *J. Phys. Chem. Lett.* **2013**, *4* (16), 2745–2751. https://doi.org/10.1021/jz401440d.